# Sinclair Inlet Water Quality Assessment:

## Water Quality Surveys Conducted September 1997, March 1998, and July 1998

**January 2004**


**Prepared For:**
**Puget Sound Naval Shipyard Project ENVVEST**

**Prepared By:**
**C.N. Katz, P.L. Noble, D.B. Chadwick,**
**B. Davidson, and R.D. Gauthier**

**Environmental Quality Branch Code 2362**
**Space and Naval Warfare Systems Center**
**San Diego, CA 92152-6326**

# ADMINISTRATIVE INFORMATION

The contents of this document were prepared as part of the PSNS Project ENVVEST and do not represent the views of the United States Navy, the United States Environmental Protection Agency, or the Washington State Department of Ecology. References to brand names and trademarks in this document are for information purposes only and do not constitute an endorsement for use.

The CD contains files that are a part of the Sinclair Inlet Water Quality Assessment for the Puget Sound Wastewater Technology Evaluation and Research Project. The CD is a companion to the Report entitled "Sinclair Inlet Water Quality Assessment" delivered to Gerry Sherrell, Special Project Manager, Puget Sound Naval Shipyard on 1 October 1999, and approved for public release on January 16, 2004. The following is a description of the files on the CD:

**FinalECOSReport.doc:** Electronic version of the draft report entitled "Sinclair Inlet Water Quality Assessment" in Microsoft Word 7.0 format

**FinalECOSReport.pdf:** PDF version of the report.

**Puget_Plots.doc:** Electronic version of the companion report entitled "Companion Data Plots for Sinclair Inlet Water Quality Assessment" in Microsoft Word 7.0 format

**Currents_sd.mpg:** MPEG movie of current velocity at the mouth of Sinclair and Dyes Inlet generated from data collected on survey PS02, 18-19 September 1997

**Density_sd.mpg:** MPEG movie of density at the mouth of Sinclair and Dyes Inlet generated from data collected on survey PS02, 18-19 September 1997

**Oil_fluorescence_sd.mpg:** MPEG movie of oil fluorescence at the mouth of Sinclair and Dyes Inlet generated from data collected on survey PS02, 18-19 September 1997

**Oxygen_sd.mpg:** MPEG movie of oxygen at the mouth of Sinclair and Dyes Inlet generated from data collected on survey PS02, 18-19 September 1997

**pH_sd.mpg:** MPEG movie of pH at the mouth of Sinclair and Dyes Inlet generated from data collected on survey PS02, 18-19 September 1997

**Salinity_sd.mpg:** MPEG movie of salinity at the mouth of Sinclair and Dyes Inlet generated from data collected on survey PS02, 18-19 September 1997

**Temperature_sd.mpg:** MPEG movie of temperature at the mouth of Sinclair and Dyes Inlet generated from data collected on survey PS02, 18-19 September 1997

**TSS_sd.mpg:** MPEG movie of TSS at the mouth of Sinclair and Dyes Inlet generated from data collected on survey PS02, 18-19 September 1997

For further information regarding the files contact:
Charles N. Katz
SPAWAR Systems Center, San Diego
Marine Environmental Quality Branch D362
53475 Strothe Road
San Diego, CA 92152-6310
Tel: 619-553-5332, Fax: 619-553-3097
mailto:ckatz@spawar.navy.mil



# PUGET SOUND WASTEWATER TECHNOLOGY EVALUATION AND RESEARCH PROJECT

# Sinclair Inlet Water Quality Assessment

## Final Report

## January 2004

## By

**C.N. Katz, P.L. Noble, D.B. Chadwick, B. Davidson, and R.D. Gauthier**

**Environmental Quality Branch Code 2362**
**Space and Naval Warfare Systems Center**
**San Diego, CA 92152-6326**

# EXECUTIVE SUMMARY

This report describes water quality data collected in Sinclair Inlet, Washington and the adjacent waters of Puget Sound in September 1997, and March and July 1998. A full visualization package for all the data described here is provided under separate cover "Companion Data Plots for Sinclair Inlet Water Quality Assessment Report". The goals of the sampling were to establish baseline water quality conditions throughout the inlet, identify locations and extent of contaminants from storm water inflows, and collect water current data throughout the Inlet for use in validating a hydrodynamic model currently under development by SSC San Diego. All goals were met by simultaneously collecting circulation, hydrographic, conventional water quality parameters, and specific contaminant data at the appropriate spatial and temporal scales necessary to understand the processes controlling distributions.

Data were collected on a total of 19 surveys performed over three survey periods. All data were collected using SPAWAR System Center's Marine Environmental Survey Capability, a real-time environmental data mapping system. Circulation and hydrography measurements included current velocity, salinity, temperature, density, and sample depth. Conventional water quality parameters included total suspended solids, dissolved oxygen, pH, and chlorophyll *a*. Contaminants of concern included nutrients (nitrate, nitrite, ammonia, silicate, and phosphate), metals (arsenic, cadmium, chromium, copper, lead, selenium, silver, and zinc), and polynuclear aromatic hydrocarbons. Ancillary measures included bottom depth, sample location, and wind velocity. In addition to sampling inlet receiving waters, a limited number of samples were taken from the two major publicly owned treatment works (POTWs), or sewer plants, and three creeks.

Current measurements made during these surveys provided the most comprehensive view of the circulation made to date. A complex gyral circulation at the mouth, generated by interaction of tidal flow out of the Port Washington Narrows, was found to control mixing at the mouth of the inlet. This circulation pattern enhances flushing at the mouth with its higher current speeds and by generating a continuous outward flow of water along the northern shore. Inside the inlet, circulation is influenced by both tides and estuarine conditions. The lower current speeds and stratification observed inside the inlet combine to weaken mixing which leads to longer flushing times relative to the mouth. High resolution mapping of salinity and currents along a cross-sectional at the mouth provided and estimate of residence time of 57 days for Sinclair Inlet, 11 days for Dyes Inlet.

Conventional measures of water quality of the inlet can be characterized as conditionally good. There was visual evidence of large plankton blooms inside the inlet on all occasions and chlorophyll *a*, one measure of biological productivity, was exceptionally high. These signs of eutrophication appear to be driven by nutrient influx from the Bremerton POTW, not creek flow, in the inner portion of the inlet. The nutrient source within this region of reduced circulation and mixing provides the necessary conditions to cause the high production. The high production was reflected in relatively high suspended loads, but another source of solids in the inner inlet, either the Bremerton POTW or resuspension, may be present. The blooms also generated very high levels of oxygen and pH throughout most of the inlet. However, there was one small region along the south shore, well back in the inlet, which had dangerously low oxygen levels presumably as a result of organic decomposition. This condition was observed on only one occasion and its extent in space and time is not fully known. Long flushing times could eventually lead to further degradation, which is the basis for characterizing the inlet's water quality as conditionally good.

All metal concentrations were measured at levels well below water quality criteria set by the State of Washington. Though metal levels were low throughout the region, sufficient data were collected to assess their distribution and sources. Arsenic, copper, lead, selenium, and zinc were all significantly elevated in the POTW discharges relative to those measured in the inlet while chromium, lead, and selenium were significantly elevated in the creeks. The introduction of metals into the inner inlet with its reduced circulation results in generally higher concentration levels in this portion of the inlet. Elevated metal concentrations were also measured within the region bordered by the Puget Sound Naval Shipyard. Copper and zinc were significantly higher within the shipyard region than the rest of the inlet. Two specific areas within this region showed elevated levels, the western pier area of the mothball fleet and along pier 3. The likely source of these two metals are hull paint and cathodic protection anodes for the ships located in the western area and the dry dock discharges along pier 3. However the proximity of the Bremerton POTW discharge to the mothball fleet complicates assessing their relative source strengths.

Polynuclear Aromatic Hydrocarbons (PAH), toxic components of oil and creosote, were measured at levels below water quality criteria set by the Environmental Protection Agency and adopted by the State of Washington. Their distribution in the inlet was patchy and higher levels of total PAH did not always coincide with an obvious source. The majority (60%) of samples showed a compositional makeup of PAH typical of that derived from background pyrogenic sources, such as from atmospheric fallout. The remainder of samples had a composition at least partially derived from petrogenic sources, such as from fuels. There were no significant differences between total PAH measured within the region bordered by the Puget Sound Naval Shipyard and those outside. Though the POTWs were a source of petrogenic PAH to the inlet, there was no definitive impact on their distribution. The creeks were not a source of PAH.

In summary, the field effort was successful in establishing baseline water quality conditions throughout the inlet, identifying locations and extent of contaminants from storm water sources, and in collecting water current data for use in validating a hydrodynamic model for the inlet. Inlet water quality can be characterized as good with respect to the contaminants of concern measured. The exception to this is the potential negative impacts that may arise from nutrient influx from the POTWs and their impact on eutrophication.

All metal concentrations were measured at levels well below water quality criteria set by the State of Washington. Though metal levels were low throughout the region, sufficient data were collected to assess their distribution and sources. Arsenic, copper, lead, selenium, and zinc were all significantly elevated in the POTW discharges relative to those measured in the inlet while chromium, lead, and selenium were significantly elevated in the creeks. The introduction of metals into the inner inlet with its reduced circulation results in generally higher concentration levels in this portion of the inlet. Elevated metal concentrations were also measured within the region bordered by the Puget Sound Naval Shipyard. Copper and zinc were significantly higher within the shipyard region than the rest of the inlet. Two specific areas within this region showed elevated levels, the western pier area of the mothball fleet and along pier 3. The likely source of these two metals are hull paint and cathodic protection anodes for the ships located in the western area and the dry dock discharges along pier 3. However the proximity of the Bremerton POTW discharge to the mothball fleet complicates assessing their relative source strengths.

Polynuclear Aromatic Hydrocarbons (PAH), toxic components of oil and creosote, were measured at levels below water quality criteria set by the Environmental Protection Agency and adopted by the State of Washington. Their distribution in the inlet was patchy and higher levels of total PAH did not always coincide with an obvious source. The majority (60%) of samples showed a compositional makeup of PAH typical of that derived from background pyrogenic sources, such as from atmospheric fallout. The remainder of samples had a composition at least partially derived from petrogenic sources, such as from fuels. There were no significant differences between total PAH measured within the region bordered by the Puget Sound Naval Shipyard and those outside. Though the POTWs were a source of petrogenic PAH to the inlet, there was no definitive impact on their distribution. The creeks were not a source of PAH.

In summary, the field effort was successful in establishing baseline water quality conditions throughout the inlet, identifying locations and extent of contaminants from storm water sources, and in collecting water current data for use in validating a hydrodynamic model for the inlet. Inlet water quality can be characterized as good with respect to the contaminants of concern measured. The exception to this is the potential negative impacts that may arise from nutrient influx from the POTWs and their impact on eutrophication.

# TABLE OF CONTENTS

# LIST of FIGURES

# LIST of TABLES

# ACRONYMS

| | |
|---|---|
| ADCP | Acoustic Doppler Current Profiler |
| Chl-*a* | Chlorophyll *a* |
| CCW | Counterclockwise |
| CTD | Conductivity, Temperature, and Depth |
| CW | Clockwise |
| DAS | Data Acquisition System |
| DFM | Diesel Fuel Marine |
| DFME | Diesel Fuel Marine Equivalents |
| DGPS | Differential Global Positioning System |
| EPA | Environmental Protection Agency |
| MESC | Marine Environmental Survey Capability |
| MLLW | Mean Lower Low Water |
| NaN | Not a Number |
| NOAA | National Oceanic and Atmospheric Administration |
| PAH | Polynuclear Aromatic Hydrocarbons |
| POTW | Publicly Owned Treatment Works |
| PSNS | Puget Sound Naval Shipyard |
| QA/QC | Quality Assurance/Quality Control |
| RTF | Rich Text Format |
| SSC San Diego | Space and Naval Warfare Systems Center, San Diego |
| TMA | Trace Metal Analyzer |
| TPAH | Total Polynuclear Aromatic Hydrocarbons |
| TSS | Total Suspended Sediments |
| UV | Ultraviolet |
| 3-D | 3-Dimensional |

# 1.0 INTRODUCTION

This report describes water quality data collected in Sinclair Inlet, Washington and the waters of Puget Sound immediately adjacent (Figure 1) in September 1997, and March and July 1998. The data were collected as part of the Puget Sound Naval Shipyard (PSNS) Wastewater Technology Evaluation and Research Project funded by the Naval Facilities Command. Data were collected using a real-time data acquisition system designed and operated by the Marine Environmental Quality Branch (Code D362) of the Space and Naval Warfare Systems Center, San Diego (SSC San Diego). An electronic Word 7.0 and Rich Text Format (RTF) version of this report is included on the accompanying CD.

The goals of the sampling were threefold:

- Establish baseline water quality conditions throughout the inlet
- Identify locations and extent of contaminants from storm water inflows
- Collect water current data throughout the Inlet for use in validating a hydrodynamic model under development by SSC San Diego

# 2.0 TECHNICAL APPROACH

SSC San Diego utilized its Marine Environmental Survey Capability (MESC) to thoroughly characterize the spatial and temporal water quality conditions in the inlet and adjacent waters. The MESC is a real-time data acquisition and processing system designed and built by the Navy to provide integrated, rapid, continuous measurement and mapping of oceanographic and environmental parameters in coastal and estuarine environments (Lieberman et al., 1989, Chadwick and Salazar, 1991, Katz and Chadwick, 1993). MESC measures physical, chemical, and biological characteristics from a moving vessel utilizing state-of-the-art sensors, computer systems, and navigation equipment. This approach allows for direct, *in situ* measurements that avoid extrapolation, and provides simultaneous measurements at a frequency commensurate with scales of natural and anthropogenic variability. The MESC therefore provides the near-synoptic real-time data collection necessary to effectively map the highly dynamic nature of the coastal environment. A description of MESC and its capabilities can be found in the Methods section.

To assess baseline and storm water inflow conditions, a set of surveys was scheduled for September 1997 (dry) and again in March 1998 (wet). However, because of transitional meteorological conditions (early winter rains) present in September, a third set of surveys was added in July 1998 to better represent the dry season. A total of 19 surveys, over 22 days, were conducted for this project. The name, date, and general type of surveys are listed in Table 1 below. The surveys fell into one of five general types: Axial, Surface Mapping, Cross-Sections, 3-Dimensional, and Shoreline. The different survey types were designed to each capture a specific aspect of the spatial and temporal variations in water quality. The purpose and general methodology employed for each type of survey was as follows:

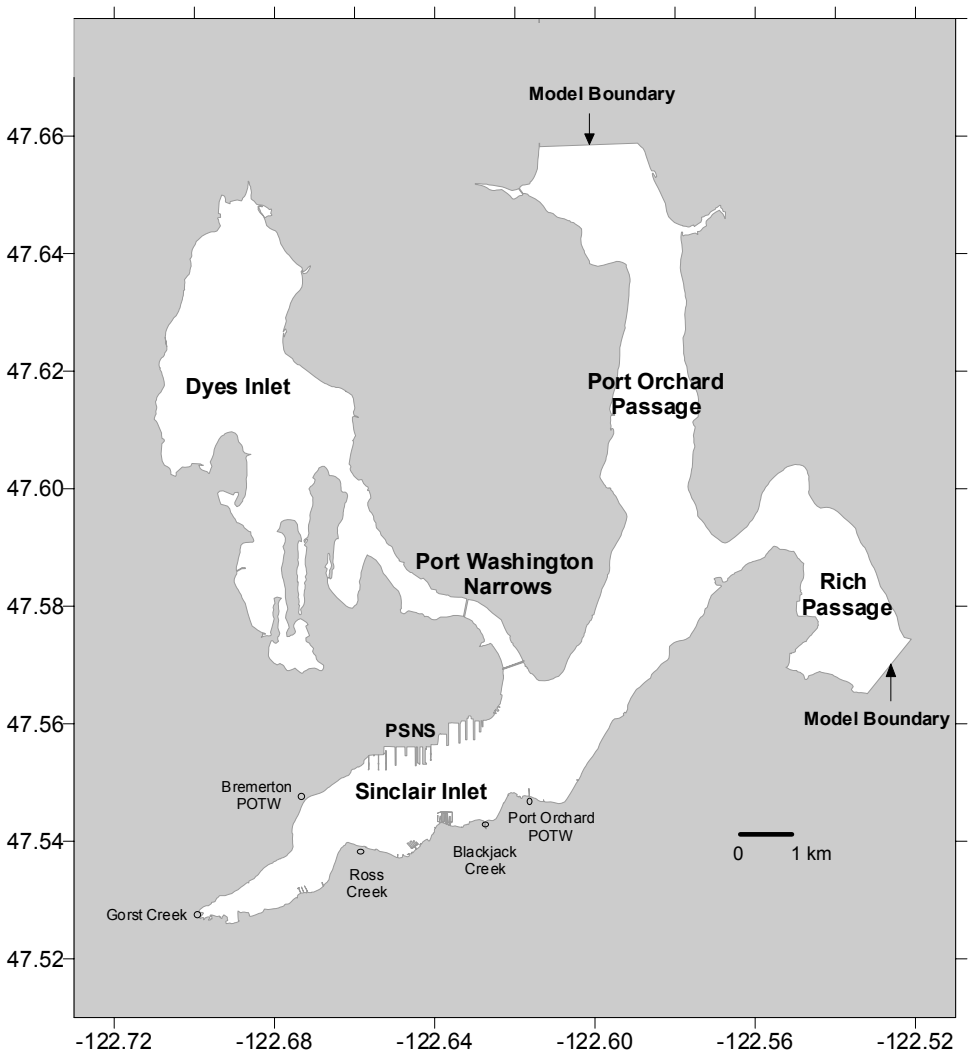


**Figure 1.** Study area showing Sinclair Inlet and its adjacent waters. The general location of the Puget Sound Naval Shipyard in Sinclair Inlet is identified as PSNS. The adjacent water regions are shown only out to the boundaries of the hydrodynamic model. Major creeks and Publicly Operated Treatment Works (POTWs) in Sinclair Inlet are also shown.

**Axial Surveys.** Axial surveys were designed to look at variations in water quality. For simplicity, water current measurements are bundled in with the term "water quality" and were always collected throughout the vertical water column from inside to outside the inlet, specifically out to the physical boundaries of the hydrodynamic model. Data were collected along a single, or in some cases, a dual transect, mainly along the centerline of each region. An example of this transect is shown in Figure 2. Outside Sinclair Inlet, data were collected mostly near the surface, nominally at 1.5 m. Inside Sinclair Inlet, data were collected underway while raising and lowering the MESC instrument package as quickly as possible (tow-yoing) thereby providing data throughout the full water column. Additionally, vertical profiles were performed at various stations systematically throughout the entire region. Most of these stations were also locations for collecting discrete seawater samples that were used to calibrate *in situ* sensors, or to extend the measurement capability of MESC. One axial survey was performed during each visit.

**Surface Mapping Surveys.** Surface mapping surveys were designed to provide full spatial coverage of the inlet during a variety of tidal conditions. Water quality data were collected near the surface on a transect that zig-zagged along mostly north-south lines (Figure 3) providing spatially dense coverage. The transect was repeated throughout a variety of tidal conditions to capture changes in water quality parameters as a function of the tide. Discrete samples were collected at a number of stations during these surveys. Two surface mapping surveys were performed on each of the first two visits, and one survey was performed on the third visit.

**Cross-section Surveys.** Cross-sections were performed at the mouth of Sinclair and Dyes Inlet (Figure 4) to assess the mass flux of water borne components through these sections as a function of tidal condition. Data were collected over full tidal cycles while tow-yoing the MESC instrument package so as to obtain a full 3-Dimensional view of each section. No discrete sampling was performed during these surveys. Two surveys were performed during the first visit.

**3-D Surveys.** These surveys were performed to assess the inlet-wide variation of water quality parameters as a function of water depth. Data were collected on the same transect as the surface mapping survey (Figure 3) but instead of mapping only at the surface, data were collected underway while tow-yoing the MESC instrument package as quickly as possible. In this way, data were collected from near surface to near bottom in a continuous fashion at a reasonably high spatial density. No discrete sampling was performed during these surveys. One 3-D mapping survey was performed on each visit.

**Shoreline Surveys.** Shoreline mapping surveys were performed to identify source areas along the shoreline of Sinclair Inlet, with particular emphasis on the pier area of PSNS. Data were collected mostly near the surface, though some vertical profiles were performed. Discrete samples were collected at a number of stations during these surveys. Three shoreline surveys were performed on the first visit, two on the second, and one on the third visit. Though the transect varied on each survey, one example from survey PS18 is shown in Figure 5.

**Table 1.** MESC survey dates, name, and general type.

| Visit | Survey Date | Survey | Survey Type |
|---|---|---|---|
| 1 | 17 September 1997 | PS01 | Axial |
| 1 | 18-19 September 1997 | PS02 | Cross-sections |
| 1 | 20-21 September 1997 | PS03 | Surface mapping |
| 1 | 22 September 1997 | PS04 | Shoreline |
| 1 | 23 September 1997 | PS05 | Shoreline |
| 1 | 24 September 1997 | PS06 | Shoreline |
| 1 | 25 September 1997 | PS07 | Surface mapping |
| 1 | 26 September 1997 | PS08 | 3-D |
| 1 | 27 September 1997 | PS09 | Cross-sections |
| 2 | 11 March 1998 | PS10 | Axial |
| 2 | 12 March 1998 | PS11 | Surface mapping |
| 2 | 13 March 1998 | PS12 | 3-D |
| 2 | 14 March 1998 | PS13 | Surface mapping (back-bay only) |
| 2 | 15 March 1998 | PS14 | Shoreline |
| 2 | 16 March 1998 | PS15 | Shoreline |
| 3 | 16 July 1998 | PS16 | Axial |
| 3 | 17-18 July 1998 | PS17 | Surface mapping |
| 3 | 19 July 1998 | PS18 | Shoreline |
| 3 | 20 July 1998 | PS19 | 3-D |

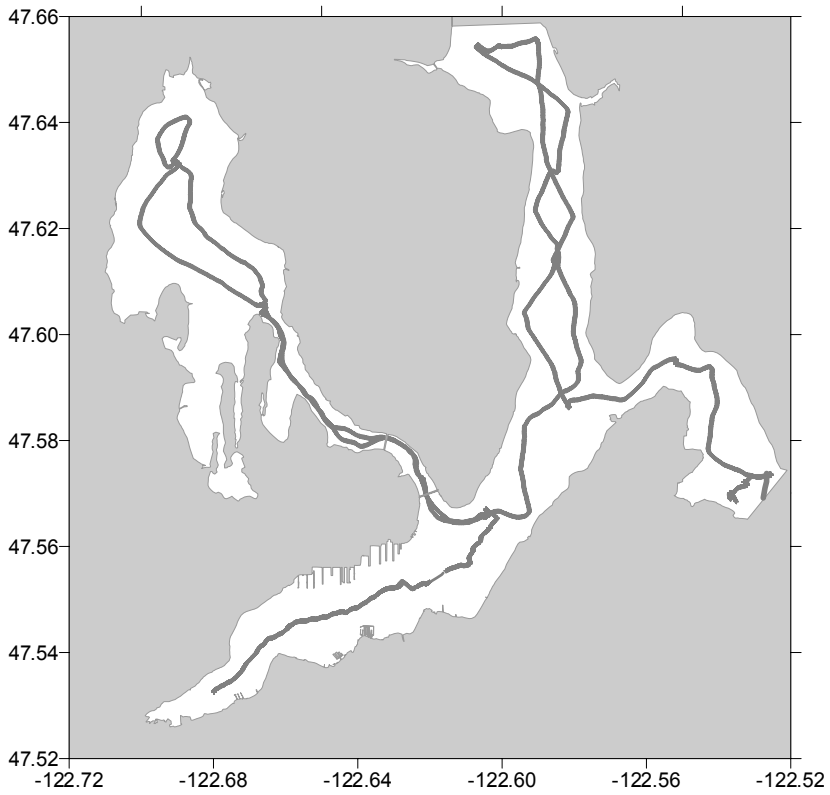


**Figure 2.** Example of an axial survey transect (PS10) starting out at the hydrodynamic model boundary in Rich Passage, and continuing on through Port Orchard Passage, Dyes Inlet and into Sinclair Inlet.


**Figure 3.** Example of a surface mapping survey transect (PS03) starting at the mouth of Sinclair. The transect was repeated during different tidal conditions. This transect was also used to collect data for the 3-D surveys

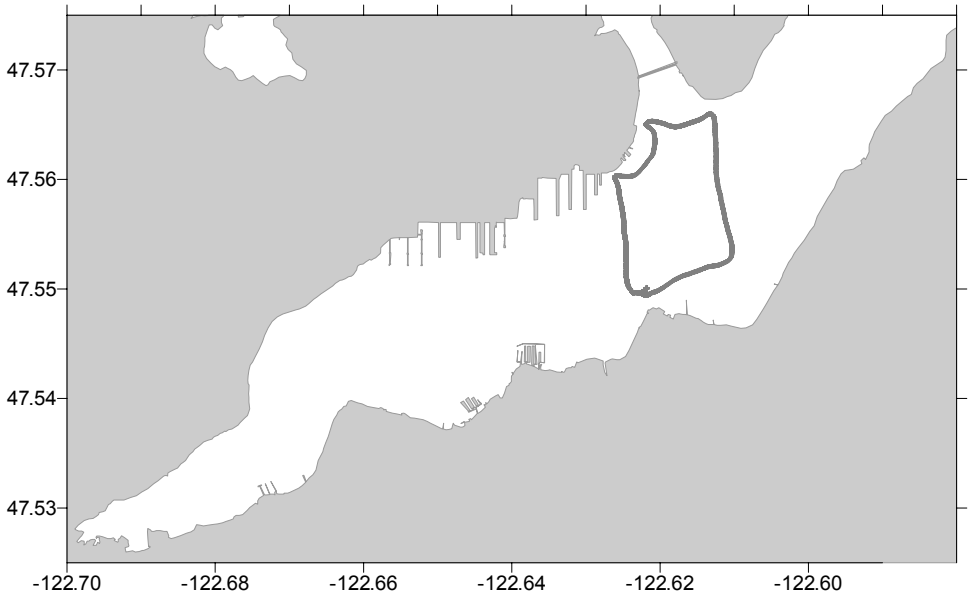


**Figure 4.** Example of a cross-section survey transect (PS09) at the mouths of Sinclair and Dyes Inlet. The transect was repeated continuously throughout a full tidal cycle.

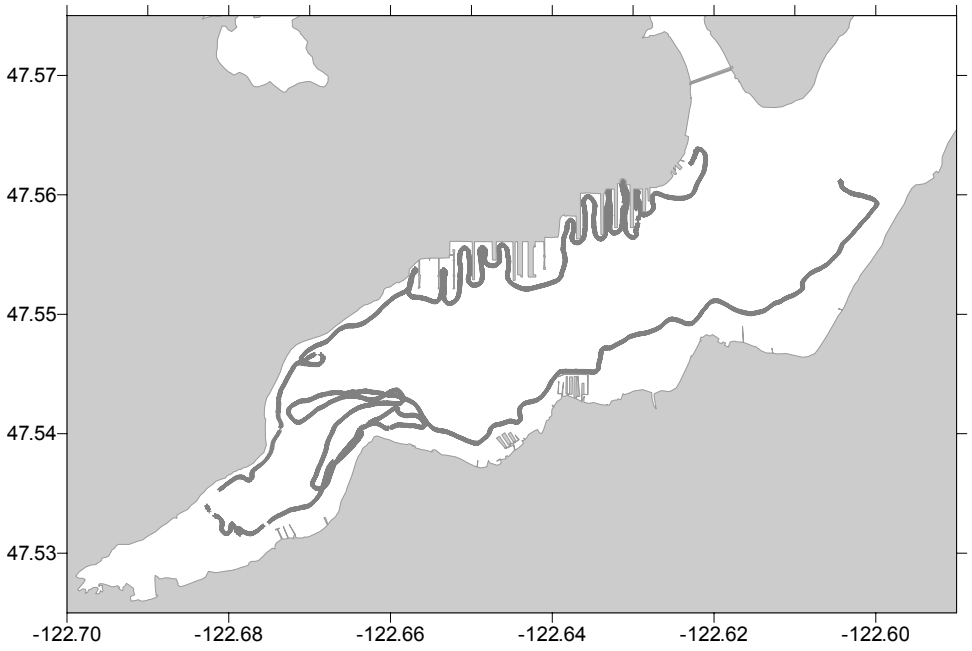


**Figure 5.** Example of a shoreline survey transect (PS18). The exact transect varied on each occasion.

# 3.0 STUDY AREA

Sinclair Inlet lies in the central part of Puget Sound, Washington. It is roughly 6 km long extending in an east-northeast direction from its head at Gorst Creek out to the mouth where it intersects with the Port Washington Narrows. At this intersection, the mouth is roughly 1.5 km across. The inlet has a maximum mean low-low water (MLLW) depth of about 20 m and averages 9.4 m. The wetted surface area is approximately $7.8 \cdot 10^6$ $m^2$ and has a MLLW volume of approximately $7.4 \cdot 10^7$ $m^3$. The bottom bathymetry gently decrease from the mouth to the head (Figure 6). Large areas of tide flats are exposed at low tide, particularly in the inner third of the inlet and along the southern shore near the mouth. Water exchanges through the mouth with waters of the Port Washington Narrows leading into Dyes Inlet, Rich Passage, and Port Orchard Channel.

The region is bounded to the north and south by forested hills, though the shorelines have been extensively developed, primarily along the north-eastern shore with the city of Bremerton and industrial area of PSNS, and along the south-eastern shore with the city of Port Orchard. Two POTWs discharge into the area, the Bremerton POTW discharging along the north-western shore just west of PSNS, and the Port Orchard POTW discharging just outside the mouth of the inlet on the south shore. Several small creeks discharge into the inlet, the largest of which are Gorst at the head, Blackjack at the mouth along the south shore, and Ross, about midway along the south shore. The flow from these creeks is low and highly variable (Albertson et al., 1995).

A number of studies have been conducted in Sinclair Inlet and surrounding waters. Prior to this project, two major studies were conducted that provide information on the general circulation and hydrographic conditions of Sinclair Inlet. These were conducted by the Washington State Department of Ecology (Albertson et al., 1995) and by the US Navy (Tetra Tech, 1988). These studies used limited spatial measurements.

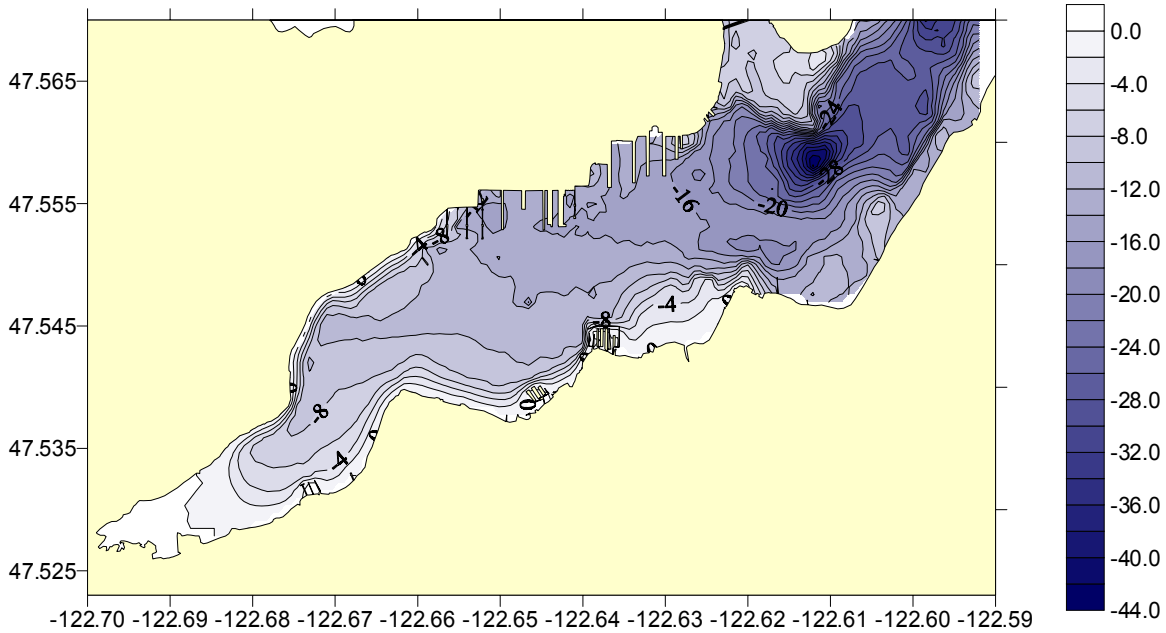


**Figure 6.** Bathymetry of Sinclair Inlet in meters at mean lower low water based on surface mapping survey data.

# 4.0 METHODS

## MESC Real-Time Data

Water quality data were collected using the MESC installed aboard the 12-m RV *Ecos*. The MESC real-time system employs both a towed sensor package and a sea water flow-through system that provides a continuous stream of seawater to a suite of on-board sensors. Sensors in the towed package consisted of a conductivity, temperature, and depth profiler (CTD), outfitted with pH and dissolved oxygen sensors, a light transmissometer, and an ultraviolet (uv)-fluorometer for hydrocarbon detection. A V-Fin depressor was used to keep the instrument package stable and submerged to the appropriate depth, while a hydraulic winch was used to raise and lower the package to the desired water depth. The on-board sensors included multiple fluorometers, an automated trace metal analyzer (TMA), an acoustic doppler current profiler (ADCP), a digital fathometer, and a differential Global Positioning System (DGPS) navigation receiver. The on-board fluorometers were independently set up to measure hydrocarbon and chlorophyll fluorescence.

In addition to the real-time measurements, the MESC flow-though system was used to collect discrete seawater samples that were used to either calibrate the real-time sensors or to provide data not available by the real-time sensors. Discrete samples were collected and analyzed for Total Suspended Sediments (TSS), chlorophyll *a* (Chl-*a*), nutrients including nitrate ($NO_3$), nitrite ($NO_2$), ammonia ($NH_3$), silicate ($SiO_2$, and phosphate ($PO_4$), polynuclear aromatic hydrocarbons (PAH), dissolved and total metals including copper (Cu), lead (Pb), cadmium (Cd), arsenic (As), silver (Ag), selenium (Se), zinc (Zn), and chromium (Cr). A list of all the parameters measured or derived, and their frequency of measurement is shown in Table 2. The metals analyzed were chosen from a list of contaminants of concern for both the waters and sediments of Sinclair Inlet prior to the start of the project. Though mercury would have also been included on the list, its analysis was considered too cost prohibitive for the purposes of this study.

Real-time data were typically collected while moving at speeds up to 6 kts. During the cross-section and 3-D surveys, the vessel was slowed to 2 to 3 kts to accommodate the raising and lowering of the tow package through the water column. At a 4-Hz sampling rate, the along-track spatial resolution of the data was less than one meter. The vertical resolution of the 4-Hz data while tow-yoing was roughly 0.1 m. Current measurements, averaged over 10s, had an along-track spatial resolution of 30 m and a vertical resolution of 1 m. The vessel was stopped to perform vertical profiles and, in most instances, was stopped to collect discrete seawater samples. On a few occasions, when only a small subset of the discrete sample suite was collected, the vessel was slowed, but did not stop. While discrete samples were collected, the MESC real-time system continued to collect data, thereby providing a simultaneous record of all parameters. This method allowed for direct intercalibration of the real-time sensors with the discrete sample analyses.

**Table 2.** Chemical, physical, and biological parameters, and the frequency of each measurement made with the MESC.

| Parameter | Units | Measured | Derived | Frequency ($s^{-1}$) |
|---|---|---|---|---|
| Local Time | Decimal hours | x | | 4 |
| Latitude | Decimal degrees | x | | 2 |
| Longitude | Decimal degrees | x | | 2 |
| Ship Velocity | $m \cdot s^{-1}$ | x | | 2 |
| Relative Wind Velocity | degrees, $m \cdot s^{-1}$ | x | | 1 |
| True Wind Velocity[a] | degrees, $m \cdot s^{-1}$ | | x | 1 |
| Current Velocity (full water column) | Degrees, $m \cdot s^{-1}$ | x | | 0.1 |
| Sample Pressure | decibars | x | | 4 |
| Sample Depth[b] | m | | x | 4 |
| Conductivity | siemens$\cdot m^{-1}$ | x | | 4 |
| Temperature | degrees centigrade | x | | 4 |
| Salinity[c] | Psu | | x | 4 |
| Density[d] | Sigma-t | | x | 4 |
| Bottom Depth[b] | M | x | | 1 |
| Light Transmission | Percent | x | | 4 |
| Total suspended solids[e] | $Mg \cdot L^{-1}$ | | x | 4 |
| pH | NBS | x | | 4 |
| Dissolved Oxygen | $ML \cdot L^{-1}$ | x | | 4 |
| Oxygen Saturation[f] | Percent | | x | 4 |
| Oil fluorescence | relative volts | x | | 4 |
| Oil (DFME)[g] | $ug \cdot L^{-1}$ | | x | 4 |
| TPAH[h] | $ng \cdot L^{-1}$ | | x | 4 |
| Chlorophyll fluorescence | relative volts | x | | 4 |
| Chlorophyll-*a*[i] | $ug \cdot L^{-1}$ | | x | 4 |
| Nutrients $NO_3$, $NO_2$, $NH_3$, $PO_4$, $SiO_2$[j] | $mg \cdot L^{-1}$ | x | | Various |
| Metals Cu, Pb, Cd, As, Ag, Se, Zn, Cr[k] | $ug \cdot L^{-1}$ | x | | Various |

Derived measurements use data from multiple sensors and/or are calibrated against discrete measurements. These are as follows:

a) True wind velocity is derived from relative wind and ship velocity.
b) Sample Depth is derived from sample pressure. Both sample and bottom depth values were corrected to Mean Lower Low Water (MLLW) using tide table data.
c) Salinity is derived from conductivity, depth, and temperature.
d) Density is derived from salinity, depth, and temperature.
e) TSS is derived from a calibration of light transmission with discrete TSS measurements.
f) Oxygen saturation is derived from oxygen concentration, salinity, temperature, and depth.
g) Oil in Diesel Fuel Marine Equivalents (DFME) is derived from oil fluorescence calibrated with DFM.
h) Total Polynuclear Aromatic Hydrocarbons (TPAH) is derived from a calibration of oil fluorescence with discrete TPAH measurements.
i) Chlorophyll-*a* is derived from a calibration of chlorophyll fluorescence with discrete Chlorophyll-*a* measurements.
j) Nutrients were measured at discrete stations only.
k) Metals were both measured at discrete stations as well as with an automated trace metal analyzer.

## *MESC Real-Time Analyses*

Though many of the sensors used in the MESC system are common off-the-shelf oceanographic sensors with standard operating procedures, a brief description of each is provided here. The reader is directed to the specific vendors listed for more detailed information. A complete listing of the parameters, sensor type, manufacturer, and measurement accuracy and resolution can be found in Table 3.

**DGPS.** The MESC uses a Trimble Model 4000 RLII transceiver in combination with a Trimble NavBeacon XL receiver to obtain position data. Positions were determined from the satellite-based U.S. Global Positioning System with corrections obtained from the U.S. Coast Guard's local reference station broadcasts (differential system). Ship velocity data were computed internally by the 4000 RLII unit. The DGPS clock was used to set local time at the start of MESC data acquisition while the MESC computer clock maintained time thereafter.

**ADCP.** A RD Instruments Inc., 1.2 MHz DR/SC ADCP was used to acquire current velocity data. The instrument was set up to ping at roughly 6 Hz (36 pings per ensemble) and the ensembles averaged over 10 seconds. Data were collected throughout the entire water column in 1-m bins from 0.4 m to the bottom. The unit is not able to provide data in water shallower than about 4 m. ADCP data were collected using manufacturer-supplied software on a dedicated computer. The system clock was set at the beginning of each survey to match the MESC data acquisition clock to allow data integration.

**CTD.** Conductivity, temperature and sample depth (pressure) were determined using a SeaBird Electronics Model 911 CTD. These sensors were factory-calibrated in 1996. The CTD utilized an *in situ* pump to keep water flowing over the temperature probe and through the conductivity cell at a fixed rate. Salinity was derived from these sensors using the sensor factory calibration coefficients, and algorithms provided by SeaBird which are based on the IEEE (1980). Sample depth, in meters, was also determined using the coefficients supplied by SeaBird and was final corrected to read 1 m at a measured sensor depth of 1 m. Density was derived from the measurements of conductivity, temperature, and pressure using the equations provided by the manufacturer.

**Dissolved Oxygen.** Dissolved oxygen was measured using a Seabird Model 13, polarographic element membrane sensor attached to the Model 911 CTD. The CTD pump was used to maintain a continuous flow of water over the membrane. The sensor was calibrated during each set of surveys using a two-point calibration scale, 0 $mL \cdot L^{-1}$ and 100% saturation, as described in the sensor manual. Oxygen values were computed using the equation given by Owens and Millard (1985). Oxygen saturation was determined by comparing the measured oxygen value with its equilibrium value at the sample's given pressure, temperature, and salinity.

**pH.** The measurement of pH was made with a SeaBird Model 18 pressure-balanced glass-electrode /Ag/AgCl-reference pH probe attached to the Model 911 CTD. The sensor was calibrated during each set of surveys using a three-point calibration curve using buffers of pH 4, 7, and 10, according to the methods described in the sensor manual.

**Transmissometer.** Light transmission was measured using a SeaTech Inc.25 cm pathlength light transmissometer attached to the Model 911 CTD. The sensor emits a collimated light beam at 670 nm, and detects changes in the light transmitted over a 25 cm path, primarily as a result of particle scattering. The sensor was calibrated each survey set using a two-point calibration curve

measuring voltage output as a function of 0 and 100% light transmission in air. The coefficients used to determine light transmission in seawater (percent) were generated using the equations described in the sensor manual. The transmissometer data were intercalibrated with discrete seawater samples analyzed for TSS.

**Fathometer.** Bottom depth was measured using an Innerspace Technology, Inc. Model 445 digital fathometer. The system was set to use a speed of sound of 1536 $m \cdot s^{-1}$ with a surface offset of 0.3 m to accommodate for the depth of the transducer.

**Anemometer.** Wind data were obtained using a Silva Sweden AB/40 anemometer with flux gate compass. The flux gate compass was manually calibrated against the ship's compass at the start of the September surveys. The local magnetic variation was entered into the unit manually. Wind velocity, measured relative to the ship's velocity was corrected to true wind velocity by accounting for the ship's velocity vector.

**Oil Fluorometer.** Oil fluorescence was measured using two independent fluorometer sensors. While the measured parameter is designated as "oil" fluorescence, in fact, any compound present in seawater that fluoresces at the method wavelengths will produce a signal. Previous work by Katz et al. (1991, 1995) suggests that the method can be successfully used to quantify seawater PAH, carcinogenic compounds commonly found in petroleum, creosote, and combustion products. While the term "oil" is used, the method actually measures PAH compounds from a variety of sources.

The two sensors included an on-board flow-through uv-fluorometer (Turner Designs, Model 10AU) and an *in situ* uv-fluorometer (UV Aquatracka by Chelsea Instruments Ltd.) attached to the Model 911 CTD. The on-board fluorometer is considered the primary sensor because it has been used for a much longer time with the MESC and is more easily calibrated. The reason to employ both sensors was to provide independent measures of the same parameter and create a calibration database for future work with the *in situ* sensor. Because both sensors operate similarly, only the flow-through method is described here.

The on-board Model 10AU uses a 254 nm light source to excite seawater passing through a 2.5 cm pathlength quartz cell and measures the fluorescence emission at 300 to 400 nm (peak at 360 nm) as a voltage. The voltage output was calibrated against a diesel fuel marine standard using serial additions in a recirculating loop to allow quantitation against a common US Navy fuel source. The oil fluorometer was also intercalibrated with discrete seawater samples analyzed for PAH.

**Chlorophyll Fluorometer.** The on-board chlorophyll fluorometer was also a Turner Designs Model 10AU. The instrument was used a 340 to 500 nm light source to excite seawater passing through a 2.5 cm pathlength quartz cell and measured the fluorescence emission between 665 and 880 nm (peak at 670 nm) as a voltage. The chlorophyll fluorometer was also intercalibrated with discrete seawater samples analyzed for chlorophyll-*a*.

**TMA.** The TMA is an automated Hg-film, potentiometric stripping analysis method for determining dissolved metals. Approximately 3 mL of water from the MESC's flow-through system was brought into an analysis cell where hydrochloric acid (HCl) , sodium citrate, mercuric chloride were added to aid in the transfer of metal ions to the Hg film. Dissolved metals were plated onto the Hg film using a potential of –1.1 volts for 60 seconds, then stripped off at a constant 2 uA current. Serial additions of a Cu, Pb, and Cd standard were made with each run to quantitate the amount of these metals present in the seawater sample. The nominal sampling

interval for the analysis was 6 minutes. The TMA was run in a real-time continuous mode using proprietary software on an independent computer. This computer was linked to the MESC main acquisition computer to integrate the data with other MESC measurements. Discrete samples were collected for analysis on the TMA in discrete mode. These analyses were used to intercalibrate the TMA data with the metals analyses provided by the contract laboratory.

### *MESC Data Processing*

Primary processing of MESC data was uniform for all survey types. The goal of the primary processing was to produce a calibrated, outlier-free, single matrix data set. Once processed, the data were used to generate a variety of graphical representations for interpretive purposes. Figure 7 shows the overall MESC data processing scheme.

Each day of real-time MESC data was originally stored in a binary file by the data acquisition system (DAS). Each parameter was stored with its specific time stamp. All calibrations and algorithms were applied to the binary file and converted to ASCII format using the DAS. Once converted, the data were imported into Matlab© 5.1 for the primary processing. Here the data were parsed by instrument type into several matrices (time, parameter) based on the time synchronization of the instruments. Because each instrument collects data at slightly different times, all the parameters from a single instrument formed an individual matrix. These data were used to produce time series plots and statistical summaries for data review. Using the time series plots and statistical data as a guide, the instrument data were then subjectively edited for outliers produced by instrument noise, malfunction, or other error. Once the data set was filtered in this manner, final intercalibrations and unit conversions were applied as necessary.

The filtered data for the various instruments were time matched together based on the CTD time to create a single matrix of time and all parameters. DGPS data (latitude and longitude) collected at 2-Hz were matched and linearly interpolated to the 4-Hz rate of the CTD. The remaining parameters were time matched using a nearest neighbor technique providing a match of all data to the nearest ¼ second. Parameter data that had times outside the ¼-second match with the CTD time were replaced with a "NaN" or Not a Number as a text qualifier for that record. The final outcome of these processing steps was a file for each survey day containing a single data matrix of time and all parameters. This file was used for all further processing including statistical evaluations. While these steps proceeded for all 35 measured or derived parameters by MESC, further processing and assessment was focused on the following nine parameters for all surveys:

- Salinity
- Temperature
- Density
- Total Suspended Solids
- Chlorophyll-*a*
- Oxygen
- Oxygen Saturation
- pH
- Oil Fluorescence

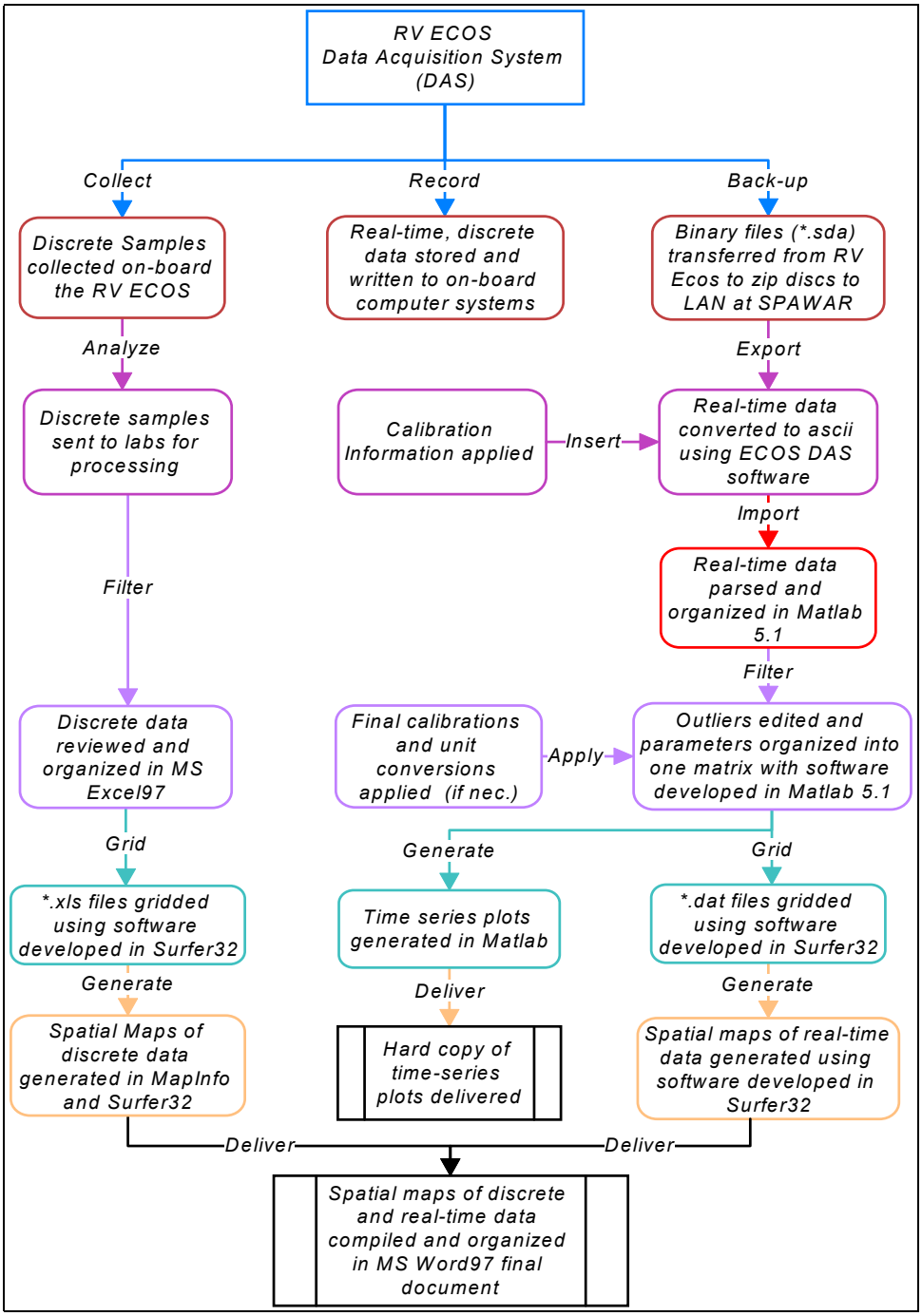


**Figure 7.** Data processing flow chart for real-time and discrete sample data collected for the PSNS Testbed Project.

### *MESC Data Presentation*

The processed MESC data files were used to generate graphical representations of the spatial and temporal distributions. The type of graphical representation used was specific to each type of survey. A description by survey type follows:

**Axial Surveys.** Filtered axial survey data were spatially mapped in Golden Software's Surfer32© using the classed post method. The classed post method uses the latitude, longitude, and parameter to create a spatial track map of the data. The data were color coded by concentration using the full range of data for all three surveys. The concentration-position map was overlayed onto digitized map of the Sinclair Inlet, Dyes Inlet, Port Orchard and Rich Passage survey area. (The digital map was generated by manually digitizing National Oceanic and Atmospheric Administration (NOAA) nautical charts 18452 and 18449). These two layers represented the final graphical presentation of any one of the various parameters recorded on an individual axial survey.

**Surface Mapping Surveys.** Filtered surface mapping data sets were separated into files corresponding to each unique transect recorded during a survey. The primary parameters of each transect were gridded in Surfer32© using the Kriging interpolation method. Each grid had 3 components: latitude, longitude, and parameter (X,Y,Z). The grids were smoothed then blanked. Spatial contour maps of the grids were created in Surfer32© and then overlayed onto a digitized map of the survey area. The contour colors were scaled to fit the full range of all data for each survey time period.

**Cross-section Surveys.** Filtered cross-section survey data sets were separated into files corresponding to each unique transect recorded during a survey. The latitude and longitude were normalized to one common transect and then converted to meters along the standard transect. The primary parameters of each transect were gridded in Surfer32© using the Kriging interpolation method. Each grid had 3 components: distance along transect, sample depth, and parameter (X,Y,Z). The grids were smoothed then blanked. Spatial contour maps of the grids were created in Surfer32© showing the cross section of distance across (x-axis), depth (y-axis) with color used to represent variations in concentration. Contour colors were scaled to fit the full range of all data for each survey time period.

**3-D Surveys.** Filtered 3-D survey data sets were divided up into files for each survey corresponding to data for a specified depth range. The primary parameters of each transect were gridded in Surfer32© using the Kriging interpolation method. Each grid had 3 components: latitude, longitude, and parameter (X,Y,Z). The grids were smoothed then blanked. Spatial contour maps of the grids were created in Surfer32© and then overlayed onto a digitized map of the surrounding survey area. The contour colors were scaled to fit the full range of all data for each survey time period.

**Shoreline Surveys.** Filtered shoreline survey data were spatially mapped in Golden Software's Surfer32© using the classed post method. The classed post method uses the latitude, longitude, and parameter to create a spatial track map of data that is color coded on the basis of concentration. The track map was overlayed onto a digitized map of the survey area. These two layers (in concert) represented the final presentation of any one of the various parameters recorded on an individual shoreline survey.

### *MESC Quality Assurance/Quality Control*

MESC sensors that can be calibrated outside the factory (pH, Oxygen, light transmissometer) were calibrated during each set of surveys using manufacturer's procedures. The calibrations are usually based on a two-point calibration curve with known standards. In addition, the oil fluorometers were calibrated against a diesel fuel marine standard All MESC data are reviewed for quality using visual chronological displays. Spikes were removed subjectively in the absence of corroborating evidence that the data were not real. This was done after reviewing survey logs, and comparing data across parameters to assess the accuracy of the individual measurement. Statistical analyses were sometimes employed to assist in the review though the final decision was usually made subjectively.

**Table 3.** List of MESC sensors, manufacturer and model number, the parameters measured or derived, and the accuracy and resolution of the measurements. Some values do not reflect the manufacturer's specification, but rather, reflect a level that in practice is consistently achievable in the field.

| MESC Sensor | Instrument Manufacturer / Model | Measured or Derived Parameters | Measurement Accuracy | Measurement Resolution |
|---|---|---|---|---|
| **DGPS** | Trimble / 4000 RLII+NavBeacon XL | Local Time | $10^{-6}$s | $10^{-7}$ s |
| | | Latitude | $2{\cdot}10^{-5}$ degrees | $10^{-6}$ degrees |
| | | Longitude | $2{\cdot}10^{-5}$ degrees | $10^{-6}$ degrees |
| | | Ship Velocity | 0.1 m·s$^{-1}$ | 0.01 m·s$^{-1}$ |
| **ADCP** | RD Instruments Inc./ 1.2 MHz DR/SC | Current Velocity (1-m depth bins) | 2 degrees, 0.01 m·s$^{-1}$ | 0.1 degrees, 0.001 m·s$^{-1}$ |
| **CTD** | Seabird Electronics Inc./ SBE 911 | Sample Pressure | 0.1 bars | 0.007 bars |
| | | Sample Depth | 0.02 m (0-100m) | 0.01 m |
| | | Conductivity | 0.0003 siemens·m$^{-1}$ | 0.00004 siemens·m$^{-1}$ |
| | | Temperature | 0.001 °C | 0.0002 °C |
| | | Salinity | 0.01 psu | 0.001 psu |
| | | Density | 0.01 sigma-t | 0.001 Sigma-t |
| **Oxygen** | Seabird Electronics Inc./ SBE 13 | Dissolved Oxygen | 0.01 mL·L$^{-1}$ | 0.01 mL·L$^{-1}$ |
| | Seabird Electronics Inc./ SBE 13 | Oxygen Saturation | 0.1% | 0.01% |
| **pH** | Seabird Electronics Inc./ SBE 18 | PH | 0.1 NBS | 0.01 NBS |
| **Transmissometer** | SeaTech Inc. / 25 cm pathlength | Light Transmission | 0.1 % | 0.02 % |
| **Fathometer** | Innerspace Technology, Inc. / 445 | Bottom Depth | 0.2 m | 0.1 m |
| **Anemometer** | Silva Sweden AB / 40 | Relative Wind Velocity | 5 degrees, 0.5 m·s$^{-1}$ | 0.1 degrees, 0.05 m·s$^{-1}$ |
| | Silva Sweden AB / 40 | True Wind Velocity | 5 degrees, 0.5 m·s$^{-1}$ | 0.1 degrees, 0.05 m·s$^{-1}$ |
| **Oil Fluorometer** | Turner Designs / 10AU | Oil fluorescence (flow-through) | 0.01 volts | 0.002 volts |
| | Turner Designs / 10AU calibrated by SSC San Diego | Oil (DFME) | 0.1 ug·L$^{-1}$ | 0.01 ug·L$^{-1}$ |
| | Chelsea Instruments Ltd./ UV Aquatracka | Oil fluorescence (*in situ*) | 0.01 volts | 0.001 volts |
| **Chlorophyll Fluorometer** | Turner Designs Inc./ 10AU | Chlorophyll fluorescence | 0.01 volts | 0.002 volts |
| **TMA** | SSC San Diego / TMA | Dissolved Metals: Cu, Pb, Cd | 0.1 ug·L$^{-1}$ | 0.01 ug·L$^{-1}$ |

## Discrete Seawater Data

### *Discrete Seawater Sample Collection*

Discrete seawater samples were collected during axial, mapping, and shoreline surveys. The number and exact geographical positions of stations varied from survey to survey though most sites were reoccupied on each visit to provide a comparison over the project timeframe. The sites for the axial were chosen a priori to provide a systematic spatial coverage inside and outside the Inlet. The remainder of the sampling sites was originally chosen "on the fly" to capture variations observed with the real-time sensors, as well as to obtain a reasonably even spatial coverage of the inlet, with some emphasis within pier area of PSNS. A total of 49 sites were occupied on the first visit, and 40 sites were occupied during the following two visits (Table 4).

The MESC's TEFLON® seawater flow-through system (the submersible pump is made of stainless steel and TEFLON®) was used to obtain all discrete seawater samples. Seawater was pumped to the deck into pre-cleaned 2-L glass bottles for PAH, 250 mL polyethylene bottles for metals, 1-L polycarbonate bottles for chl-*a* and TSS, and 40 mL polypropylene, screw-capped centrifuge tubes for nutrients. The PAH bottles were filled to preclude any headspace. Two sets of metal samples were collected, one for outside contract lab analysis and one for discrete measurements on the TMA. All samples were stored in the dark at <10º C until analysis. PAH and metal samples were shipped on ice to contract laboratories by overnight mail to ensure meeting holding time requirements, which is 2 days for metals, and 7 days for PAH. Nutrient, chl-*a*, and TSS samples were frozen until analyzed at the end of each visit. Table 4 lists the type and number of discrete samples taken and analyzed on each visit.

### *Discrete Effluent Sample Collection*

During the September visit, discrete effluent samples were obtained shoreside from the two local POTWs. However, only the PAH sample taken at the Bremerton POTW was analyzed because the other samples were lost in transit to the analytical laboratory. During the March and July visits, discrete samples were obtained from the effluent stream of the two POTWs and from the outflow of Gorst and Blackjack Creek. In July, samples were additionally collected from the outflow of Ross Creek. The creek samples were collected using the same sample container types described above by placing the neck of each bottle under the surface of the water until it filled to the appropriate level. At the POTW, sample bottles were filled using a sampling port direct from the effluent outflow. The effluent samples were analyzed for the same parameters as those measured in the marine waters taken during the MESC surveys. The samples analyzed from the POTWs and creeks are included in the sample count shown in Table 4.

**Table 4.** Number and type of discrete seawater samples analyzed on this project. The numbers include effluent samples taken from the POTWs and creeks.

| Discrete Sample Analysis | Visit 1 September 1997 | Visit 2 March 1998 | Visit 3 July 1998 | Total for 3 Visits |
|---|---|---|---|---|
| Total Sites Sampled | 49 | 40 | 40 | 129 |
| Chl-*a* | 17 | 16 | 23 | 56 |
| TSS | 18 | 17 | 21 | 56 |
| Nutrients | 0 | 40 | 38 | 78 |
| PAH | 13 | 24 | 21 | 58 |
| Dissolved Metals | 38 | 40 | 37 | 115 |
| Total Metals | 3 | 10 | 11 | 24 |

### *Discrete Sample Chemical Analyses*

**Polynuclear Aromatic Hydrocarbons.** PAH samples were analyzed using the National Oceanic and Atmospheric Administration's Status and Trends version of the Environmental Protection Agency (EPA) Method 8270M, SIM by A.D. Little in Cambridge MA on the first two surveys, and by Battelle Ocean Sciences, Duxbury, MA on the third survey. Upon arrival, samples were acidified to pH 2.0 with 6N HCl, spiked with PAH surrogates, then solvent extracted in dichloromethane using a method similar to EPA Method 3510, Separatory Funnel Liquid-Liquid Extraction. The extracts were dried using sodium sulfate and concentrated to approximately 1 mL using Kuderna-Danish concentrators followed by nitrogen evaporation.

The concentrated samples were analyzed by Gas-Chromatography-Mass-Spectrometry run in Single Ion Mode. Up to 53 individual PAH analytes, including alkylated homologs, were each quantified with method detection limits better than 12 $ng \cdot L^{-1}$ for all analytes. Quality Assurance/Quality Control analyses showed matrix spike recoveries ranged between 44 and 116%, and averaged 80% for all surrogates. Checks made against standard reference oils showed individual analytes were within 29% of targeted values and averaged about 7%. A more complete description of the methods used and analytical results are included in Appendix A.

**Metals.** Dissolved and total metal samples were analyzed using EPA Method 1640 by Battelle Marine Sciences Laboratory in Sequim, WA. Upon arrival at Battelle's laboratory, the samples analyzed for dissolved metals were filtered through a 0.45-µm capsule filter, then acidified with 10% nitric acid (HNO3) to bring the sample to a pH <2. Samples analyzed for total metals were acidified without filtration. The samples were then preconcentrated by tetrahydroborate reductive precipitation (Nakashima et al., 1988) and determined by Inductively Coupled Plasma-Mass Spectrometery. Effluent samples were not preconcentrated prior to the analysis step.

The method detection limit for these analyses was nominally 0.1 $ug \cdot L^{-1}$, though it ranged from 0.005 $ug \cdot L^{-1}$ for Ag, to 0.3 for Se. Quality Assurance/Quality Control analysis results showed that for all analytes, blanks were less than 0.4 $ug \cdot L^{-1}$ and replicates averaged less than 17%. Matrix spike recoveries averaged about 91%, and comparisons to Standard Seawater Reference Materials averaged less than a 17% difference for all analytes. A more complete description of the methods used and analytical results are included in Appendix B.

**TSS and Chl-*a*.** Samples collected for TSS were analyzed by filtering approximately 900 mL through pre-dried and pre-weighed glass-fiber filters (1.2 um nominal pore size). The filters were rinsed with deionized water to remove dissolved salts, then dried and weighed to determine the

mass of the filtered solids. Samples collected for chl-*a* were analyzed using standard techniques described in ASTM, 1995. Seawater was filtered through microfiber filters and the filtrate extracted in 90% acetone. The solution was analyzed in triplicate on a Turner Designs Model 10 fluorometer that was calibrated against a standard chl-*a* reference standard. The sample was analyzed before and after acidification with HCl to account for pheophytin interference.

**Nutrients.** Nutrient analyses ($NO_3$, $NO_2$, $NH_3$, $PO_4$, $SiO_2$) were performed on an ODF-modified 4-channel Technicon AutoAnalyzer II or a Skalar SanPlus Autoanalyzer by Scripps Institute of Oceanography. Samples received frozen, were brought to room temperature prior to analysis. Silicate was analyzed using the technique of Armstrong (1967), which uses ammonium molybdate and stannous chloride to form a blue compound, which is then quantified on a colorimeter relative to a standard curve. A modification of the Armstrong (1967) procedure was used for the analysis of nitrate and nitrite. Nitrite was analyzed for the red azo dye it forms by reaction with sulfanilamide and N-(1-naphthyl)ethylenediamine dihydrochloride. Nitrate was also determined in this way after it was first reduced to nitrite by a cadmium reduction column. Phosphate was analyzed using a modification of the Bernhardt and Wilhelms Technique (1967), which uses ammonium molybdate and dihydrazine sulfate to produce a blue compound, which is quantified on a colorimeter against know standards. Ammonium is analyzed via the Berthelot reaction in which hypochlorous acid and phenol react with ammonium in an alkaline solution to form indophenol blue, which is then quantified colorimetrically. All samples were run in duplicate.

### *Discrete Data Processing/Presentation*

Discrete sample analytical data were obtained from the various laboratories and compiled into a single Microsoft Excel® spreadsheet file along with the associate MESC real-time data. The data were organized by survey and geographic position. The data file was used for all statistical evaluations. For the purposes of graphical presentation, all data from a single survey were pooled together and gridded in Surfer32© using the Kriging interpolation method. Each grid had 3 components: latitude, longitude, and discrete parameter concentration (X,Y,Z). The grids were smoothed, then blanked. Spatial contour maps of the grids were created in Surfer32© and then overlayed onto a digitized map of the survey area. The contour colors were scaled to fit the full range of all data for each survey time period.

## MESC and Discrete Data Intercalibrations

Real-time sensor data are typically intercalibrated with discrete sample measurement data to derive absolute calibration or to provide correlation data that can be used to enhance the spatial resolution of the more limited, more costly, and time consuming traditional analyses. This is usually done for the real-time chl-*a* fluorescence, uv-fluorescence, light transmissometer, and the TMA. The real-time data from these sensors are averaged for each discrete sample collection time period and compared with the values derived from laboratory analyses. However, on these surveys, exceptionally low dissolved metal and TPAH concentrations precluded meaningful relationships between the real-time data and samples analyzed in the laboratory. As a result, TPAH and metal data were derived only from the discrete sampling performed with MESC.

In the case of chl-*a*, discrete samples analyzed with traditional laboratory methods provided an absolute calibration for the real-time flow-through fluorometer. Calibrations were based on a regression equation generated for each set of surveys. During the first set of surveys the presence of a red tide required the use of two regression equations, one in the range of 0 to 9 $ug \cdot L^{-1}$ Chl-*a*,

and a second for data values above 9 ug·L$^{-1}$ Chl-*a*. For all survey sets, the regression equations had $r^2$ values that ranged from 0.72 to 0.99. An example of the regression for the first visit is shown in Figure 8.

Discrete samples analyzed for TSS data were used to develop a regression equation between TSS and light transmission data. A database developed over the past five years has shown these two variables are well correlated using an exponential regression equation, as predicted by scattering theory. For all survey sets, the $r^2$ of the exponential regression line ranged from 0.76 to 0.82. An example of the regression for the second visit is shown in Figure 9.

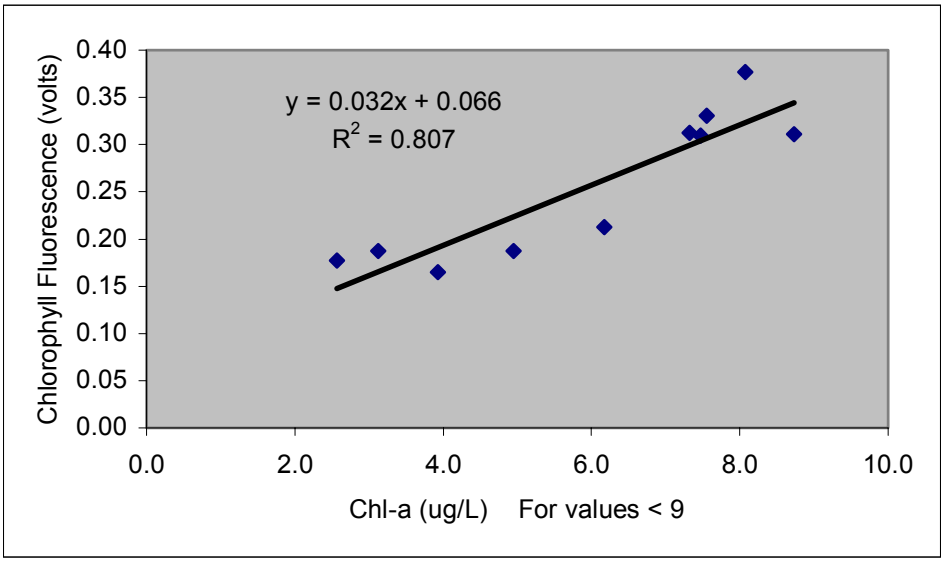


**Figure 8.** Regression of real-time chlorophyll fluorometer voltage with discrete chl-*a* analyses for the September set of surveys. A separate regression equation (not shown) was generated for values greater than 9 ug·L$^{-1}$ to better calibrate for red tide conditions.

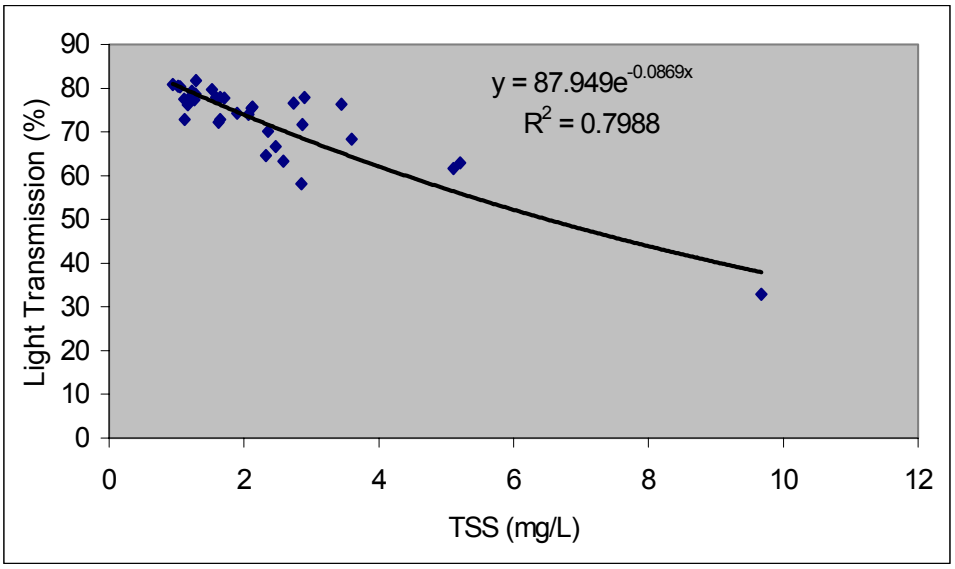


**Figure 9.** Regression of real-time light transmission data with discrete analyses of TSS for the September set of surveys. The log-linear relationship is predicted by scattering theory.

# 5.0 RESULTS

Excluding the ADCP data, over 36 million data points were collected with MESC during this project. Given this large volume of data and the requirement for color visualization, the complete set of survey results is included separately on the accompanying CD in both RTF and Word 7.0 format. In this section, only representative data plots will be shown to describe the observed conditions. Climate, circulation, hydrography, conventional water quality parameters, and contaminant data are described separately. Spatial variations, both horizontal and vertical, are described first in each section, followed by a description of temporal variations including tidal and seasonal trends, and a discussion of sources and processes.

## Climatological Conditions

The survey monitoring periods were designed to capture wet and dry weather conditions. The September monitoring period was scheduled to capture a time period when weather conditions around the inlet were relatively stable and dry for a reasonable amount of time. Conversely, the March monitoring period was scheduled to capture a time period after a relatively consistent period of winter rains. However, a period of winter-like storms brought considerable rain and high winds just prior to the start of the September survey period after a couple of months of relatively low rainfall (Figure 10). The rains continued on into the first survey day (PS01) before they gave way to sunny, hot, and generally calm conditions for the following eight days. Rain again occurred during the last two days of work (PS08 and PS09). The effect of these transitional weather conditions and the episodic inflow of storm water were evident on individual surveys.

The March surveys successfully captured a time period in which the inlet had seen relatively high and continuous rainfall. Though it did not rain hard or continuously during the monitoring period, the wet weather leading up to the surveys (Figure 10) met the goal of capturing the effects of long term storm water inflows on the inlet. A third monitoring period in July 1998 was added to try and capture a more consistent dry weather condition. It can be seen from the rainfall chart

(Figure 10) that this condition was met on the third set of surveys. Light drizzle of about 0.13" occurred the day before the third set of surveys began, but otherwise conditions were dry.

Wind conditions measured with MESC were generally low and averaged 7 kts for all surveys. Daily averages ranged from about 3 kts to 16 kts, both of which occurred during the September set of surveys. The highest winds occurred on PS08 during one of the rainstorms. No significant differences in average wind speeds were measured seasonally. Directions varied seasonally but were mostly from the south-southeast. The directions measured by MESC were more easterly than reported in URS, 1996. Though the differences might be real year-to-year variations, they may also be a result of differences in the height of the measurements.

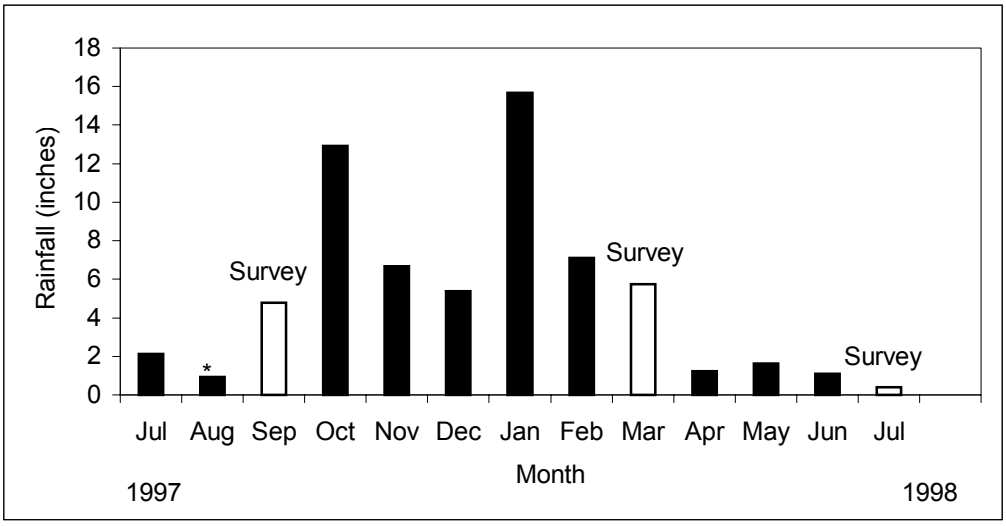


**Figure 10.** Rainfall measured at the Bremerton Airport during the project timeframe. The value shown for August 1997 (*) was missing in the data set and was estimated from measurements made at Seattle using an average rainfall ratio for the two locations.

## Circulation

Understanding circulation of the inlet is critical in assessing the distribution, fate, and transport of contaminants in the inlet. Previous studies of the inlet suggest that currents are tidally dominated though wind may possibly be important in some regions (Albertson et al., 1995). The semidiurnal tides produce two but unequal high and low tides daily with an average amplitude of 3.3 m (Lavelle et al., 1988, Micronautics Inc.). Maximum currents of about 10 to 15 $cm \cdot s^{-1}$ were measured at selected sites inside the inlet and over 100 $cm \cdot s^{-1}$ was measured outside Port Washington Narrows (Lincoln and Collias, 1975). Typical currents measured at three moored current meter sites USGS were between 5 and 10 $cm \cdot s^{-1}$. According to Tetra-Tech (1988) the circulation is typical of a two-layer estuarine system with cold saltier water moving in at the bottom replacing warmer less salty water at the surface. While these studies captured some important aspects of the circulation, the data collected in this study provide the most comprehensive spatial and temporal views of the circulation available. A thorough description of the circulation is presented in a separate report on hydrodynamic modeling.

The most interesting as well as most important aspect of the circulation derived from the current data set is that the inlet is dominated by a complex gyral circulation pattern at its mouth. This gyre results from interaction with the strong tidal flow out of the Port Washington Narrows

(Figure 1). The higher flows are coincident with the deeper bathymetry of this region outside the inlet (Figure 6). At the transition from ebb to flood tide, a clockwise (CW) gyre forms at the mouth with an intertwined counterclockwise (CCW) gyre forming immediately to the west (Figure 11). As the flood tide progresses, the gyres break down and current flow is uniformly into the inlet except at the most northeastern part of the mouth where water is entrained into the water flooding into the Port Washington Narrows and continues to move out of the inlet (Figure 12). This small outflow continues throughout the entire flood tide condition. As the ebb tide begins, the current flow starts out more or less uniformly out of the inlet, increasing through the peak of ebb tide (Figure 13). Near the end of the ebb tide, the gyres at the mouth reform and the cycle repeats (Figure 14). It should be noted that a lag time of about two hours between the phase of the tide and the current flow was observed during these surveys at the mouth of the inlet and may have been longer at the head.

Inside the inlet current speeds are considerably reduced from those at the mouth which reach in excess of 150 $cm \cdot s^{-1}$. The flow reduction can be attributed to higher bottom friction caused by decreasing water depths toward the head. At the start of flood tide flow direction inside the inlet is somewhat random with speeds ranging from 2 to about 10 $cm \cdot s^{-1}$. As the flood tide progresses, current direction becomes highly uniform into the inlet and current speeds along the centerline of the axis below the shipyard progressively increase to a maximum of about 20 $cm \cdot s^{-1}$ at the peak of ebb tide. The reverse occurs on the ensuing ebb tide though current speeds were slightly lower at about 15 $cm \cdot s^{-1}$.

This tidally induced circulation pattern enhances flushing along the eastern end of the shipyard affecting both the distribution and mass transport of dissolved and suspended constituents. The higher magnitude flows at the mouth and the continuous outflow along the northeastern shore serve to mix water more effectively than would occur without this flow pattern. The lower current speeds toward the head of the inlet lead to weaker mixing and longer flushing times relative to the outer part of the inlet. This is particularly true for flows along the shorelines. The longer flushing times inside the inlet potentially lead to larger impacts from fresh water and contaminant loading.

While the current plots shown represent vertically averaged values, variations from surface to bottom were observed and sometimes showed flows in opposite directions. Example cross-sections at the mouth of the inlet (Figure 15) show how the gyral circulation produces strong lateral gradients as well as vertical variations. The vertical variations in flow result from variations in the density distribution and effects of bottom friction. This complicated flow pattern must be addressed when considering flushing as is done later in this report.

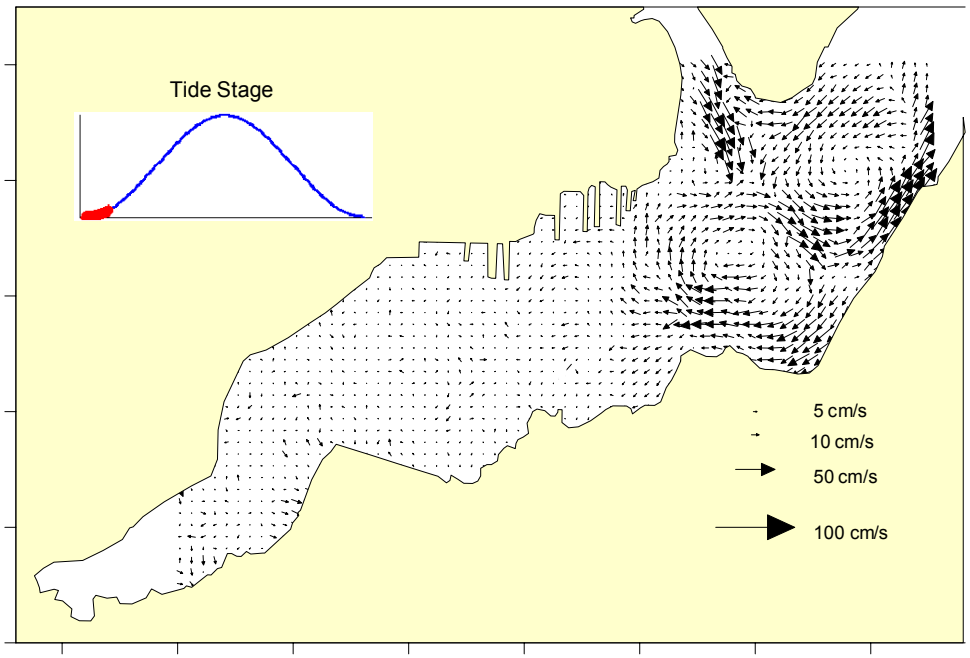


**Figure 11.** Vertically averaged current velocity at the start of flood tide. Data were pooled from all surveys for the same stage of the tide.

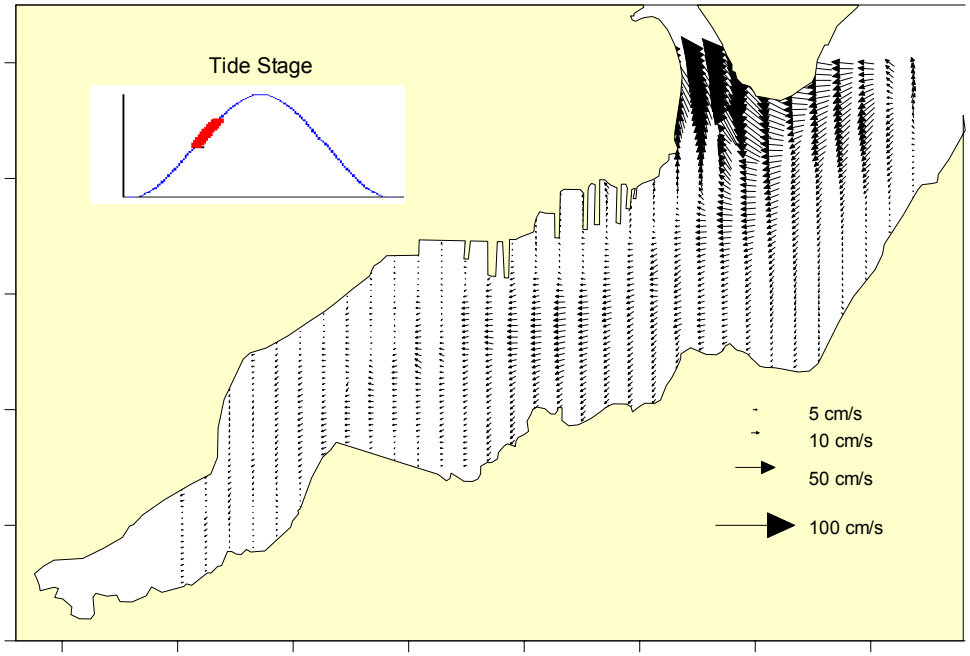


**Figure 12.** Vertically averaged current velocity during flood tide. Data were pooled from all surveys for the same stage of the tide.

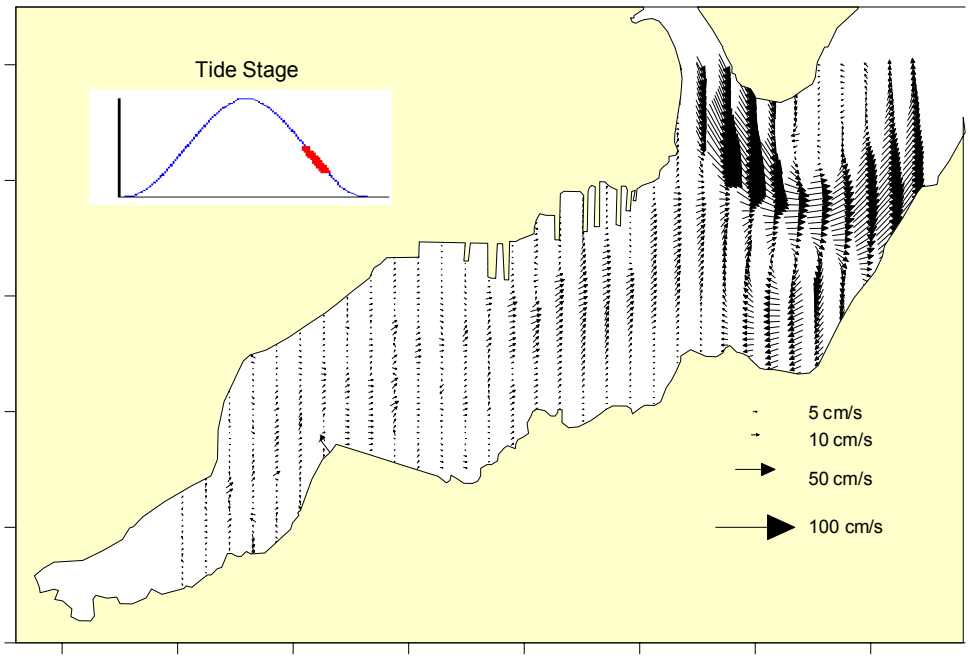


**Figure 13.** Vertically averaged current velocity during ebb tide. Data were pooled from all surveys for the same stage of the tide.

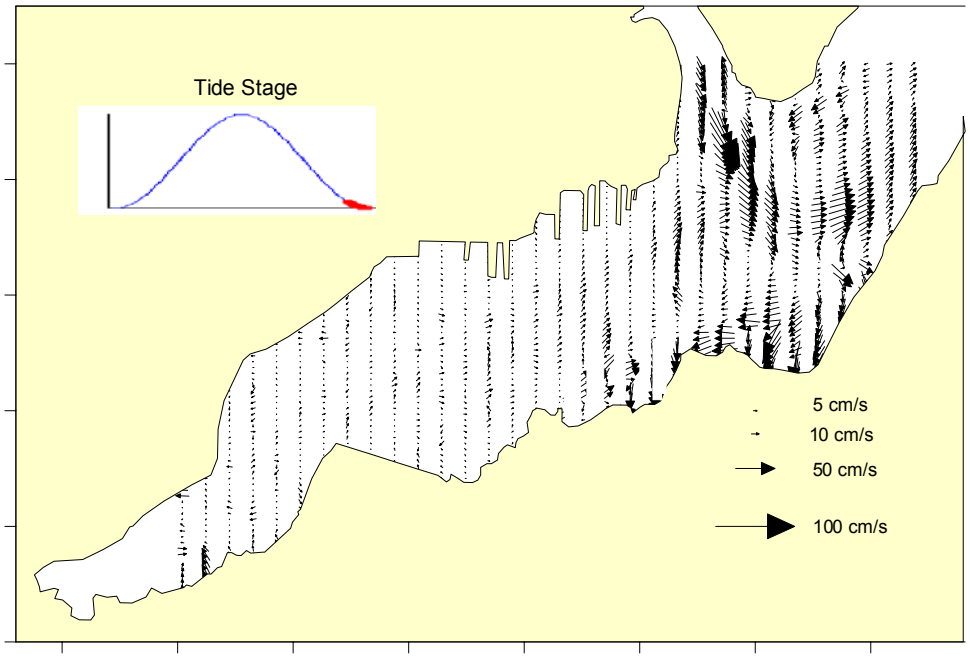


**Figure 14.** Vertically averaged current velocity at the end of ebb tide. Data were pooled from all surveys for the same stage of the tide.

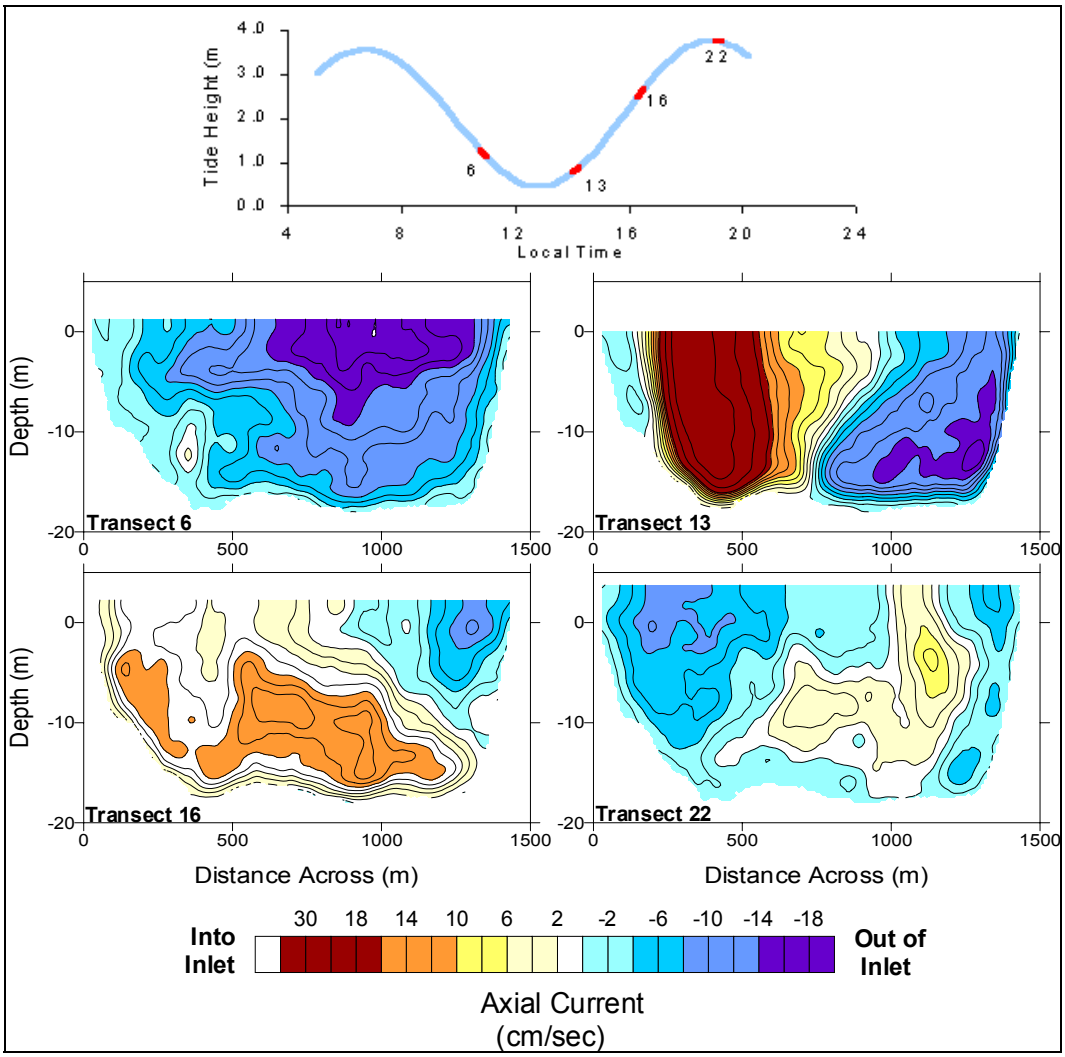


**Figure 15.** Cross-sections of axial current speed ($cm \cdot s^{-1}$) at the mouth of Sinclair Inlet made 18 and 19 September 1997, PS02.

## Hydrographic Conditions

An understanding of the general hydrography, or seawater temperature, salinity, and density of the inlet, is important in assessing the processes that control contaminant distributions, mixing, and transport. In particular, the distribution of salinity provides a tool to quantitatively assess the magnitude and extent of conservative mixing, which in this context, refers to conservation of mass. In this way, the hydrographic data provide a first order approximation of mixing for all water borne constituents. In addition to conservative mixing however, dissolved and suspended contaminants can be altered by non-conservative processes such as sinking, air-sea exchange, and biological modification, to name a few. These processes are much more difficult to quantify but can be at least be assessed qualitatively by looking at the individual parameter distributions. Comparison of the individual distributions relative to the hydrography provides a way to assess the relative importance of the controlling processes.

### *Spatial Variations*

Salinity, temperature, and density data are summarized in Table 5 and Table 6. Table 5 lists the mean, minimum, maximum, range, and number of data points for each time period for measurements made inside the inlet only. These were summarized from the surface mapping and 3-D surveys performed each time period. The summary statistics listed in Table 6 are representative for measurements made regionally using data from axial surveys performed each time period. Summary statistics for each survey can be found in Appendix C.

Salinity and temperature data summarized in the tables were typically lower than comparable data collected in 1992 by Albertson et al., 1995. Salinity minimum/maximum values were lower by 0.5 to nearly 2 psu. Temperature values were lower by as much as 2 °C in September but higher by about the same amount in July. Average density values were higher by about 0.5 sigma-t. These variations are reasonable given the limited areal extent of the 1992 data and expected year-to-year climatological variations.

Salinity generally decreased axially into the inlet while temperature showed the opposite distribution and increased into the inlet. Axial changes in salinity of up to 2 psu and temperature up to 5 °C were observed, depending on season. The density distribution mirrored that of salinity with variations of about 2 sigma-t from mouth to head. All three parameters also showed a lateral, or cross-channel gradient as well (Figure 16 and Figure 17). While the axial gradient was persistent and seen on nearly all occasions, the lateral gradient varied with tidal condition. The general decrease of salinity and density into the inlet was a result of warm freshwater inflow, primarily from Gorst Creek and the Bremerton POTW. While creek inflow is low and variable (Albertson et al., 1995), there is a year-round freshwater flow into the inlet from both sources. The gradient of salinity generates an inflow of higher salinity water from outside the inlet to maintain salt balance. The vertical distribution of salinity suggests that higher salinity water moves in along the bottom from outside the inlet while fresher water moves out at the surface (Figure 18). This is a typical two-layer estuarine circulation pattern as mentioned previously. The source of the higher salinity water comes primarily from Rich Passage, which is derived from Puget Sound surface water (Ridley and Ostericher, 1960) though the jet flow out of Dyes Inlet appears to mix in at the mouth.

The strength of the axial gradient was strongest in the inner portion of the inlet. This results from a combination of reduced circulation and proximity to sources, particularly the discharge from the Bremerton POTW along the north shore. Towards the mouth, the gyral circulation and freshwater discharge from Dyes Inlet help to develop the lateral gradient. Freshwater inputs from Blackjack Creek and the Port Orchard POTW likely play a role in this as well. The gradient continues, though lessens into the adjacent waters of Rich Passage, Port Orchard Channel, and on up into Dyes Inlet were warmer freshwater sources there alter the distribution (Figure 19). While the magnitude of the gradient varied for each of the three monitoring periods, there was always a general increase of salinity and density from inside to outside the inlet with maximum surface values occurring in Rich Passage. The opposite was true for temperature.

The inlet was vertically stratified in salinity, temperature, and density (Figure 20) throughout most of the inlet on all occasions. Vertical variations in these parameters were typically about 25% of the axial variation, i.e. about 0.5 psu, 1 °C, and 0.5 sigma-t, respectively, but varied with season. Stratification, which inhibits vertical mixing, develops from combination of the two-layer circulation pattern and relatively low flow conditions. Freshwater inflow, particularly in winter and solar heating particularly in summer produce a low density surface layer that is maintained by low flow conditions. These conditions, characteristic of a partially stratified

estuary as defined by Bowden, 1966 (in Kjerfve, 1978), can lead to reduced dilution of contaminants introduced into surface waters such as those derived from storm water. Outside the inlet, stratification was reduced as a result of higher flows and mixing. Based on the vertical profile data collected during the axial surveys, the waters of Rich Passage were vertically homogeneous in salinity on all occasions, as were those in the constricted high-flow region of the Port Washington Narrows. In these regions contaminant dilution would be enhanced.

**Table 5.** Summary statistics for salinity, temperature, and density for each survey period. The data, summarized from surface mapping and 3-D surveys, are representative of values for inside Sinclair Inlet only.

| Inside Inlet Only | | Salinity (psu) | Temperature (deg C) | Density (sigma-t) |
|---|---|---|---|---|
| **September** | Mean | 28.94 | 14.62 | 21.38 |
| | Min | 27.57 | 13.29 | 20.01 |
| | Max | 29.43 | 16.65 | 22.01 |
| | Range | 1.86 | 3.36 | 2.00 |
| | n | 191211 | 191591 | 191214 |
| **March** | Mean | 27.85 | 9.32 | 21.48 |
| | Min | 26.32 | 8.98 | 20.15 |
| | Max | 28.35 | 10.93 | 21.91 |
| | Range | 2.03 | 1.96 | 1.76 |
| | n | 152585 | 152636 | 152124 |
| **July** | Mean | 28.90 | 15.48 | 21.17 |
| | Min | 28.08 | 13.46 | 19.87 |
| | Max | 29.19 | 18.82 | 21.80 |
| | Range | 1.11 | 5.36 | 1.94 |
| | n | 307531 | 307671 | 307534 |

**Table 6.** Summary statistics for salinity, temperature, and density for each survey period. The data represent regional values summarized from axial surveys.

| Regional Data | | Salinity (psu) | Temperature (deg C) | Density (sigma-t) |
|---|---|---|---|---|
| **September** | Mean | 29.10 | 13.99 | 21.64 |
| | Min | 27.41 | 13.08 | 20.03 |
| | Max | 29.43 | 15.48 | 22.07 |
| | Range | 2.02 | 2.40 | 2.04 |
| | n | 68491 | 68491 | 68491 |
| **March** | Mean | 28.09 | 9.03 | 21.71 |
| | Min | 26.70 | 8.84 | 20.55 |
| | Max | 28.84 | 10.43 | 22.30 |
| | Range | 2.13 | 1.59 | 1.74 |
| | n | 88681 | 88689 | 88681 |
| **July** | Mean | 29.01 | 14.38 | 21.48 |
| | Min | 28.59 | 11.98 | 20.54 |
| | Max | 29.37 | 17.73 | 22.23 |
| | Range | 0.78 | 5.76 | 1.68 |
| | n | 74522 | 74535 | 74510 |

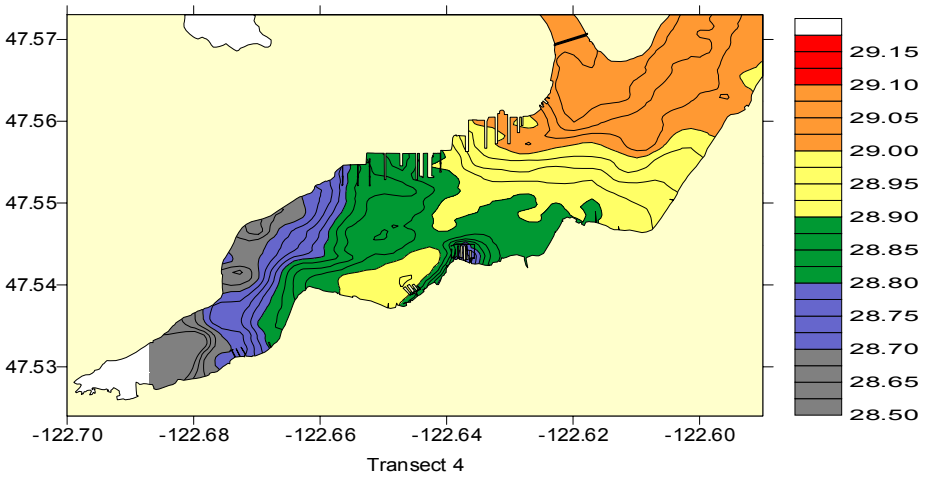


**Figure 16.** Surface salinity (psu) distribution measured on 17July 1998, PS17, Transect 4, Ebb tide.

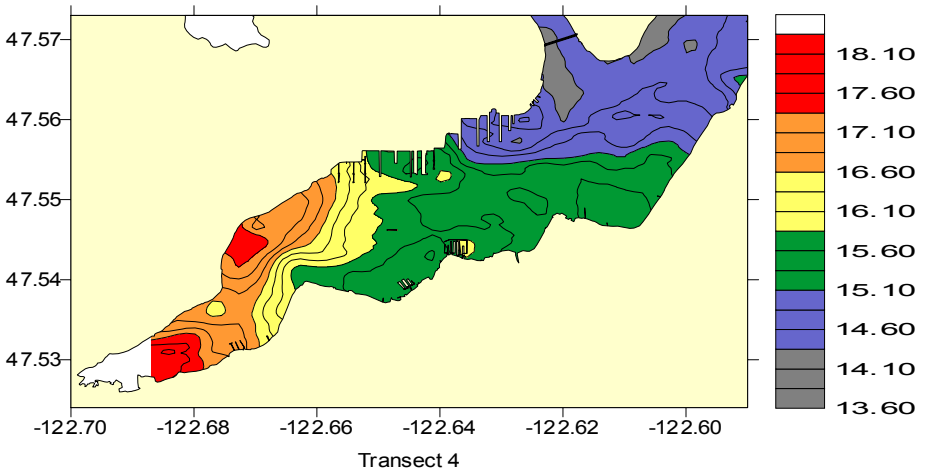


**Figure 17.** Surface temperature (° C) distribution measured on 17July 1998, PS17, Transect 4, Ebb tide.

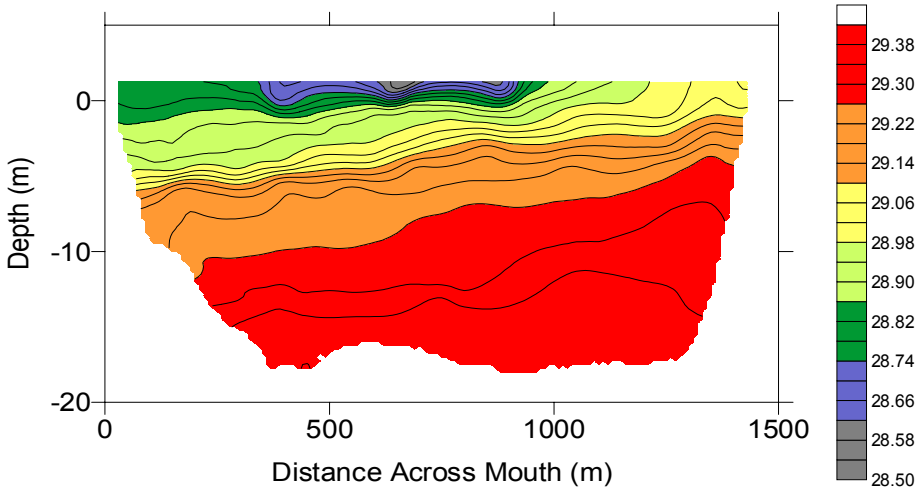


**Figure 18.** Cross-section of salinity (psu) at the mouth of Sinclair Inlet measured on 18 September 1998, PS02, Transect 6.

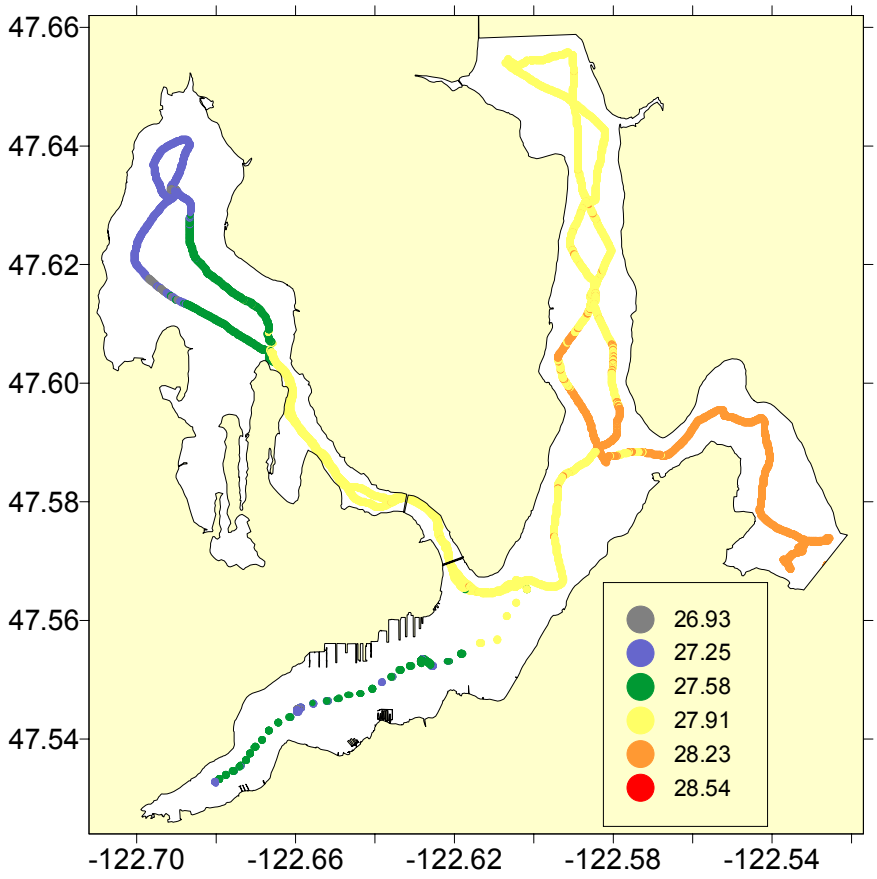


**Figure 19.** Axial surface salinity (psu) distribution measured on 11 March 1998 (PS10). The sparse nature of the data inside the inlet results from collecting tow-yo data.

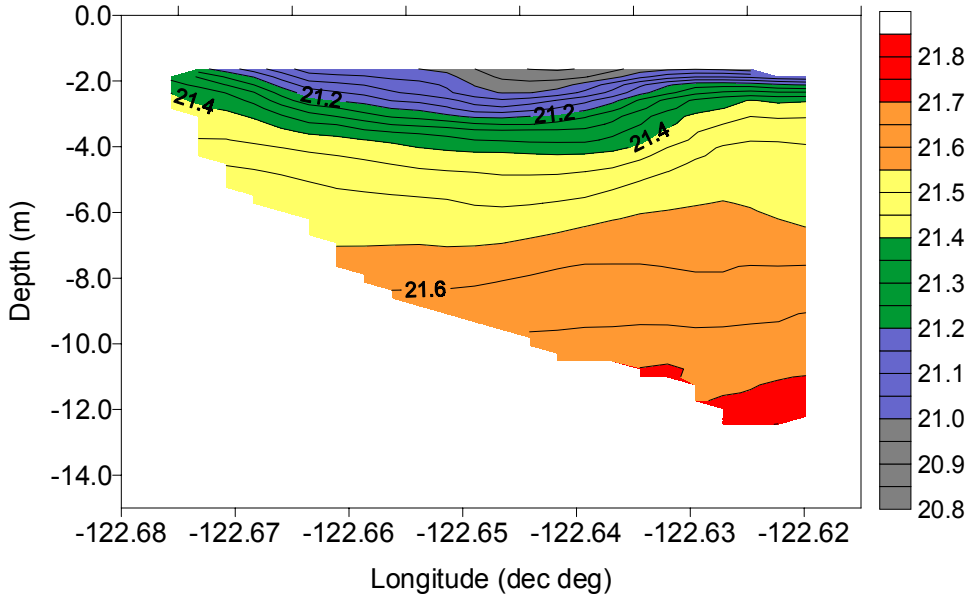


**Figure 20.** Density cross-section along the axis of Sinclair Inlet, plotted as a function of longitude for 16 July 1998 (PS16). The section was derived from the axial tow-yo data.

## *Temporal Variations*

***Tidal Variations.*** Tidal flow is the dominant process for short-term fluctuations in the spatial distribution and mixing of seawater constituents in the inlet. These variations can best be seen from the spatial distribution plots generated from the surface mapping surveys, particularly those shown for 17 to 18 July when measurements were made over a complete tidal cycle (Figure 21). Figure 22 shows relatively high salinity water pushing into the inlet over a 6 hr flood period (transects 1 to 3) mostly along the northern shore and forming a cross-axis gradient. Water found at the mouth at the start of the tide was pushed in to roughly the mid-point of the Shipyard piers, a distance of about 2000-m. During the subsequent ebb tide (transects 3 to 5), fresher water from the back of the inlet mixed back out toward the mouth, again, primarily along the northern shore, and thus reversing the cross-axis gradient. During this ebb, lower salinity water that started out at the midpoint of the shipyard piers was observed at the eastern end of the shipyard.

During the next flood to higher-high water and ebb to lower-low water, the pattern was repeated, though the ebb excursion was even greater. On flood, higher salinity water pushed along the northern shore all the way to the western end of the shipyard piers (transect 8). On the following ebb the push of low salinity can be seen out to the mouth along the northern shore, an excursion of about 2800-m. Lower salinity water that had formed along the south shore was also mixed out past the mouth. This ebb is slightly different from the preceding one in that a complex pattern in the cross-axis gradient forms with a high to low salinity gradient forming in the eastern half of the inlet and the reverse forming in the western half. This condition is similar to that observed at the start of the survey, except that the lowest salinity water has pooled up in mid-inlet. This pooling was also observed in the axial cross-section shown in Figure 20 that was generated for data collected during a similar tidal condition. The low salinity water appears to have been derived from a combination of inflows from the Bremerton POTW and Gorst Creek.

The short-term spatial variations observed in the salinity distribution can be explained primarily by the tidal circulation. The apparent excursion of salinity observed during the mapping survey transects requires an average surface current flow of approximately 9 to 13 $cm \cdot s^{-1}$ for each phase of the tide. The average surface current velocity in the top four meters inside the inlet during this survey was 11 $cm \cdot s^{-1}$, easily accounting for the necessary magnitude of flow required. In this way, freshwater introduced at the head of the inlet is dispersed toward the mouth on each ebb flow, mixing both axially and laterally. Though not measured, it is expected that during periods of very high freshwater inflow that an advective flow of freshwater could add to the tidal dispersion.

***Seasonal Variations.*** Year-to-year variations in hydrography were already noted when the current data set was compared to the 1992 data set of Albertson et al. (1995). Seasonal changes were also evident in both data. Salinity and temperature both generally decreased from September to March and then increased again into July as were shown in Table 5 and Table 6. The reverse was true for density. The seasonal variations observed were about 1 psu in salinity, 5 °C in temperature, and 0.2 sigma-t in density. The variations were about the same for measurements made both inside the inlet as well as regionally suggesting that the inlet was in steady state with its adjacent waters. This is expected for the generally moderate climatological conditions typical of the Puget Sound region, particularly those occurring during the measurement period.

While seasonal variations produced an overall change in hydrographic values in the inlet, the spatial distribution and short-term variations already discussed were present throughout the year. However, the degree of variation changed with season. The along axis gradient in salinity was considerably higher in March as a response to the higher freshwater inflow. One quantitative measure of this was to compare average levels calculated for each of the five regions shown in Figure 24 and summarized in Table 7. The salinity difference between Rich Passage and the head of the inlet in September and July was about 0.4 psu while the difference in March was nearly double at 0.7 psu. The opposite condition was true for the axial temperature gradient that was a minimum in March (0.5 °C), maximum in July (2.8 °C), and intermediate in September (1 °C). The impact of changing salinity and temperature on the density distribution was evident here with salinity dominating the density changes in March and temperature dominating in July. Seasonal variations in hydrography were of similar magnitude for the regions outside the inlet.

As mentioned previously, seasonal variations were also evident in the vertical distributions. Based on tow-yo data collected in the inlet, the typical variation from surface to depth was maximum for salinity (0.5 psu) and minimum for temperature (0.5 °C) in March (Table 8). The opposite was true in July. However, the interplay of salinity and temperature on the density distribution results in reasonably constant density stratification for all three time periods. While salinity variation dominates the density distribution in March, temperature dominates the density stratification in July and September. Of course the relative strengths vary spatially with proximity to fresh water sources and shallow regions where solar heating is most effective. The consistency in stratification suggests that the observed estuarine circulation and mixing conditions are a long-term characteristic of the inlet.

As discussed previously, regions outside the inlet subject to higher tidal flow conditions such as Rich Passage and the Port Washington Narrows were vertically well mixed on all occasions. However, seasonal changes were evident in the Port Orchard Passage and in Dyes Inlet. In both locations the effects of temperature dominate and create a higher degree of density stratification in July than in March (no measurements were made in September). While vertically well-mixed in March, the waters of Port Orchard Passage became stratified to a slightly lower level that

observed in the inlet. Stratification in Dyes Inlet was slightly greater than that of the inlet, by about 0.2 sigma-t units, for both time periods.

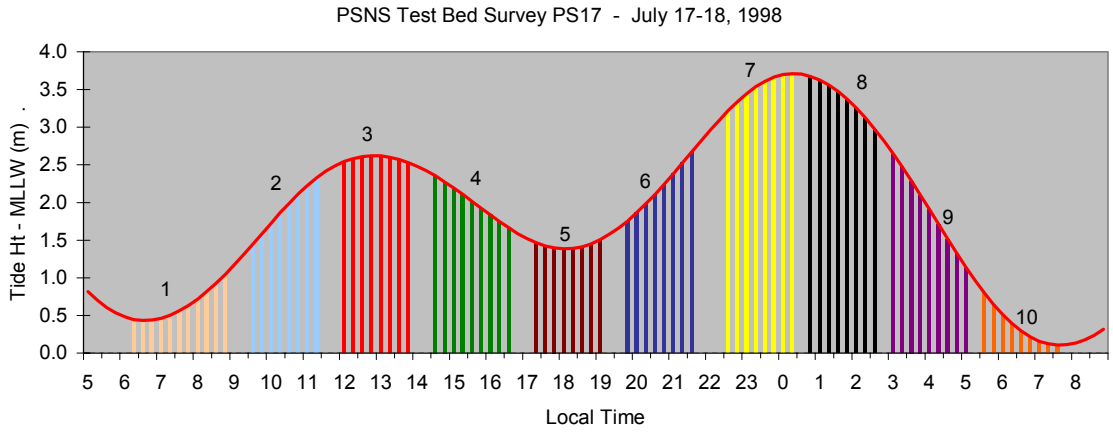


**Figure 21.** Plot of tidal amplitude during PS17 Survey on 17 and 18 July 1998. The numbered segments refer to individual full-inlet transects completed through the tide.

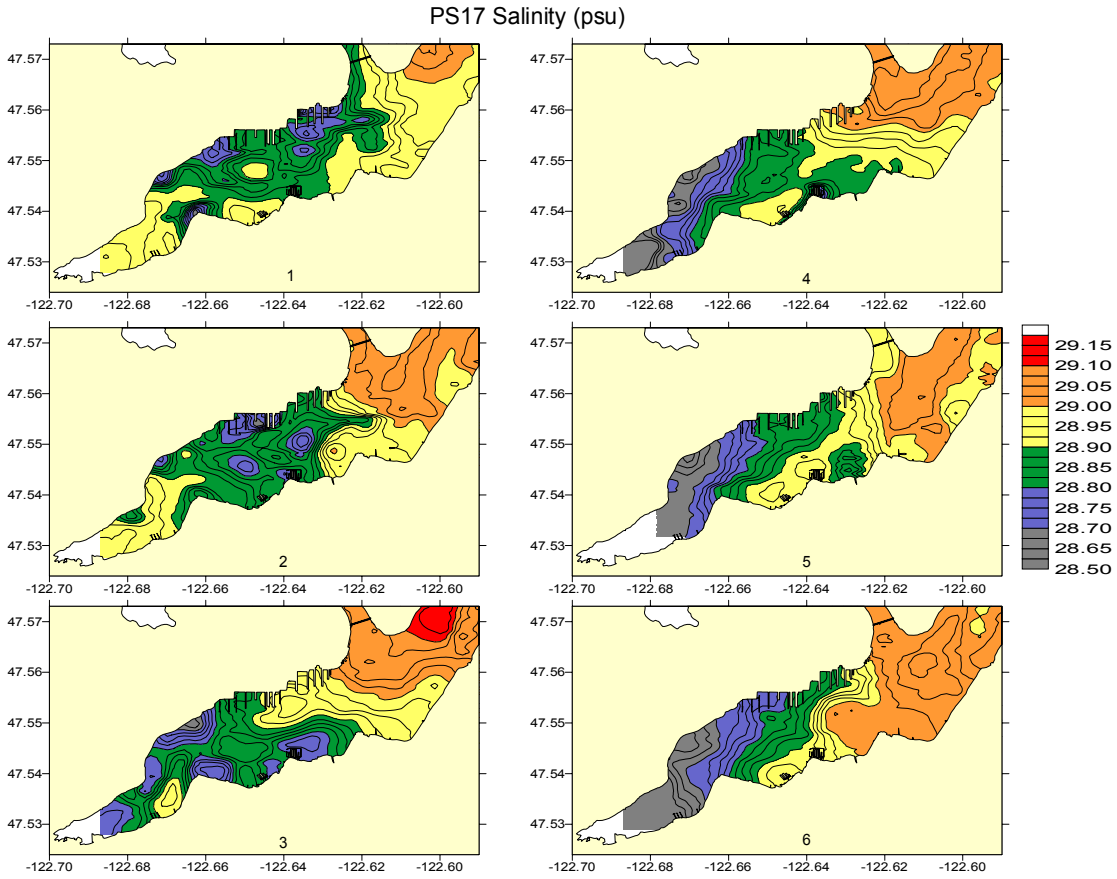


**Figure 22.** Tidal variation in salinity (psu) distribution for first 6 transects of PS17 Surface Mapping Survey.

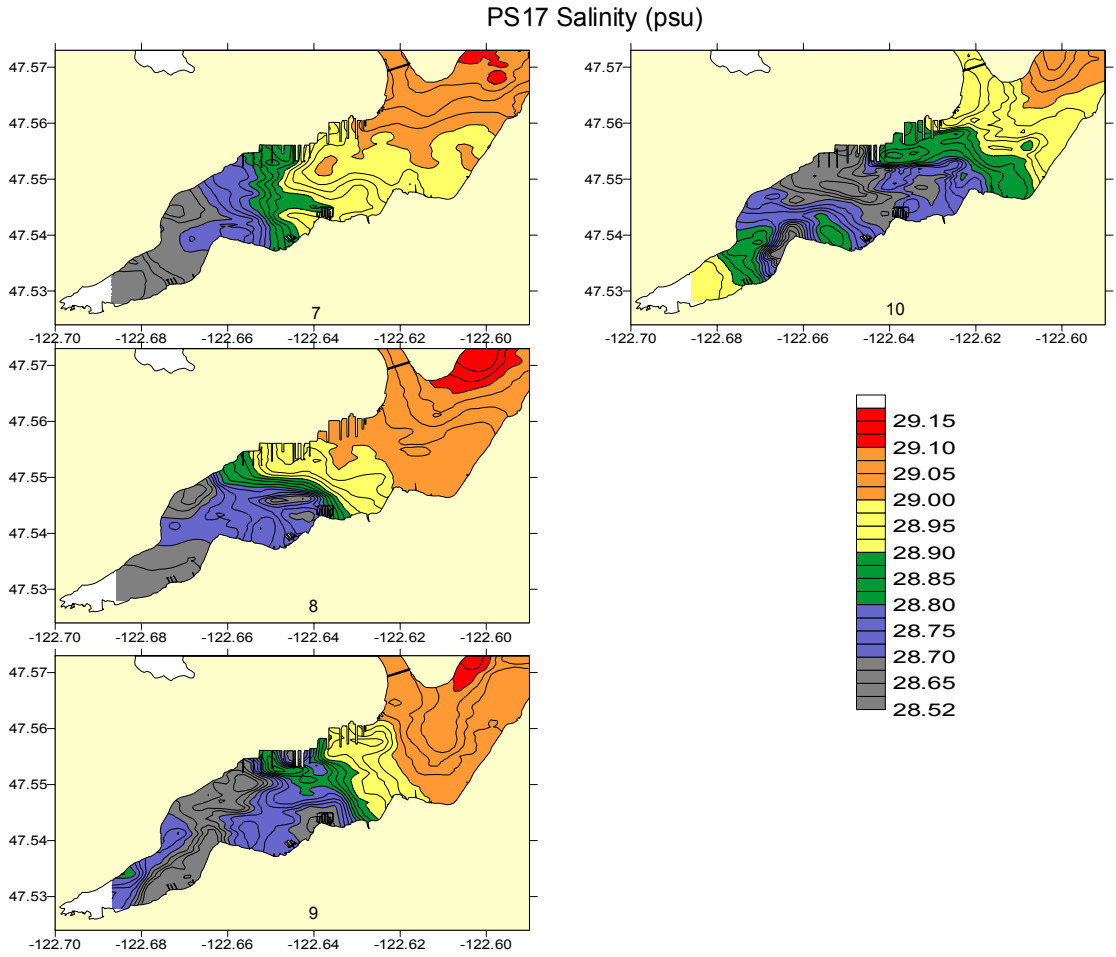


**Figure 23.** Tidal variation in salinity (psu) distribution for last four transects of PS17 Surface Mapping Survey.

**Table 7.** Mean surface seawater parameter values for each the sub-regions shown in Figure 24. The mean values are based on approximately 2000 points chosen arbitrarily within each of the regions shown in the figure. (NaN= not a number).

| Location | Salinity (psu) | Temp (deg C) | Density (sigma-t) | Oxygen ($mL \cdot L^{-1}$) | Oxygen Sat (%) | pH (NBS) | TSS ($mg \cdot L^{-1}$) | Chl-*a* ($ug \cdot L^{-1}$) | Sample Depth (m) |
|---|---|---|---|---|---|---|---|---|---|
| **PS01 September** | | | | | | | | | |
| Rich Passage | 29.36 | 13.29 | 21.97 | 4.48 | 73.87 | 8.09 | 1.29 | 3.59 | -1.82 |
| Port Orchard | 29.12 | 14.14 | 21.62 | 5.11 | 85.75 | 8.19 | 2.48 | 6.80 | -1.19 |
| Dyes Inlet | 27.94 | 15.40 | 20.45 | 7.04 | 120.44 | 8.58 | 3.83 | 57.76 | -1.15 |
| Sinclair Mouth | 28.91 | 14.10 | 21.46 | 5.42 | 90.24 | 8.25 | 1.86 | 7.24 | -1.22 |
| Sinclair Head | 28.94 | 14.27 | 21.46 | 5.21 | 87.41 | 8.20 | 2.87 | 22.90 | -1.37 |
| Data Range | 1.42 | 2.11 | 1.52 | 2.57 | 46.57 | 0.49 | 2.54 | 54.17 | 0.67 |
| **PS10 March** | | | | | | | | | |
| Rich Passage | 28.39 | 8.95 | 21.96 | 6.13 | 90.88 | 7.82 | 1.29 | NaN | -1.38 |
| Port Orchard | 28.17 | 8.96 | 21.78 | 6.52 | 96.41 | 7.87 | 0.99 | NaN | -1.65 |
| Dyes Inlet | 27.35 | 9.09 | 21.12 | 7.67 | 113.43 | 8.05 | 2.23 | 19.31 | -1.41 |
| Sinclair Mouth | 27.97 | 9.12 | 21.60 | 6.27 | 92.50 | 7.86 | 1.54 | 2.09 | -1.52 |
| Sinclair Head | 27.66 | 9.40 | 21.32 | 6.62 | 97.91 | 7.91 | 1.55 | 7.16 | -1.58 |
| Data Range | 1.04 | 0.44 | 0.83 | 1.54 | 22.55 | 0.22 | 1.24 | 17.22 | 0.27 |
| **PS16 July** | | | | | | | | | |
| Rich Passage | 29.28 | 12.41 | 22.08 | 5.64 | 91.15 | 8.05 | 0.62 | 3.92 | -1.42 |
| Port Orchard | 28.82 | 15.21 | 21.17 | 7.17 | 122.52 | 8.32 | 1.06 | 3.37 | -1.75 |
| Dyes Inlet | 28.80 | 16.78 | 20.81 | 7.99 | 140.57 | 8.45 | 2.44 | 5.35 | -1.79 |
| Sinclair Mouth | 28.80 | 15.56 | 21.08 | 7.60 | 127.50 | 8.45 | 3.78 | 19.57 | -1.85 |
| Sinclair Head | 28.85 | 15.25 | 21.18 | 8.50 | 146.57 | 8.45 | 4.00 | 14.50 | -1.50 |
| Data Range | 0.49 | 4.38 | 1.27 | 2.86 | 55.42 | 0.41 | 3.37 | 16.20 | 0.43 |

**Table 8.** Vertical variation in hydrographic data based on axial tow-yo data inside the inlet.

| Survey Period | Salinity (psu) | Temperature (deg C) | Density (sigma-t) |
|---|---|---|---|
| September | 0.3 | 0.6 | 0.3 |
| March | 0.5 | 0.5 | 0.5 |
| July | 0.2 | 1.9 | 0.6 |

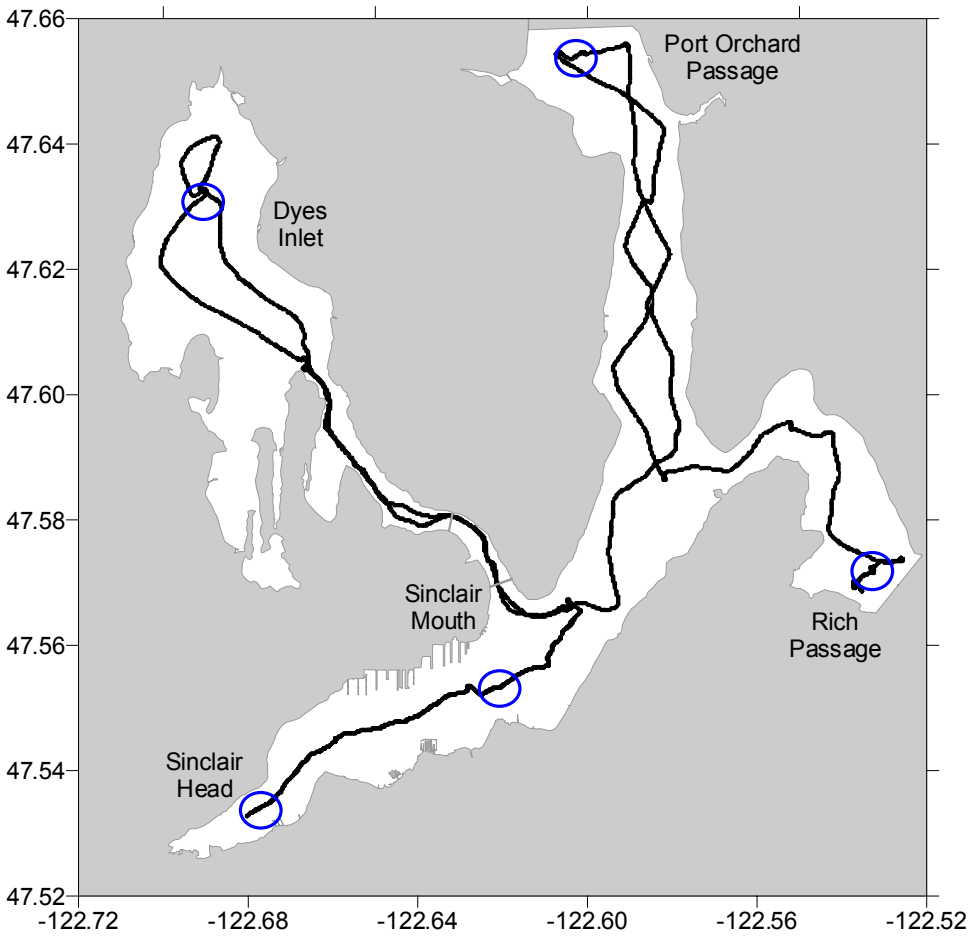


**Figure 24.** Regions used to calculate parameter values shown in Table 5.

***ResidenceFlushing Time Calculation.*** As mentioned previously, the distribution of salinity can be used to assess conservative mixing processes. Using the conservation of mass, salinity can be used as a tool to quantitatively determine the extent of flushing in the inlet, an important determinant in assessing the assimilative capacity of the inlet to contaminants. To get a quantitative assessment of inlet flushing times, the salt balance of Sinclair and Dyes Inlets were evaluated based on the cross-sectional surveys at the mouth of each inlet (PS02). Current velocities and salinity concentrations were measured throughout the vertical water column on 51 transects over a 24-hour period at the mouths of Sinclair and Dyes Inlets (Figure 25). The purpose of the analysis was to provide estimates of residence time, and to determine the primary mechanisms controlling flushing at the mouth of the inlets.

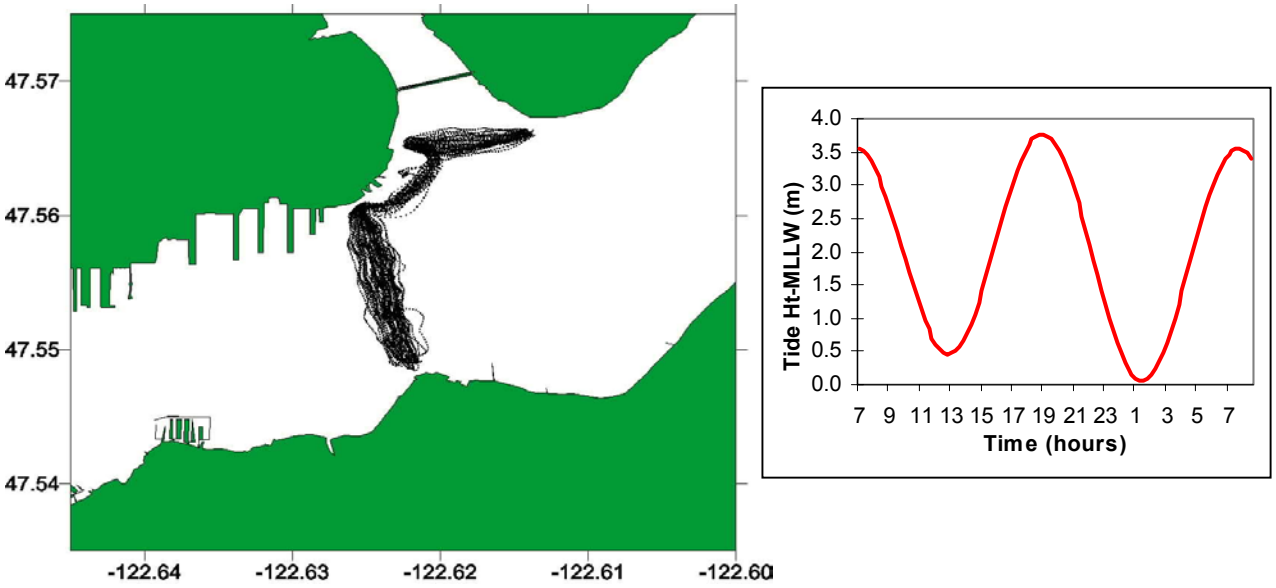


**Figure 25.** Cross-sectional tow-yo survey tracks with corresponding tide profile on September 18-19, 1997 (PS02)

Under steady state conditions, the salinity in an estuary is controlled by a balance between the advective transport of salt out due to the downstream mean flow, versus the transport of salt in due to tidal and density driven exchange flows. While the steady state assumption is seldom realized, the magnitude of the salt transport fluxes through the mouth of the inlet can provide a reasonable estimate of the overall salt balance for the system.

The data sets collected during PS02 provide the basis for evaluating the relative contribution to the salt balance of the inlets following the classical decomposition approach of Fisher (1972) and others. In this approach, the salt flux is broken down into a number of terms that can then be related to possible exchange mechanisms. The results of the salt balance analysis for Sinclair and Dyes Inlets are presented in Table 9.

**Table 9.** Contribution to the salt balance from various components of the tidal exchange and mean flow ($kg \cdot s^{-1}$).

| Water Body | Salt Flux Component | | | |
|---|---|---|---|---|
| | Mean Flow | Tidal Pumping | Stokes Drift | Tidal Shear |
| Sinclair Inlet | -344 | -17 | 404 | 6 |
| Dyes Inlet | -9691 | 162 | 4033 | 9 |

The results for Sinclair Inlet indicate that a rough balance between the downstream mean flow, and an upstream tidal exchange mechanism controls the salinity. This results from the correlation between the mean tidal velocity and the tidally-varying cross-sectional area at the mouth of the inlet, the so called "Stokes drift" (Figure 26). Salt is transported upstream because the phase of the tidal velocity lags the tidal height (and thus the cross-sectional area) by about one hour. In effect, there is more water flowing into the inlet because the cross-sectional area is generally larger during flood tide, and smaller during ebb tide. In order for water mass to be conserved, this inflow must be balanced by an outflow, the "Stokes drift compensation flow". This mean flow combined with any freshwater driven flow serve to export salt from the inlet, thus maintaining a rough salt balance.

The results for Dyes Inlet are qualitatively the same, the primary difference being that the salt fluxes are close to an order of magnitude higher (Table 9). However, it appears that the same mechanism tends to control the salt balance in Dyes Inlet.

Knowing the approximate mass flux of salt through the inlets, and estimating the total salt content, it is possible to derive an estimate of the residence time for the inlets assuming steady state conditions from

$$\tau = \frac{m}{m_t} = \frac{Vs_a}{m_t}$$

where $m$ is the salt content of the inlet, $m_t$ is the salt flux through the inlet, $V$ is the volume of the inlet, and $s_a$ is the average salinity concentration of the inlet. For Sinclair Inlet, a good estimate of $s_a$ can be determined from the 3-D and surface water surveys (Table 5), while for Dyes inlet, a reasonable estimate can be obtained from the axial surveys. The volume of each inlet was estimated from the bathymetric charts and data collected during all surveys (Figure 6). The estimated residence times for Sinclair Inlet and Dyes Inlet are 57 days and 11 days, respectively.

The residence time of 57 days calculated for Sinclair Inlet water is considerably longer than those reported previously (Ridley and Ostericher, 1960; US Navy, 1983 as reported in Albertson et al., 1995). Ridley and Osterricher (1960) estimated the overall residence time for the combined Dyes Inlet/Sinclair Inlet/Rich Passage region. The estimates were made by two methods, mean flow flushing based on tidally averaged flows at Point Glover, and freshwater replacement based on salinity measurements at five regional stations and estimated freshwater inflows. These two methods gave approximate residence times of 43 tidal cycles (~21 days) and 48 tidal cycles (~24 days), respectively. Unfortunately, the net flow estimates, average salinity estimates, and freshwater inflow estimates were all based on very limited data. While freshwater inflow estimates remain limited, the flow and salinity data collected during this project are significantly improved over the previous work and should provide more reliable estimates of the flushing time

for Sinclair and Dyes Inlets. The second report was not located so comparison of the calculations could not be made.

An alternate estimate of the residence time can be obtained based on knowledge of the freshwater flow and the salinity or "freshness" of the estuary. According to Fisher et al. (1979)

$$\tau = \frac{V_f}{Q_f}$$

where $V_f$ is the volume of freshwater in the inlet, and $Q_f$ is the river flow. Since the creek flow for the inlets is not well established, we can use this relation to estimate it, and check the value for order-of-magnitude agreement. We find that the estimated freshwater flow for Sinclair Inlet is about 5 mgd, and for Dyes Inlet about 25 mgd. For Sinclair Inlet, dry weather flows from the Bremerton POTW is about 5 mgd. It is expected that this estimate is probably good within a rough order of magnitude even in the absence of creek inflow data. For Dyes Inlet, the estimate of 25 mgd is within the wide range of freshwater inflow estimates given in Albertson et al. (1995).

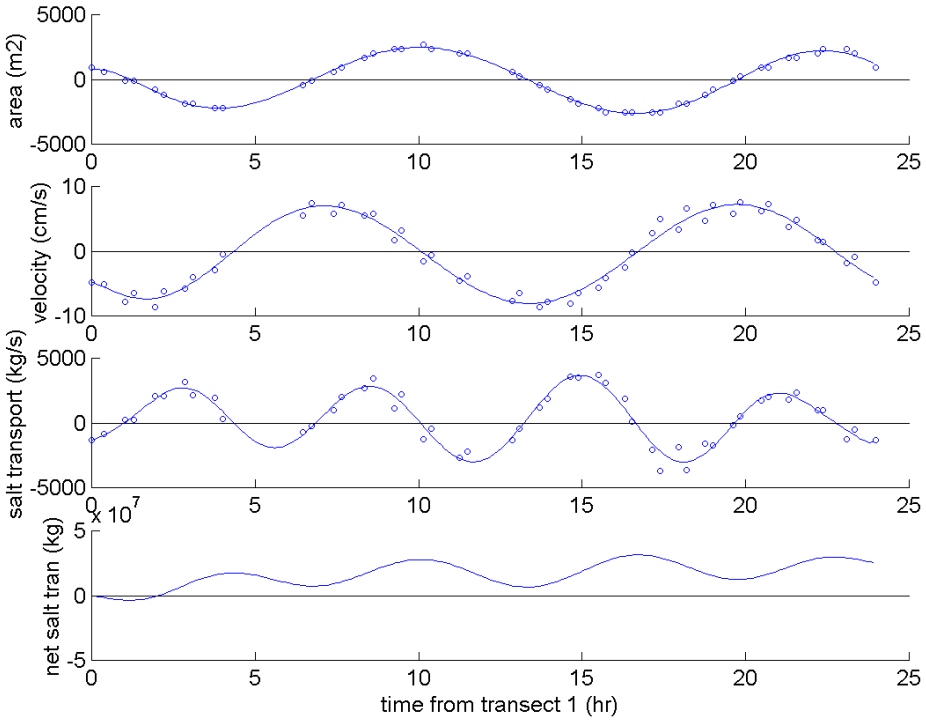


**Figure 26.** Tidal variation in the cross-sectional area (mean removed), sectional-average velocity, Stokes drift salt flux, and net Stokes drift salt flux at the mouth of Sinclair Inlet.

## *Summary of Circulation, Hydrography, and Flushing Time*

The circulation of Sinclair Inlet is influenced by tides and estuarine conditions. Freshwater sources in the inlet set up axial, lateral, and vertical gradients in the hydrography. Combined with low flow, these conditions produce a characteristic outflow of warmer, fresher water at the

surface that is balanced by colder, saltier water at depth. These conditions were consistent over both tidal and seasonal time scales. During the observation period, the hydrography of the inlet was in steady state with its adjacent waters.

A complex gyral circulation pattern with higher current speeds is generated at the mouth by interaction with the tidal flow through the Port Washington Narrows. This flow characteristic enhances flushing at the mouth of the inlet. Conversely, lower current speeds and a higher degree of stratification within the inner inlet lead to longer flushing times. The result is that the input of contaminants into the inner part of the inlet leads to higher exposure levels. Given that the major freshwater inflows of the Bremerton POTW and Gorst Creek occur toward the head of the inlet suggests that there will also be an enhanced exposure inside the inlet from storm water. Residence time calculated for Sinclair Inlet was 57 days and for Dyes Inlet was 11 days.

## Conventional Water Quality Parameters

Water quality parameters measured during these surveys included TSS, dissolved oxygen, pH, and chl-*a*. Some of these are "conventional water quality measures", or at least capture similar characteristics to those used in assessing the overall health of a water body within a regulatory framework. Thus, the term "conventional" will be used to describe this group of parameters separately from those considered as contaminants of concern to the inlet such as nutrients, metals, and PAH.

Of particular concern for marine waters is how these parameters might vary outside normal levels as a result of eutrophication. In particular, there is a general concern that dissolved levels may become too low after large plankton blooms dye off and cause detrimental conditions for the inlets' biology. Simultaneous measurement of all parameters provides the required data for assessing these issues and the relative importance in the processes controlling distributions.

Plankton bloom conditions were visibly evident on all three surveys. There was a bloom of dinoflagellates characterized by large patches of reddish-brown water, primarily in the inner third of the inlet on the first two visits. The areal extent of the "red-tide" was considerably larger in September than in March. On the July set of surveys there was also a bloom of green algae that formed large free-floating fibrous bundles. These were seen well outside the inlet, in other portions of Puget Sound, as well as inside the inlet. Another interesting biological phenomenon observed on all three occasions was the presence of huge numbers of large jellyfish, primarily in the inner third of the inlet. Like the red-tide bloom, their areal extent was largest in September. The presence of large plankton blooms suggests that concern about eutrophication is not misplaced.

### *Spatial Variations*

Conventional seawater parameters are summarized inTable 10 and Table 11. Table 10 lists the mean, minimum, maximum, range, and number of data points for each time period for measurements made inside the inlet only. These were summarized from the surface mapping and 3-D surveys performed each time period. The summary statistics listed in Table 11 are representative for measurements made regionally using data from axial surveys performed each time period. Summary statistics for each survey can be found in Appendix C.

The relatively large range of values shown in the tables reflects the bloom conditions visible during all three periods. Though mean concentration levels appear reasonable when compared to other estuarine environments (Lapota, 1993) and other measurements made in the inlet (Albertson et al., 1995), maximum values were particularly high. Maximum chl-*a* levels of over 500 ug·$L^{-1}$ surpassed those of Albertson et al., (1995) by well over an order of magnitude. Relatively high levels of dissolved oxygen as measured by percent saturation (measured concentration/atmospheric equilibrium concentration) and pH both reflect the high productivity, a process which produces oxygen and assimilates carbon dioxide. At the other end of the spectrum, the lowest oxygen level of 2.7 mL·$L^{-1}$ observed in September was below the 3.5 mL·$L^{-1}$ value termed as "low" by Albertson et al., (1995), but above 2.1 mL·$L^{-1}$, the level termed as "hypoxic". These low oxygen values were observed in a small region along the southwestern shore and only during one set of mapping surveys in September (Figure 27).

The same general spatial distribution pattern seen for salinity was similarly observed for all conventional parameters. Axial and lateral gradients in all parameters were evident on all occasions with values generally increasing into the inlet. An example of this is shown in Figure 28 for TSS. The similarity of the general distribution pattern with that of salinity suggests a certain degree of conservative mixing characteristics. However, the general distribution was modified with patches of relatively high levels (Figure 29), particularly within the inner third of the inlet generated by localized biological or other processes such as resuspension. The locations and extent of these patches varied tidally, with survey, and with season. While hydrography plays a role on where the processes take place, the processes themselves are non-conservative and the distributions generated by them and their dispersion characteristics are therefore non-conservative as well.

Vertical distributions of conventional water quality parameters in the inlet varied slightly from one another, with some parameters showing strong seasonal variations. Based on the distribution plots generated for the 3-D surveys and reviewing axial tow-yo data, oxygen and pH were consistently highest at the surface and decreased with depth throughout the inlet. TSS concentrations were commonly highest at the surface toward the mouth of the inlet, then reversed and were highest at the bottom or subsurface in mid-inlet and reversed again toward the head. This distribution suggests a bottom source in mid-inlet that might be derived from either the Bremerton POTW or possibly from resuspension of fine grained sediments. Alternatively, some degree of vertical mixing may explain this as well. Chl-*a* commonly had a subsurface maximum but like TSS, sometimes reversed from a surface or subsurface maximum at the mouth to a bottom maximum in mid-inlet and reversed once again toward the head. These reversals again suggest a changing source and/or a vertical mixing component. The vertical offset in oxygen and pH concentrations with that of chl-*a* likely results from higher consumption at depth.

Like salinity, the spatial distribution of dissolved and suspended seawater parameters also showed gradients into the adjacent regions outside the inlet. The result is that the waters of the inlet were always fresher, warmer, and higher in particulates, oxygen, pH, and chl-*a* than adjacent waters. Using average seawater values calculated for each of the five regions shown Figure 24 and summarized in Table 7, it can be seen that the surface waters of Rich Passage were nearly always lowest in TSS, dissolved oxygen, pH, and chl-*a*. The waters of northwestern Dyes Inlet had the opposite distribution while the waters in the Port Orchard Channel and at the head of the inlet had intermediate values. The range in most values was smallest in the March data set indicating that conditions during this time period were more uniform and approached steady-state.

### *Temporal Variations*

Tidal variations in the spatial distributions of all parameters were similar to that discussed for salinity in which short-term spatial variations were explained primarily by the tidal circulation. The example shown for oxygen (Figure 30) shows the flow of relatively high oxygen water out toward the mouth on ebb and the push in on flood. At mid-inlet, the larger mass of high oxygen water appears to break up into a few smaller masses toward the end of flood. This variation lends some weight to the interpretation that there may be some degree of vertical mixing affecting the distribution of water quality parameters in the mid-inlet.

There was a clear change in inlet seawater conditions with season (Table 10). On average, all conventional parameters decreased from September to March and then increased again from March to July. The changes were greatest for chl-*a*, which varied by as much as a factor of five. The higher average chl-*a* concentration in July resulted from the regional bloom condition while the higher maximum chl-*a* values in March resulted from an intense but spatially limited red tide condition. The lower levels in March likely result from light limited conditions. The seasonal trend is that water in the inlet is saltier, warmer, more oxygenated, and higher in pH, particulates, and chl-*a* in summer than in winter. The summer increases in oxygen, pH, and particulates result directly from increased biological productivity that is expected given the region's climate and light-limited conditions. However, the lower TSS in winter was not necessarily expected since it was thought that storm water inflow would increase particulate flux to the inlet. The lower winter values indicate that the amount of particulates is low in storm water or that particulates associated with the storm water settle out quickly near their source and are not seen in the suspended matter of the inlet. Though no measurements were made, visual inspection of creek flows in March and July looked to be exceptionally clear, suggesting that the creeks were not a source of high suspended loads to the inlet during these times.

### *Summary of Conventional Water Quality Parameters*

Conventional water quality parameters measured during this study included TSS, dissolved oxygen, pH, and chl-*a*. These parameters provide an indication of the conditions that can affect the inlet's health, in particular with regard to the effects of eutrophication. Large blooms of plankton and masses of jellyfish were visible on all occasions giving an indication that some degree of eutrophication occurs in the inlet.

On average, the levels of these parameters were reasonably comparable to other estuarine environments. However, exceptionally high levels of chl-*a* were found on all occasions. High biological production led to supersaturation of dissolved oxygen in surface waters. Only in a very limited area of the inner inlet in September did oxygen consumption produce "low" or "hypoxic" conditions. As such, this was the only location that met the full characteristics of eutrophication.

While the general spatial distribution of these parameters followed the patterns established by the general circulation and hydrography, localized biological and mixing processes modified some of them considerably. In particular, there were reversals in the vertical distribution of chl-*a* and TSS in the mid-inlet region that suggested that vertical mixing processes were potentially important in their distribution. There also appeared to be a source of TSS near the bottom in the mid-inlet region which made the Bremerton POTW or resuspension of fine-grained sediments the likely sources.

The inlet was always fresher, warmer, and higher in particulates, oxygen, pH, and chl-*a* than its adjacent waters on all occasions. Seasonal variations were commensurate with climatological changes and increased biological production. The result is higher levels of all constituents in the summer and fall than in winter. This was generally true for the waters of the adjacent regions as well. While this was expected for the biologically mediated parameters, the lower TSS in winter was unexpected, as stormwater was an anticipated source of particulates.

**Table 10.** Summary statistics for conventional water quality parameters for each survey period. The data, summarized from surface mapping and 3-D surveys, are representative of values for inside Sinclair Inlet only.

| Inside Inlet Only | | TSS ($mg \cdot L^{-1}$) | Oxygen ($mL \cdot L^{-1}$) | $O_2$ Saturation (%) | pH (NBS) | Chl-a ($ug \cdot L^{-1}$) |
|---|---|---|---|---|---|---|
| **September** | Mean | 1.96 | 6.74 | 114.45 | 8.69 | 21.71 |
| | Min | 0.48 | 2.69 | 44.81 | 8.16 | 6.65 |
| | Max | 48.29 | 9.36 | 157.65 | 9.22 | 519.15 |
| | Range | 47.81 | 6.67 | 112.84 | 1.06 | 512.50 |
| | n | 191101 | 191590 | 191590 | 191591 | 191461 |
| **March** | Mean | 1.49 | 6.48 | 96.55 | 7.89 | 4.15 |
| | Min | 0.47 | 5.88 | 87.63 | 7.79 | 0 |
| | Max | 10.70 | 9.49 | 141.99 | 8.36 | 342.02 |
| | Range | 10.23 | 3.61 | 54.36 | 0.57 | 342.06 |
| | n | 150346 | 151868 | 151831 | 148524 | 130133 |
| **July** | Mean | 3.38 | 8.08 | 139.79 | 8.39 | 14.30 |
| | Min | 0.56 | 5.64 | 94.08 | 8.08 | 2.47 |
| | Max | 11.03 | 10.87 | 188.32 | 8.73 | 67.33 |
| | Range | 10.47 | 5.23 | 94.25 | 0.64 | 64.86 |
| | n | 307370 | 307517 | 307514 | 307673 | 251178 |

**Table 11.** Summary statistics for conventional water quality parameters for each survey period. The data represent regional values summarized from axial surveys.

| Regional Data | | TSS ($mg \cdot L^{-1}$) | Oxygen ($mL \cdot L^{-1}$) | O2 Saturation (%) | pH (NBS) | Chl-a ($ug \cdot L^{-1}$) |
|---|---|---|---|---|---|---|
| **September** | Mean | 2.07 | 5.13 | 85.78 | 8.20 | 15.18 |
| | Min | 1.10 | 4.04 | 67.86 | 8.06 | 2.99 |
| | Max | 6.17 | 8.04 | 137.99 | 8.64 | 163.39 |
| | Range | 5.06 | 4.00 | 70.13 | 0.58 | 160.40 |
| | n | 68094 | 68491 | 68491 | 68491 | 68069 |
| **March** | Mean | 1.52 | 6.38 | 94.60 | 7.87 | 4.32 |
| | Min | 0.62 | 5.96 | 88.26 | 7.62 | 0.38 |
| | Max | 3.42 | 8.05 | 118.91 | 8.13 | 23.84 |
| | Range | 2.80 | 2.09 | 30.65 | 0.51 | 23.46 |
| | n | 88577 | 88672 | 88677 | 88691 | 28082 |
| **July** | Mean | 1.69 | 6.69 | 113.21 | 8.23 | 9.16 |
| | Min | 0 | 5.30 | 85.68 | 8.00 | 0.56 |
| | Max | 16.33 | 9.30 | 160.08 | 8.56 | 262.81 |
| | Range | 16.34 | 4.00 | 74.40 | 0.56 | 262.24 |
| | n | 73283 | 74534 | 74535 | 74535 | 61087 |

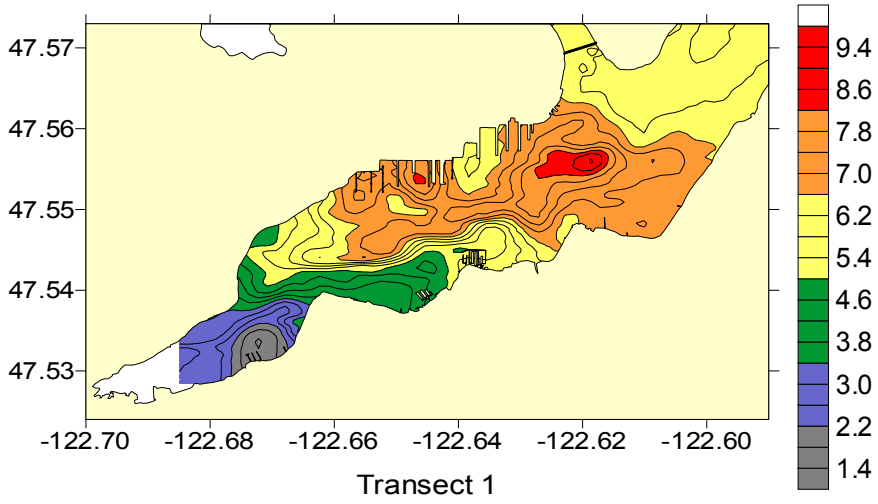


**Figure 27.** Surface distribution of dissolved oxygen (mL·L$^{-1}$) showing the region of "low" and "hypoxic" values in the inner inlet, measured 25 September (PS07, Transect 1).

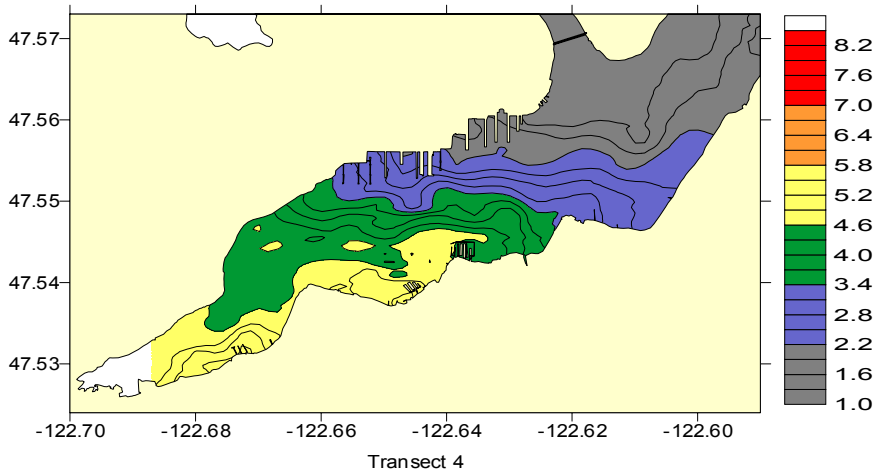


**Figure 28.** Surface TSS (mg·L$^{-1}$) distribution measured on 17July 1998, PS17, Transect 4, Ebb tide.

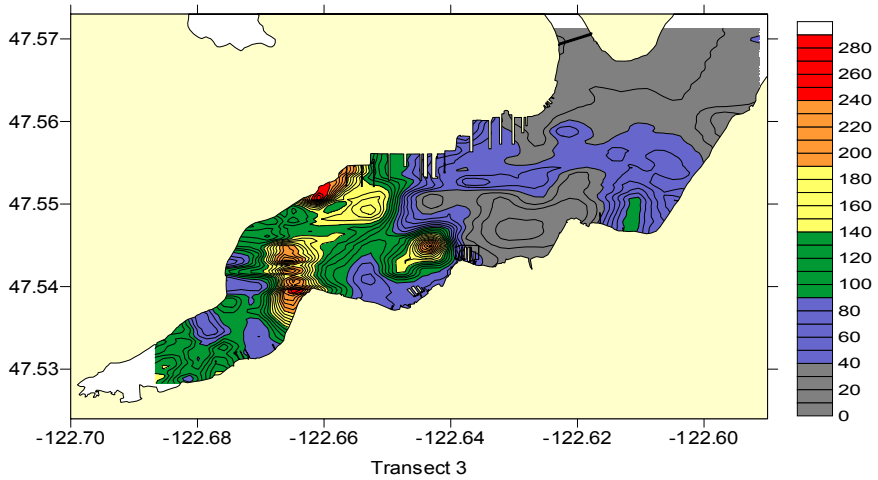


**Figure 29.** Surface chl-*a* (ug·L$^{-1}$) distribution measured on 25 September 1997 (PS07, Transect 3).

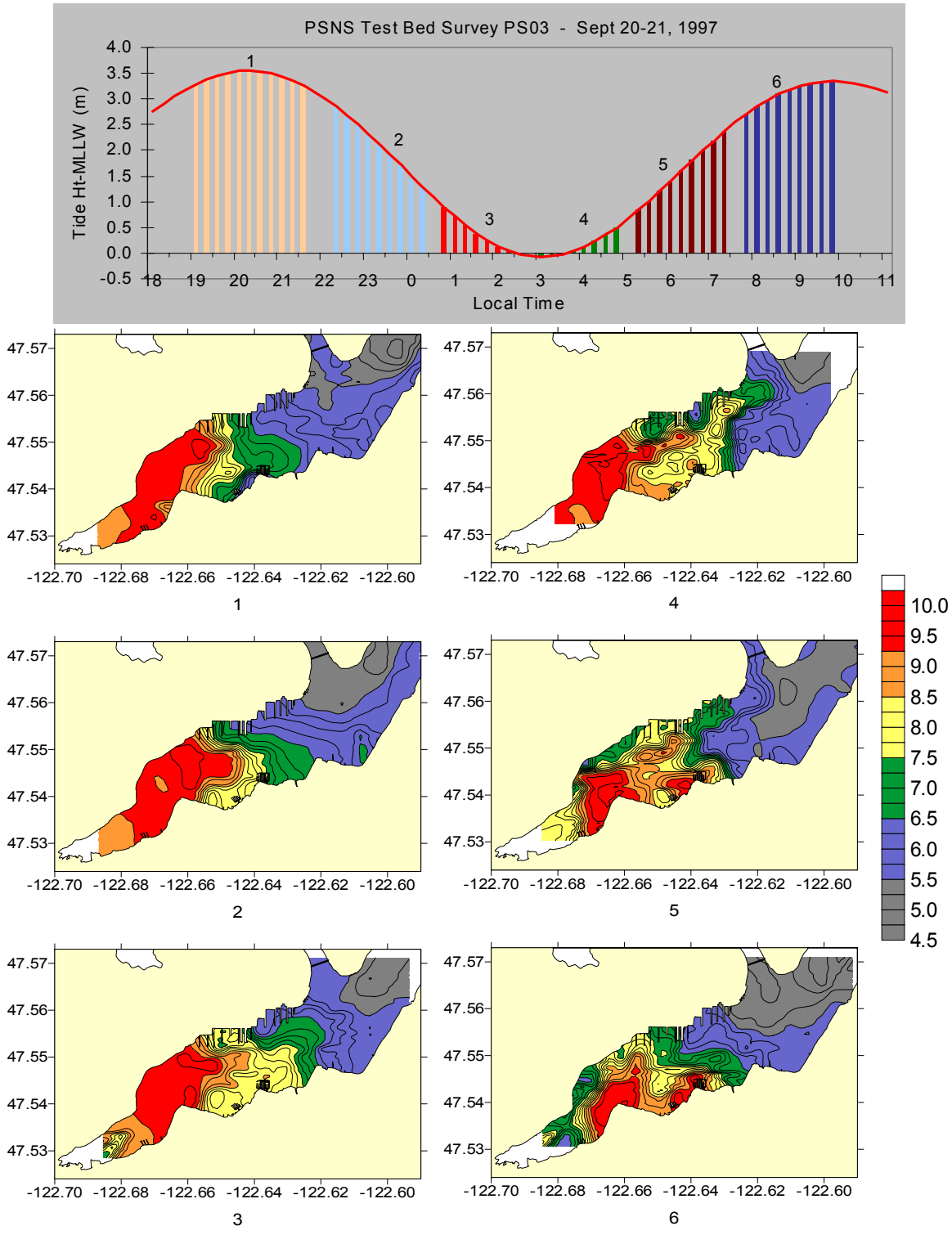


**Figure 30.** Tidal variation of dissolved oxygen ($mL \cdot L^{-1}$) for six surface mapping transects performed 20 to 21 September, 1997 (PS03). Transect numbers refer to tidal amplitude diagram at top.

## Nutrients

The introduction of excessive amounts of nutrients into coastal waters can lead to eutrophication. A specific PSNS concern for how nutrient inputs from storm water impact the inlet led to measurements being made on the second two survey sets. Discrete surface samples were collected for the full suite of nutrients throughout the survey area. The samples were collected over several days to obtain the desired spatial coverage. Because of this, the data were pooled for evaluation and visualization, though in doing so, tidal variations are lost, and the discussion of distributions is limited to broad generalizations.

The distribution of all nutrients in the inlet for March and July closely follow those shown for phosphate and ammonia in Figure 31 and Figure 32. The principal feature of these distributions was the high concentrations observed in the vicinity of the Bremerton POTW. Out from this region, concentrations typically decreased rapidly and became somewhat uniform out to the mouth where concentrations increased slightly. Outside the inlet, concentrations did not vary significantly from those measured at the mouth. While the basic distributions were similar, there was a slight difference in that the phosphate distribution also had a localized high defined by a few stations in the south-central part of the inlet. This localized high was also seen for nitrate and to a lesser extent for silica. The source of these high values is not known though their spatial orientation suggests a source associated with the marinas along the southern shoreline. There were no other indications of significant shoreline sources of nutrients.

The other principal feature of the nutrient distribution is the significant decrease in receiving water concentrations from March to July. While this seasonal change is evident in Figure 31 and Figure 32, the numerical data are summarized in Table 12 below. The observed concentrations appear to be above levels that would be considered "limiting" to plankton growth. Average concentrations in the inlet and surrounding waters decreased by as much as a factor of 7 for nitrate and as little as a factor of 1.6 for phosphate. The relative changes resulted in a significant change in the nitrogen (sum of $NO_3$, $NO_2$, $NH_3$) to phosphate ratio (N:P) from a value of 12 in March to a value of about 3 in July. Because these ratios are typically fixed by primary production, the reduction by varying amounts seen in the inlet most likely comes from a reduction in mass loading rather than uptake by organisms. The lower concentrations measured in the effluents in July combined with generally lower dry weather discharge rates support this.

Other nutrient concentration data for the inlet come from Albertson et al., 1995. Their measurements were made at six stations along the axis of the inlet in 1992. Considerable differences exist between their data set and the current one. For the same months, concentrations of nitrate+nitrite (their methods did not separate the two compounds) were between 50% and 300% higher, phosphate was higher by about 300%, and ammonia was lower by about 50 to 400%. Their data also indicated a general decrease of nitrate+phosphate and an increase of ammonia into the inlet, and no spatial variation in phosphate. While their data did show a similar seasonal decrease in nitrate+nitrite from winter to summer, ammonia showed episodic highs in summer, and phosphate showed little seasonality. The differences between data sets can be attributed to a number of factors including differences in spatial coverage, variations in climatological conditions (e.g., 1992 had higher rainfall in July than March), as well as variations in both the magnitude and distribution of biological activity.

From Table 12 it can be seen that the POTWs were a considerable source to the inlet for all nutrients while the creeks were only a source of silica. To highlight the influence of these discharges, the effluent data were pooled with the receiving water data and plotted together in hypothetical plots shown in Figure 33 and Figure 34. The discharge from the POTWs clearly influenced all the nutrient distributions similar to the example shown for ammonia (Figure 33)

while the additional source of silica from the creeks was seen in Figure 34. These figures along with Table 12 highlight the POTW as a source for ammonia and the POTW and creeks as a source of silica to the Inlet, as well as the minimal seasonal signal from the creeks. These plots suggest that silica might be a useful indicator for looking at the influence of freshwater in this region.

The impact of nutrient inputs from the POTWs and the effects of relative flushing rates are particularly highlighted in Sinclair Inlet. The source of nutrients in the inner inlet corresponds with the exceptionally high biological productivity levels found there. In this region the low tidal flow and long flushing rates lead to a condition in which the excess nutrients enhance the production. In comparison, the inflow of nutrients from the Port Orchard POTW at the mouth enters a region of relatively high flushing. Under these conditions the impact of nutrient stimulation is minimized. While the inlet is clearly impacted by nutrient inflow, the degradation of water quality to low dissolved oxygen levels was ephemeral and limited to only a very small region.

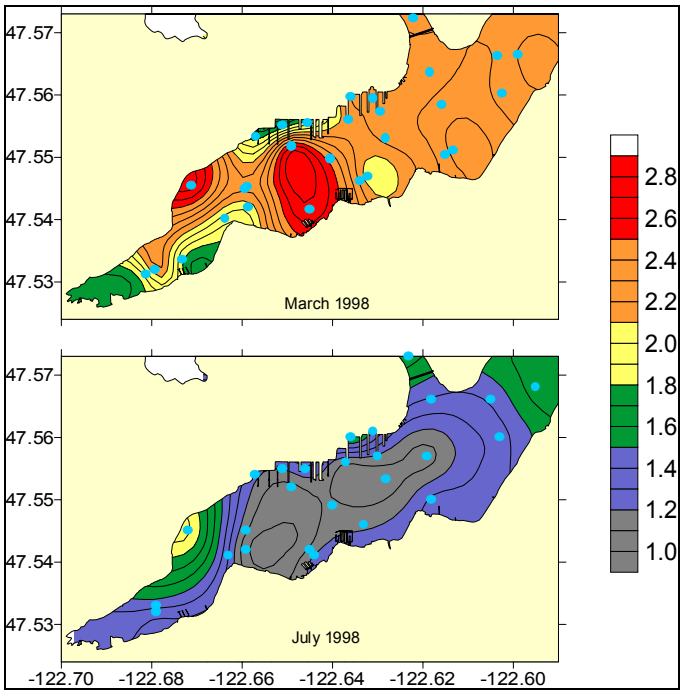


**Figure 31.** Pooled distribution of dissolved $PO_4$ ($uM \cdot L^{-1}$) in March and July 1998 based on discrete sampling completed over multiple survey days.

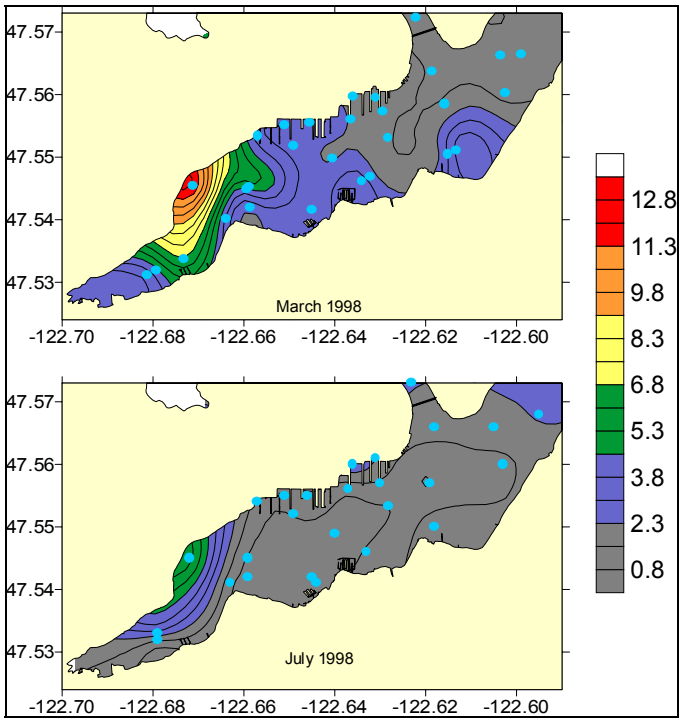


**Figure 32.** Pooled distribution of dissolved $NH_3$ ($uM \cdot L^{-1}$) in March and July 1998 based on discrete sampling completed over multiple survey days.

**Table 12.** Nutrient concentrations measured in receiving waters in March and July 1998 and from the inputs of two local sewage plants and Gorst, Blackjack, and Ross creeks.

| Statistic | $PO_4$ ($uM \cdot L^{-1}$) | $SiO_3$ ($uM \cdot L^{-1}$) | $NO_2$ ($uM \cdot L^{-1}$) | $NH_3$ ($uM \cdot L^{-1}$) | $NO_3$ ($uM \cdot L^{-1}$) | N:P |
|---|---|---|---|---|---|---|
| **MARCH** | | | | | | |
| Inlet Mean (n=36) | 2.20 | 73.36 | 0.41 | 2.58 | 22.78 | 11.8 |
| POTW (n=2) | 40.25 | 227.93 | 7.61 | 30.00 | 67.64 | 2.7 |
| Creeks (n=2) | 0.65 | 263.40 | 0.15 | 2.12 | 36.69 | 77.4 |
| **JULY** | | | | | | |
| Inlet Mean (n=33) | 1.34 | 23.20 | 0.14 | 1.53 | 3.29 | 3.3 |
| POTW (n=2) | 79.59* | 212.80 | 16.33* | 20* | 1.43 | 0.5 |
| Creeks (n=3) | 1.42 | 219.87 | 0.10 | 2.20 | 36.09 | 31.1 |
| **MARCH/JULY** | | | | | | |
| Inlet | 1.6 | 3.2 | 2.9 | 1.7 | 6.9 | - |
| POTW | 0.5 | 1.1 | 0.5 | 1.5 | 47.3 | - |
| Creeks | 0.5 | 1.2 | 1.4 | 1.0 | 1.0 | - |

*Uses maximum analysis detection limit of 80, 30, and 20 $uM \cdot L^{-1}$, respectively for one of the two samples.

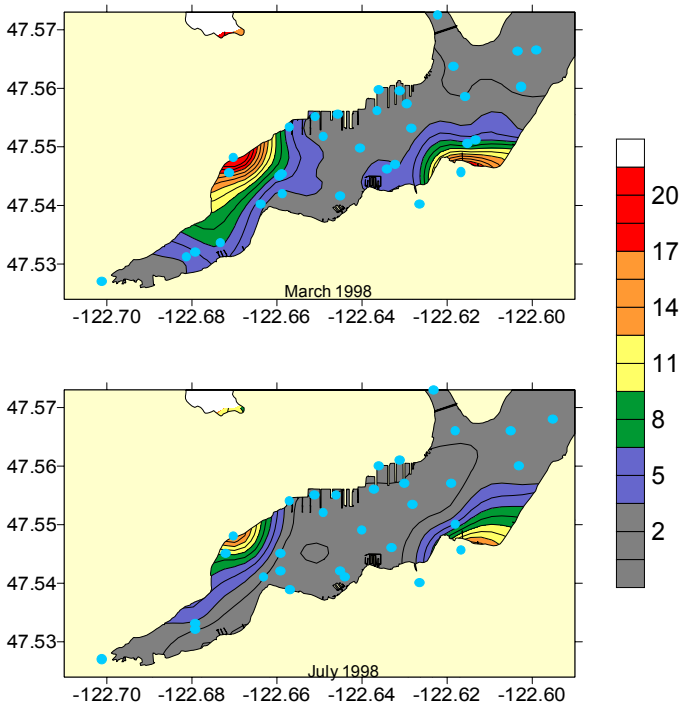


**Figure 33.** Hypothetical distribution of dissolved $NH_3$ ($uM \cdot L^{-1}$) in March and July 1998 showing POTW and creek effluent data pooled with receiving water data.

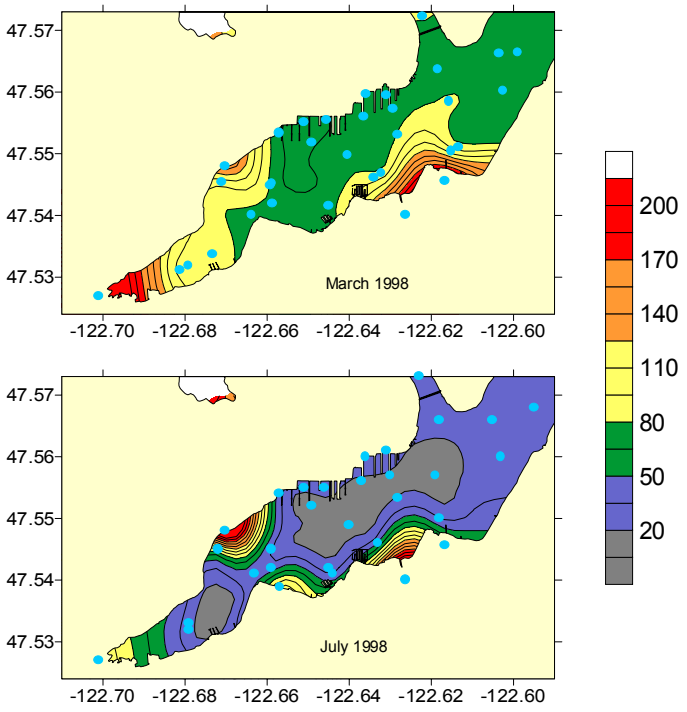


**Figure 34.** Hypothetical distribution of dissolved $SiO_3$ ($uM \cdot L^{-1}$) in March and July 1998 showing POTW and creek effluent data pooled with receiving water data.

### *Summary of Nutrients*

All nutrient distributions were driven by inflow from the POTWs. Only silica was found in the creeks and thus stormwater does not apparently have a significant role in generating the eutrophic conditions. Nutrient levels were highest in the inner portion of the inlet where a large source at the Bremerton POTW combines with lower flows and higher residence time to produce them. This condition enhanced primary production to exceptionally high levels characteristic of eutrophication. The discharge from the Port Orchard POTW at the mouth is dispersed much more quickly and has considerably lower impact on distributions and biological production. The mass loading of nutrients to the inlet was lower in summer than in winter with the result that concentration levels in the inlet were considerably lower. Though nutrient levels were highest in winter, light limiting conditions keep production levels relatively reduced at that time.

## Metals

Concern about the input of metals into the Inlet in and around the shipyard led to their measurement in the receiving water during each survey period. The metals chosen for analysis were based on a review of the contaminants of concern for Sinclair Inlet from the Clean Water Act Section 303d list, a review of the literature, and a review of shipyard NPDES outfall measurements. In particular, the shipyard has keen interest in copper concentrations because of compliance issues related to their dry dock discharges. Note that the metals on the EPA 303D list were included on the basis of sediment or tissue concentrations rather than water concentrations. The list of metals chosen for analysis included: arsenic (As), cadmium (Cd), copper (Cu), chromium (Cr), lead (Pb), selenium (Se), silver (Ag), and zinc (Zn). Mercury, which also is on the 303d list was not measured because it was cost prohibitive. Most analyses were performed on the dissolved phase of the metal, that is, the metal concentration in the water after it was filtered through a 0.45 um filter. Additionally, there were several measurements made of the total metal concentration (i.e. without filtering) in the water as well. Summary results of the discrete sample analyses are shown in Table 13 below. Unless otherwise stated, statistical t-test evaluations were made at the 95% confidence interval (two-tail).

### *Arsenic*

For all time periods, dissolved arsenic concentrations ranged from 0.54 to 2.51 and averaged 1.16 $ug \cdot L^{-1}$ (Table 13). These concentrations were well below the marine chronic water quality standard published for the State of Washington (Chapter 173-201A WAC) of 36 $ug \cdot L^{-1}$ or the proposed standard value of 21 $ug \cdot L^{-1}$ indicated in the publication. The highest average and maximum concentrations were observed in September followed by March then July. September average values were statistically higher than those measured in March and July. March values were also statistically higher than those measured in July. The ratio of dissolved to total metal for all surveys averaged 0.97, indicating that nearly all the metal in the receiving water was in the dissolved form. This ratio is consistent with the marine conversion factor of 1.0 published in Chapter 173-201A WAC.

Arsenic concentrations were relatively uniform throughout the inlet in March and July. In September, two regions of localized highs were evident (Figure 35). One region was along the southern shore in the vicinity of Blackjack Creek and the Port Orchard POTW. This area also showed a localized high in March and July, though to a much lesser extent. The second region was within Pier 3 at the shipyard and along the outer part of the piers to the east. While the spatial distribution looks as if arsenic originates within Pier 3 and flows out, the plots were developed from pooled data sets made over several survey days so only the general source

distributions should be interpreted from the plots. Arsenic concentrations do not correlate with other measured hydrographic parameters, thus limiting the ability to assess its source.

Though the receiving water distributions alone do not indicate it, the Bremerton POTW was the largest measured source of arsenic with values of 3.5 and 6.4 $ug \cdot L^{-1}$ observed in March and July, respectively. The effect of this input can be seen in Figure 36, a hypothetical plot accentuated by including the creek and POTW effluent concentrations in the spatial display. Though the average Bremerton POTW values were statistically different than those observed in the inlet, the average effluent measured at the Port Orchard POTW (1.49 $ug \cdot L^{-1}$) and the discharge from the creeks (1.14 $ug \cdot L^{-1}$), were not. While these effluent data appear incongruous with the localized high arsenic water observed on the south shore, the effluent measurements were too limited to assess their likelihood as a source. For the three survey time periods, the average dissolved arsenic concentration measured at stations within the shipyard area of 1.21 $ug \cdot L^{-1}$ (Figure 37) was statistically no different than the average value measured in the rest of the inlet (1.14 $ug \cdot L^{-1}$).

**Table 13.** Summary statistics of dissolved and total metal concentrations measured in discrete samples for each sampling period and combined statistics.

| | Dissolved (ug·L$^{-1}$) | | | | | | | | Total (ug·L$^{-1}$) | | | | | | | |
|---|---|---|---|---|---|---|---|---|---|---|---|---|---|---|---|---|
| **Statistic** | **As** | **Cd** | **Cu** | **Cr** | **Pb** | **Se** | **Ag** | **Zn** | **As** | **Cd** | **Cu** | **Cr** | **Pb** | **Se** | **Ag** | **Zn** |
| **September** | | | | | | | | | | | | | | | | |
| n | 38 | 38 | 38 | 38 | 38 | 38 | 8 | 38 | 3 | 3 | 3 | 3 | 3 | 3 | 3 | 3 |
| MIN | 1.12 | 0.03 | 0.44 | 0.13 | 0.01 | 0.40 | 0.003 | 0.73 | 1.52 | 0.06 | 1.03 | 0.22 | 0.09 | 0.89 | 0.00 | 2.21 |
| AVE | 1.47 | 0.05 | 0.79 | 0.20 | 0.04 | 0.84 | 0.004 | 2.31 | 1.70 | 0.07 | 1.17 | 0.24 | 0.12 | 1.03 | 0.00 | 2.67 |
| MAX | 2.51 | 0.08 | 1.40 | 0.66 | 0.21 | 1.73 | 0.01 | 7.28 | 2.01 | 0.07 | 1.40 | 0.28 | 0.17 | 1.12 | 0.01 | 3.25 |
| STDEV | 0.23 | 0.01 | 0.28 | 0.09 | 0.03 | 0.27 | 0.001 | 1.47 | 0.27 | 0.01 | 0.20 | 0.03 | 0.04 | 0.12 | 0.00 | 0.53 |
| % rsd | 15.93 | 18.84 | 35.69 | 44.57 | 85.56 | 32.13 | 32.90 | 63.70 | 15.86 | 8.36 | 17.41 | 14.25 | 35.83 | 11.75 | 19.96 | 19.79 |
| MAX/WQC | 0.12 | 0.01 | 0.45 | 0.01 | 0.03 | 0.02 | 0.01 | 0.09 | NaN | NaN | NaN | NaN | NaN | NaN | NaN | NaN |
| **March** | | | | | | | | | | | | | | | | |
| N | 36 | 36 | 36 | 36 | 36 | 36 | 36 | 36 | 10 | 10 | 10 | 10 | 10 | 10 | 10 | 10 |
| MIN | 0.86 | 0.04 | 0.49 | 0.16 | 0.02 | NaN | 0.01 | 1.27 | 0.86 | 0.06 | 0.58 | 0.28 | 0.05 | NaN | 0.01 | 1.36 |
| AVE | 1.02 | 0.07 | 0.74 | 0.22 | 0.03 | NaN | 0.01 | 2.28 | 1.03 | 0.07 | 0.95 | 0.38 | 0.08 | NaN | 0.01 | 2.74 |
| MAX | 1.16 | 0.07 | 1.18 | 0.32 | 0.10 | NaN | 0.02 | 3.84 | 1.14 | 0.08 | 1.33 | 0.84 | 0.13 | NaN | 0.01 | 5.50 |
| STDEV | 0.07 | 0.01 | 0.19 | 0.03 | 0.01 | NaN | 0.003 | 0.67 | 0.08 | 0.00 | 0.25 | 0.17 | 0.02 | NaN | 0.00 | 1.18 |
| % rsd | 7.29 | 9.59 | 26.14 | 15.90 | 48.28 | NaN | 35.50 | 29.15 | 7.80 | 6.41 | 26.45 | 44.57 | 29.27 | NaN | 31.59 | 43.07 |
| MAX/WQC | 0.06 | 0.01 | 0.38 | 0.01 | 0.01 | NaN | 0.01 | 0.05 | NaN | NaN | NaN | NaN | NaN | NaN | NaN | NaN |
| **July** | | | | | | | | | | | | | | | | |
| n | 32 | 32 | 32 | 32 | 32 | 32 | 32 | 32 | 11 | 11 | 11 | 11 | 11 | 11 | 11 | 11 |
| MIN | 0.54 | 0.03 | 0.47 | 0.11 | 0.02 | NaN | 0.01 | 0.72 | 0.88 | 0.05 | 0.58 | 0.16 | 0.06 | NaN | 0.01 | 0.82 |
| AVE | 0.96 | 0.05 | 0.80 | 0.18 | 0.04 | NaN | 0.01 | 1.86 | 0.92 | 0.05 | 1.24 | 0.34 | 0.09 | NaN | 0.01 | 2.00 |
| MAX | 1.13 | 0.06 | 2.21 | 0.49 | 0.18 | NaN | 0.01 | 4.40 | 0.99 | 0.06 | 2.58 | 0.70 | 0.12 | NaN | 0.01 | 4.35 |
| STDEV | 0.10 | 0.01 | 0.37 | 0.07 | 0.03 | NaN | 0.002 | 1.03 | 0.04 | 0.00 | 0.70 | 0.13 | 0.02 | NaN | 0.00 | 1.19 |
| rsd% | 10.25 | 9.83 | 45.99 | 38.12 | 78.88 | NaN | 25.20 | 55.28 | 3.94 | 6.77 | 56.66 | 39.18 | 23.05 | NaN | 14.86 | 59.36 |
| MAX/WQC | 0.05 | 0.01 | 0.71 | 0.01 | 0.02 | NaN | 0.01 | 0.05 | NaN | NaN | NaN | NaN | NaN | NaN | NaN | NaN |
| **Totals** | | | | | | | | | | | | | | | | |
| n | 106 | 106 | 106 | 106 | 106 | 38 | 76 | 106 | 24 | 24 | 24 | 24 | 24 | 24 | 24 | 24 |
| MIN | 0.54 | 0.03 | 0.44 | 0.11 | 0.01 | 0.40 | 0.00 | 0.72 | 0.86 | 0.05 | 0.58 | 0.16 | 0.05 | 0.89 | 0.00 | 0.82 |
| AVE | 1.16 | 0.06 | 0.77 | 0.20 | 0.03 | 0.84 | 0.01 | 2.16 | 1.06 | 0.06 | 1.11 | 0.34 | 0.09 | 1.03 | 0.01 | 2.39 |
| MAX | 2.51 | 0.08 | 2.21 | 0.66 | 0.21 | 1.73 | 0.02 | 7.28 | 2.01 | 0.08 | 2.58 | 0.84 | 0.17 | 1.12 | 0.01 | 5.50 |
| STDEV | 0.14 | 0.01 | 0.28 | 0.06 | 0.02 | 0.27 | 0.00 | 1.06 | 0.08 | 0.00 | 0.45 | 0.14 | 0.02 | 0.12 | 0.00 | 1.10 |
| % rsd | 11.94 | 12.60 | 35.81 | 32.20 | 72.94 | 32.13 | 30.70 | 49.14 | 7.88 | 6.81 | 40.75 | 39.45 | 27.40 | 11.75 | 22.49 | 46.07 |
| MAX/WQC | 0.12 | 0.01 | 0.71 | 0.01 | 0.03 | 0.02 | 0.004 | 0.09 | NaN | NaN | NaN | NaN | NaN | NaN | NaN | NaN |

| | |
|---|---|
| N | Number of samples |
| MIN | Minimum measured concentration |
| AVE | Average measured concentration |
| MAX | Maximum measured concentration |
| STDEV | Standard deviation |
| % rsd | Relative standard deviation (standard deviation/average) in units of percent |
| MAX/WQC | Maximum concentration/water quality criterion |
| NaN | Not a number (no data) |

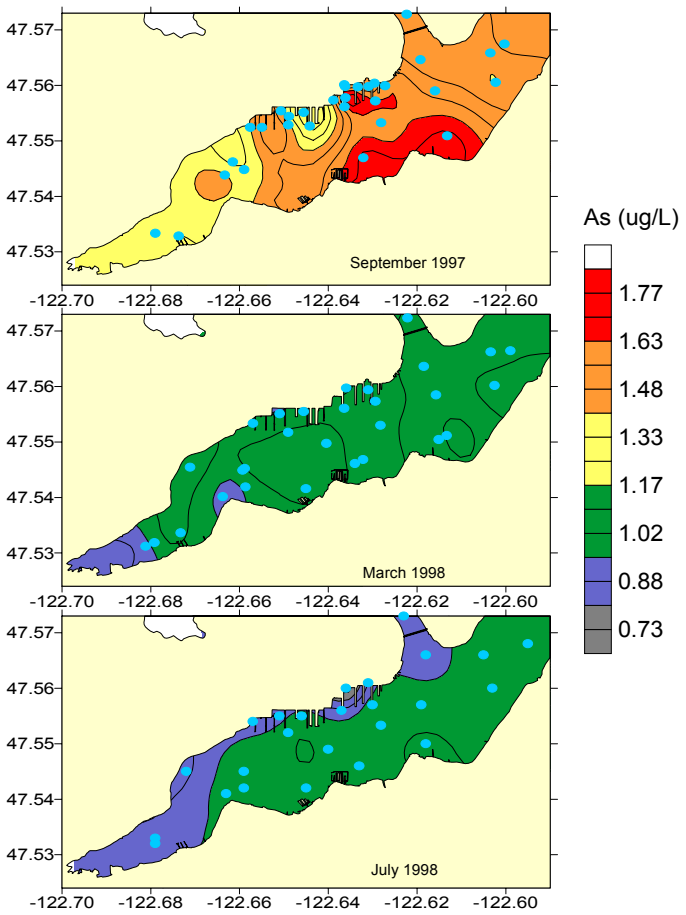


**Figure 35.** Dissolved arsenic concentration (ug·L$^{-1}$) pooled from all discrete sample data for the entire survey period.

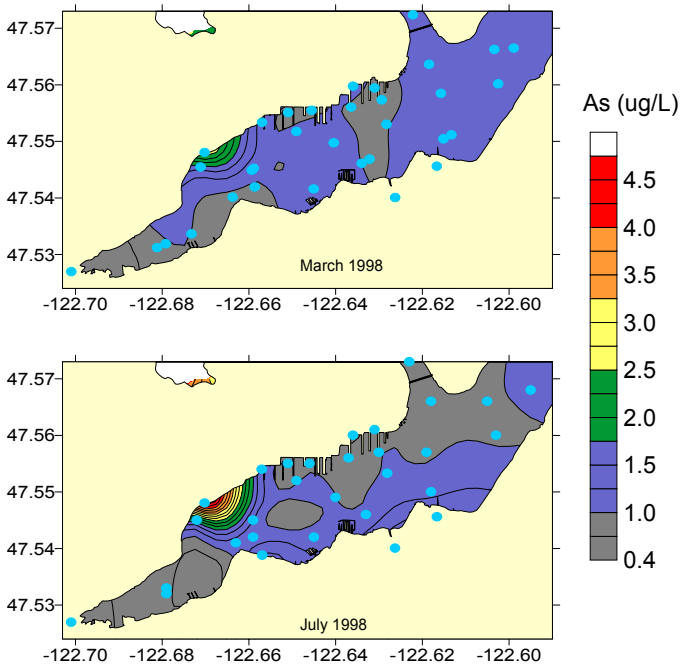


**Figure 36.** Hypothetical distribution of dissolved arsenic (ug·L$^{-1}$) in March and July 1998 showing POTW and creek effluent data pooled with receiving water data.

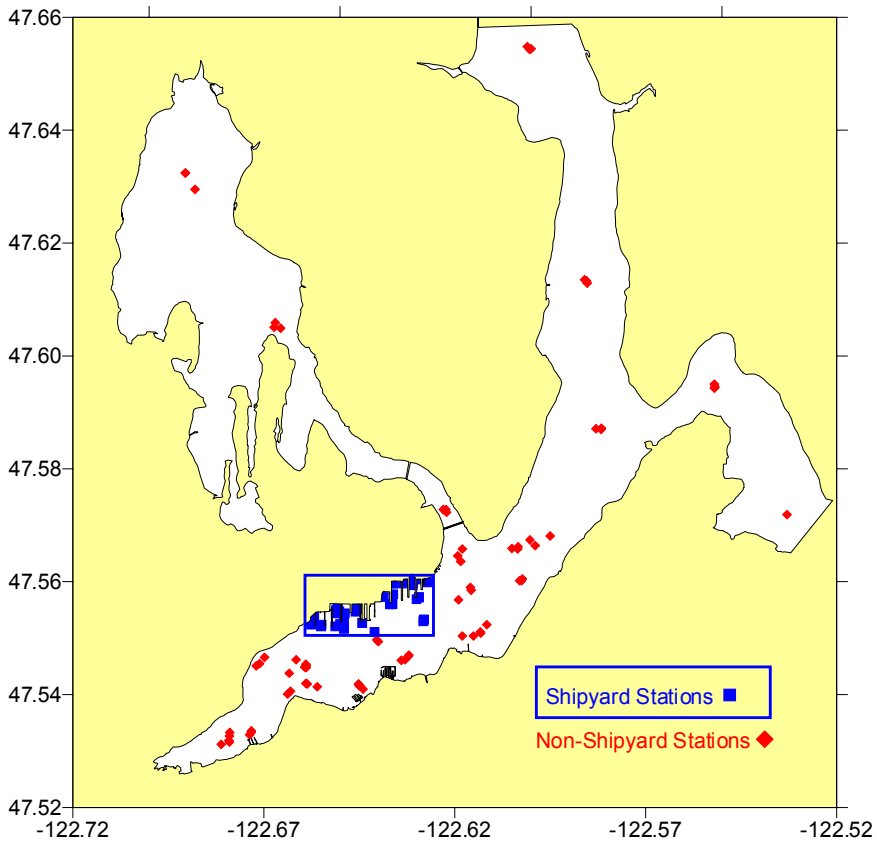


**Figure 37.** Discrete sampling sites used for statistical evaluations between shipyard and non-shipyard average contaminant concentrations.

### *Cadmium*

Dissolved cadmium ranged from, 0.05 to 0.08 ug·L$^{-1}$ for all surveys and averaged 0.06 ug·L$^{-1}$ (Table 13). These concentrations were well below marine chronic water quality standard published for the State of Washington (Chapter 173-201A WAC) of 9.3 ug·L$^{-1}$. Average concentrations were highest in March and statistically different than the average values for either September or July. July and September averages were not statistically different. The ratio of dissolved to total metal for all surveys averaged 0.94, indicating that nearly all the metal in the receiving water was in the dissolved form. This ratio is consistent with the published marine conversion factor of 0.994.

The spatial distribution of cadmium was variable for the three time periods (Figure 38). Its distribution in September showed elevated levels within the entire pier area of the shipyard as well as in back-bay. Both the March and July distributions were relatively uniform though the March values were elevated throughout. There was also a localized high of cadmium in the back-bay in March similar to that seen in September.

Cadmium concentrations measured in both the Creeks (0.1 ug·L$^{-1}$) and POTWs (0.03 ug·L$^{-1}$) were significantly lower than those found in the inlet. The source of the localized highs of cadmium observed in the back-bay do not appear to come from Gorst Creek, though the limited sampling of the creeks precludes a definitive conclusion. For the three survey time periods, the average dissolved cadmium concentration measured at stations within the shipyard area of 0.058 ug·L$^{-1}$

was statistically no different than the average value measured in the rest of the inlet (0.057 ug·$L^{-1}$).

### *Chromium*

Dissolved chromium concentrations ranged from 0.11 to 0.66 ug·$L^{-1}$ and averaged 0.20 ug·$L^{-1}$ for the three time periods (Table 13). These concentrations were below marine chronic water quality standard published for the State of Washington (Chapter 173-201A WAC) of 50.0 ug·$L^{-1}$ (hexavalent chrome only). The highest average concentration was observed in March. This average was significantly higher than that measured in July but not September. The ratio of dissolved to total metal for all surveys averaged 0.54, indicating that about half the metal in the receiving water was in the dissolved form. Unlike the other metals measured, the ratio of dissolved to total is not consistent with the published marine conversion factor of 0.993, though this ratio is specific to chrome VI.

There was no consistent spatial pattern of dissolved chromium for the three visits (Figure 39). In September, chromium was relatively elevated along the northern shoreline with localized highs in the western pier area as well as pier 3 area. In contrast, the March distribution was more uniform throughout the inlet. In July, there was a localized high at the mouth. The distributions of total chromium (not shown) were similar though the highs appeared more defined, probably as a result of the more limited nature of the data set.

On average, chromium values measured in the creeks were roughly four times higher than the average value measured in the inlet and thus appears to be a source to the inlet. This difference was statistically significant. Though average concentrations measured at the POTWs (0.21 ug·$L^{-1}$) were not statistically different than those measured in the inlet, measurements made in March were roughly 50% higher than that of receiving waters indicating the variable nature of this source. For the three survey time periods, the average dissolved chromium concentrations measured at stations within the shipyard area of 0.19 ug·$L^{-1}$ were not significantly different than the average value measured in the rest of the inlet of 0.20 ug·$L^{-1}$.

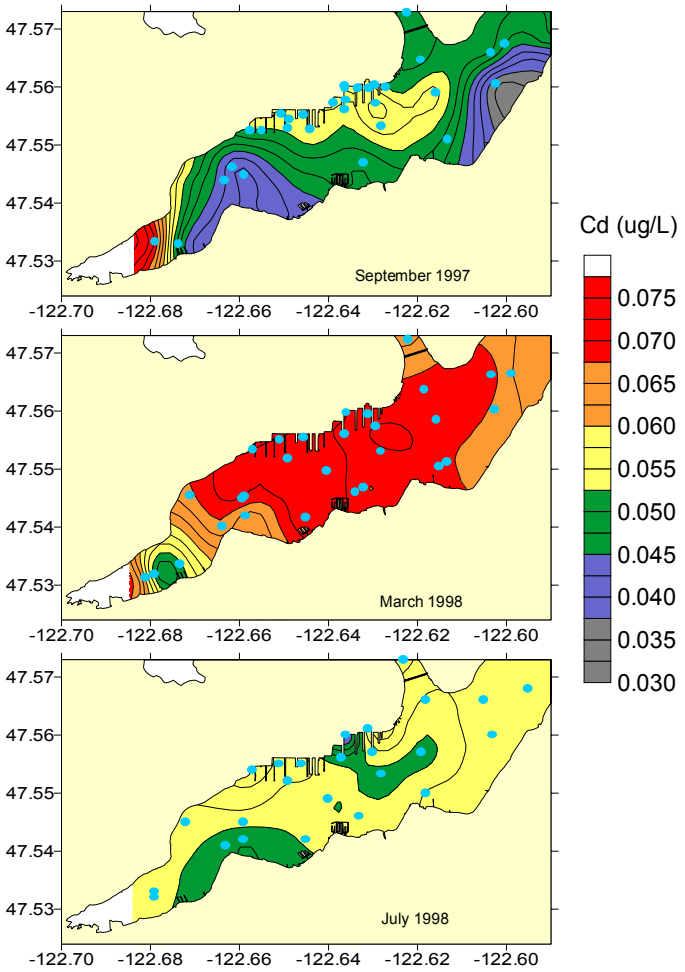


**Figure 38.** Dissolved cadmium concentration (ugL-1) pooled from all discrete sample data for the entire survey period.

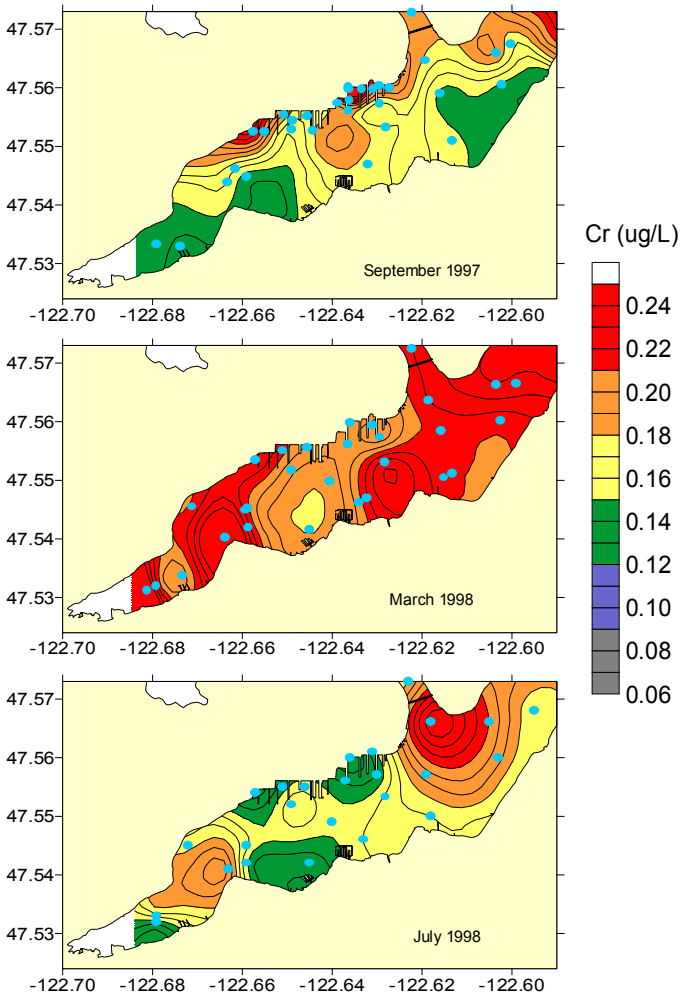


**Figure 39.** Dissolved chromium concentration (ug·L$^{-1}$) pooled from all discrete sample data for the entire survey period.

## *Copper*

Dissolved copper concentrations ranged from 0.44 to 2.21 ug·L$^{-1}$ and averaged 0.77 ug·L$^{-1}$ for the three time periods (Table 13). These concentrations were below marine chronic water quality standard published for the State of Washington (Chapter 173-201A WAC) of 3.1 ug·L$^{-1}$. The highest average concentrations were observed in March though the differences amongst the surveys were not statistically significant. The maximum concentration was measured in July. The ratio of dissolved to total metal for all surveys averaged 0.84, indicating that most of the metal in the receiving water was in the dissolved form. This ratio is consistent with the published marine conversion factor of 0.83.

The spatial distribution of copper was consistent for all three time periods. On all occasions there were localized high values along the shipyard piers, particularly in the western piers and in the vicinity of the Bremerton POTW discharge (Figure 40). Because of the pooled nature of the data, it is not clear if the POTW discharge or the large number of ships docked in the area is the source of the higher copper values found within the western pier area. The average Cu concentration measured at the POTWs (3.78 ug·L$^{-1}$) was significantly higher than the average measured in the

inlet. This average discharge value was above the receiving water quality limit of 3.1 ug·L$^{-1}$. The average copper level in the creeks (0.38 ug·L$^{-1}$) was significantly lower that the average receiving water concentration, and thus not apparently a source of copper. For the three survey time periods, the average dissolved and total copper concentrations measured at stations within the shipyard area, 1.03 ug·L$^{-1}$ and 1.46 ug·L$^{-1}$, respectively were significantly higher than the corresponding average values measured in the rest of the inlet, 0.64 ug·L$^{-1}$ and 0.81 ug·L$^{-1}$, respectively.

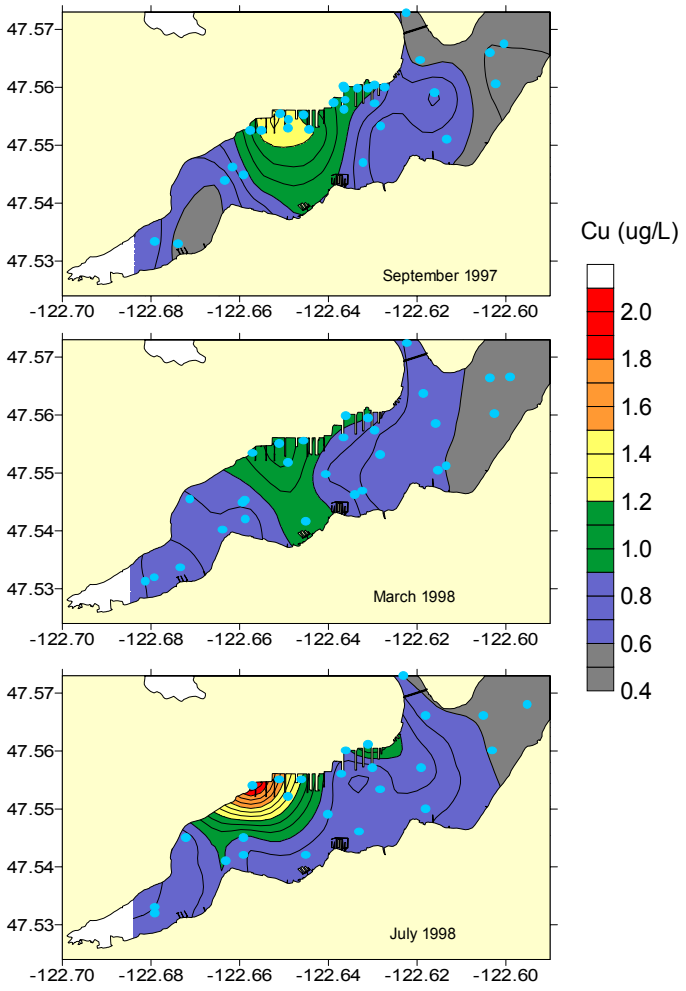


**Figure 40.** Dissolved copper concentration (ug·L$^{-1}$) pooled from all discrete sample data for the entire survey period.

## *Lead*

For all time periods, dissolved lead concentrations ranged from 0.01 to 0.21 ug·L$^{-1}$ and averaged 0.03 ug·L$^{-1}$ (Table 13). These concentrations were well below marine chronic water quality standard published for the State of Washington (Chapter 173-201A WAC) of 8.1 ug·L$^{-1}$. The highest average and maximum concentrations were observed in September, though the difference in averages amongst the surveys was not statistically significant. The ratio of dissolved to total metal for all surveys averaged 0.40, indicating that less than half the metal in the receiving water was in the dissolved form. This ratio is inconsistent with the marine conversion factor of 0.951 published in Chapter 173-201A WAC. The reasons for this discrepancy are unknown.

The distribution of dissolved lead in the inlet (Figure 41) was generally uniform on each visit except for a couple of isolated highs. In September, a localized high was observed in the north-central portion of the inlet. In July, a localized high was observed near the Bremerton POTW outfall. The Bremerton POTW was clearly a source of dissolved lead to the inlet with average concentrations that were about ten times higher than the receiving water average. Creek concentrations were, on average, twice that found in the inlet though there was considerable range in these data suggesting a variable nature to this source. Even with this variability, both the POTW and creek average values were significantly different than the average inlet value. For the three survey time periods, the average dissolved and total lead concentrations measured at stations within the shipyard area were not significantly different than the corresponding average values measured in the rest of the inlet.

The distribution of total lead concentration differed from that of dissolved lead. Though the dissolved distribution was fairly uniform in March, the total lead distribution (Figure 42) showed a localized high in the south-central part of the inlet. In addition to high total lead level seen in the vicinity of the Bremerton POTW in July, there was also a high value observed inside pier 3 of the shipyard which was not seen in the dissolved distribution. Because these distributions were based on only ten pooled data points, these distributions are slightly exaggerated.

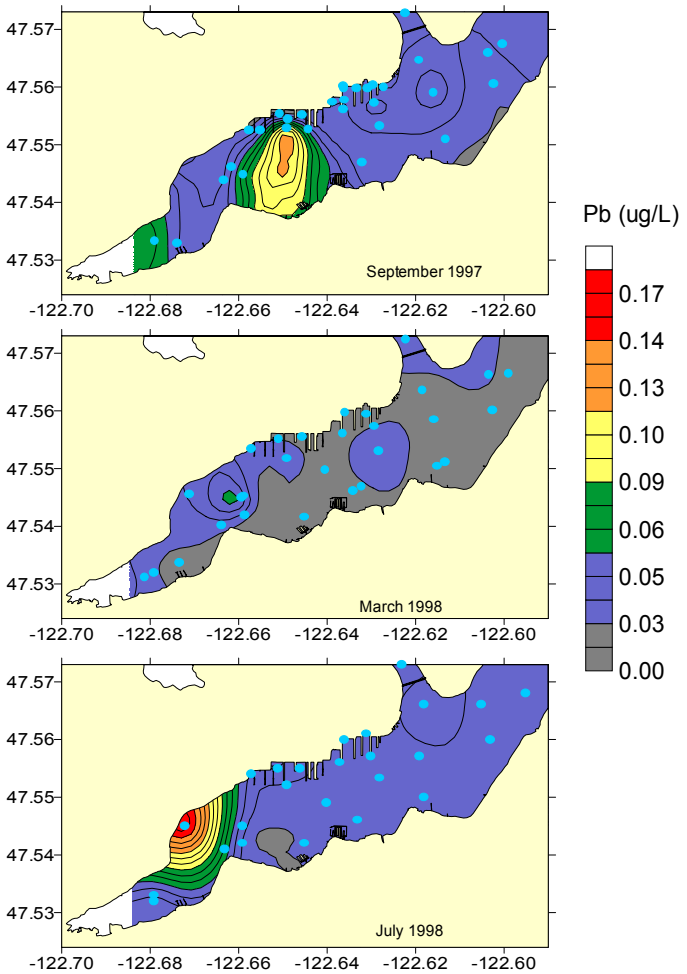


**Figure 41.** Dissolved lead concentration (ug·L$^{-1}$) pooled from all discrete sample data for the entire survey period.

## *Selenium*

Dissolved selenium concentrations ranged from the detection limit of 0.4 to 1.73 ug·L$^{-1}$ and averaged 0.84 ug·L$^{-1}$ in September. Measurements made for the other two time periods were at or below the method detection limit of 0.3 ug·L$^{-1}$. September concentrations were well below the marine chronic water quality standard published for the State of Washington (Chapter 173-201A WAC) of 71 ug·L$^{-1}$. Based on only three samples in September, the ratio of dissolved to total metal for averaged 0.76, indicating that most of the metal in the receiving water was in the dissolved form. This ratio is low relative to the marine conversion factor of 0.998 published in Chapter 173-201A WAC, though the reasons for this are not known.

The distribution of selenium was uniform throughout the inlet in September except for a localized high on the eastern side of the shipyard pier 3. However, there was no difference between average values measured within the shipyard area and those measured in the rest of the inlet. Samples obtained in the creeks and POTWs for the three periods ranged from the detection limit to about 4.4 ug·L$^{-1}$ and averaged 1.72 ug·L$^{-1}$. Thus both the creeks and POTWs were a source of selenium to the inlet.

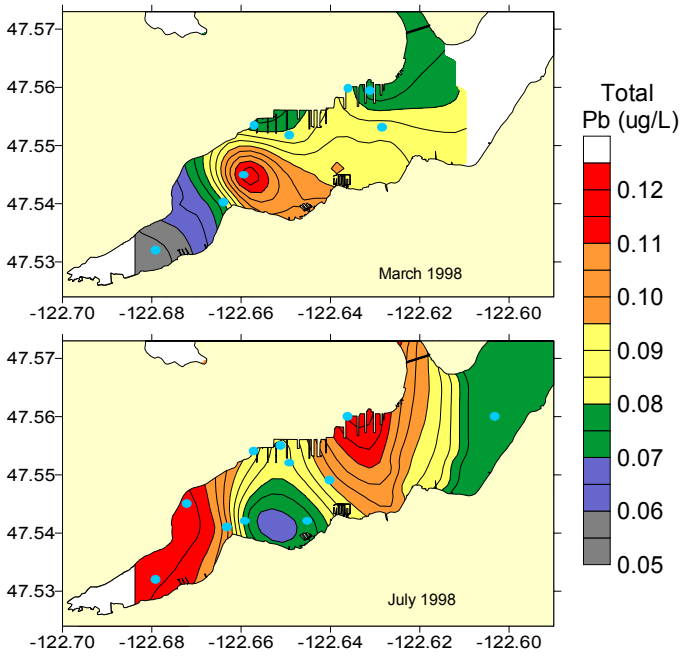


**Figure 42.** Total lead concentration (ug·L$^{-1}$) pooled from all discrete sample data for the entire survey period.

## *Silver*

Dissolved silver ranged from the method detection limit of 0.003 to 0.018 ug·L$^{-1}$ and averaged 0.008 ug·L$^{-1}$ for the three survey periods. These concentrations were well below marine acute (no chronic value) water quality standard published for the State of Washington (Chapter 173-201A WAC) of 1.9 ug·L$^{-1}$. The highest average and maximum concentrations were observed in March though the difference between March and July averages were not statistically different. However, these survey averages were both statistically higher than the average measured in September.

The ratio of dissolved to total metal for all surveys averaged 0.78, indicating that most of the metal in the receiving water was in the dissolved form. This ratio is consistent with the published marine conversion factor of 0.85.

The distribution of dissolved silver varied on each visit. While the distribution was uniform in September, there was a general increase into the back of the inlet in March with a localized high in the western pier area of the shipyard (Figure 43). In July, a localized high was again seen in the western shipyard pier area along with a few other localized highs out by the mouth and along the southwestern shore. No silver data were obtained from the creeks or POTWs though it is expected that the POTWs would normally be a source of silver. The average value of dissolved silver calculated for the shipyard region was not statistically different than for the rest of the inlet.

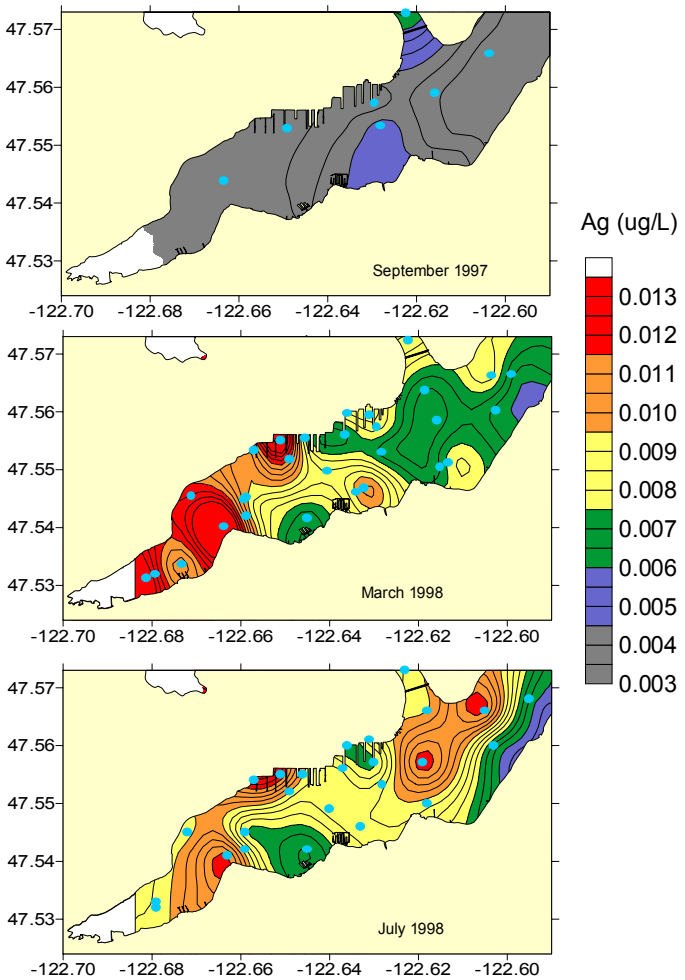


**Figure 43.** Dissolved silver concentration (ug·L$^{-1}$) pooled from all discrete sample data for the entire survey period.

## *Zinc*

Dissolved zinc concentrations ranged over an order of magnitude from 0.72 to 7.28 ug·L$^{-1}$ and averaged 2.16 ug·L$^{-1}$ for the three time periods. These concentrations were below marine chronic water quality standard published for the State of Washington (Chapter 173-201A WAC) of 81.0 ug·L$^{-1}$. The highest average concentration was observed in September though the maximum

concentration was observed in July (Table 13). Though the highest average value was measured in September, only the March survey average was statistically different than the July survey. The ratio of dissolved to total metal for all surveys averaged 0.87, indicating that most of the metal in the receiving water was in the dissolved form. This ratio is reasonably consistent with the published marine conversion factor of 0.946.

The spatial distribution of dissolved zinc showed a somewhat consistent pattern on all three occasions (Figure 44) and somewhat similar to that seen for copper. Localized highs were observed in the north-central portion of the inlet on all occasions while an additional high was seen out at the mouth in July. The highs inside extended the full length of the shipyard pier area in September and to a lesser extent on the other two surveys. The average dissolved (3.09 ug·L$^{-1)}$ and total (3.05 ug·L$^{-1}$) zinc concentrations measured within the shipyard region were statistically higher than the corresponding average values measured in the rest of the inlet, 1.69 ug·L$^{-1}$ and 1.84 ug·L$^{-1}$, respectively.

Dissolved zinc concentrations measured at both POTWs were, on average, a factor of 10 higher than the average value measured in the inlet, indicating that they are a source to the inlet. On the other hand, creek concentrations were about half the average receiving water value and are likely not a major source of zinc. The difference in the average inlet value with the average values measured for the POTWs and creeks, was statistically significant.

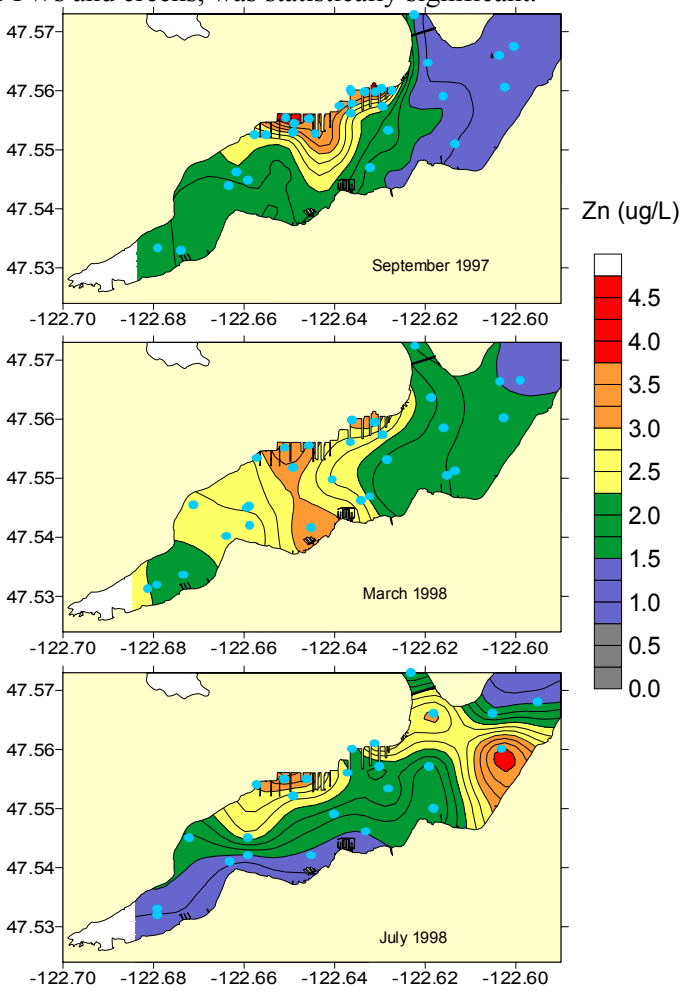


**Figure 44.** Dissolved zinc concentration (ug·L$^{-1}$) pooled from all discrete sample data for the entire survey period.

### *Summary of Metals*

A summary of the metals data is shown in Table 14. All metal concentrations measured in the inlet were well below water quality standards set by the State of Washington and EPA. The maximum receiving water metal concentration closest to its water quality standard was dissolved copper, measured at 71% of the allowed limit. The criteria for these substances were set by the state to insure protection of aquatic communities, public health, and characteristic beneficial uses of the inlet (Chapter 173-201A WAC). As such, the waters of Sinclair Inlet were in full compliance with these goals for the metals measured.

Most of the metals measured were found primarily (>75%) in the dissolved phase. Only chromium and lead showed appreciable levels of the particulate (or colloidal) phase of the metal. This is consistent with other measurements made in Puget Sound waters (Paulson et al., 1988).

Seasonal variations were significant for arsenic, cadmium, chromium, silver and zinc while copper and lead showed no significant seasonality. Selenium data were insufficient to determine seasonal variations. Though the seasonal signal was not consistent for all metals, average values were typically higher in the wet season (March and/or September) than in the dry season (July). Of the metals showing this seasonal signal, only chromium had a significant creek source though arsenic and zinc had a fresh water source from the POTWs.

The major source regions for metals were in the vicinity of the POTW and creek discharges, and within two pier areas of the shipyard. Arsenic, copper, lead, selenium, and zinc were all significantly elevated in the POTW discharges relative to values measured in the inlet. Chromium, lead, and selenium were significantly elevated in the creeks relative to values measured in the inlet. However, the impact of these sources on the inlet distribution was clearly seen only for copper and lead, and then, not on every visit. The inability to clearly and consistently observe these sources is related to both the discrete nature of the sampling and the variability in the source strength.

The western shipyard pier area, the site of the mothball fleet was a source area for chromium, copper, silver, and zinc. The area east of pier 3 was elevated in all metals except for silver and dissolved lead. However, copper and zinc were the only metals that were significantly higher within the shipyard area than outside. These were also the only metals showing a relatively consistent spatial pattern on each visit suggesting a chronic source. The likely source of these two metals are the hull paint and cathodic protection anodes for the ships located in the western area and the dry dock discharges along pier 3. The proximity of the Bremerton POTW to the mothball fleet together with the tidal flow direction complicates quantifying the relative source strength of the two potential sources.

**Table 14.** Summary of metals data.

| Metal | Dissolved Fraction | Exceeds Water Quality Criteria | Seasonal Variations | POTW Source | Creek Source | Shipyard Region Source |
|---|---|---|---|---|---|---|
| Arsenic | 0.97 | No | Sep>Mar>Jul | Yes | No | No |
| Cadmium | 0.94 | No | Mar>Sep~Jul | No | No | No |
| Chromium | 0.54 | No | Mar>Jul~Sep | No | Yes | No |
| Copper | 0.83 | No | None | Yes | No | Yes |
| Lead | 0.40 | No | None | Yes | Yes | No |
| Selenium | 0.76 | No | NaN | Yes | Yes | No |
| Silver | 0.85 | No | Mar~Jul >Sep | NaN | NaN | No |
| Zinc | 0.87 | No | Sep~Mar>Jul | Yes | No | Yes |

## Polynuclear Aromatic Hydrocarbons (PAH)

Concentrations of total PAH (TPAH) ranged from below detection (~2 to 13 $ng \cdot L^{-1}$) to 3700 $ng \cdot L^{-1}$ (Table 15). The highest concentration was observed in the middle of the Port Orchard Channel in September while the next highest concentration of 530 $ng \cdot L^{-1}$ was measured along the southwestern shore in March. In July a maximum value of 170 $ng \cdot L^{-1}$ was found along the south-central shoreline. None of the maxima were observed in a location where there was an obvious source for the PAH. The patchiness seen in the location of these high values was seen for throughout the inlet on each survey resulting in a highly variable spatial distribution from visit to visit (Figure 45). Though there was variability in the spatial distribution from survey to survey, there were no significant differences with season.

The State of Washington does not specify a water quality standard for PAH but rather, defers to standards "in consideration of USEPA Quality Criteria for Water, 1986, and as revised" (Chapter 173-201A WAC). The latest EPA recommended national water quality criteria for PAH published in April 1999 are shown in Table 16 below. There was only one instance in which any of the water quality criteria for individual PAH were surpassed. In the sample containing the highest TPAH, the concentration of chrysene was measured at 26 $ng \cdot L^{-1}$. However, it should be noted that the method detection limits varied between 2.3 and 13.6 $ng \cdot L^{-1}$ for all analytes and all samples, and there is a possibility that a criterion was surpassed but listed as non-detectable. This is true even when using the most sensitive methods available and where the laboratory reported qualified values as low as 0.2 $ng \cdot L^{-1}$.

Of the 48 receiving water samples taken and analyzed for PAH, only 19 had a definitive petrogenic component to them. The remainder of the samples had no definitive hydrocarbon source and was primarily composed of background pyrogenic PAH. Of the 19 samples having some petrogenic source, the apportionment to petroleum hydrocarbons ranged from 30% up to 90% though most were above 50%. As mentioned previously, many of these samples had no obvious physical source for the hydrocarbons. A comparison of PAH samples measured inside the shipyard region with those measured outside showed no statistically significant difference in mean values even when removing the single high value measured outside the inlet. Of the 19 samples having some petrogenic component to them, 12 were found outside the shipyard region while 7 were found within.

Ten discrete samples taken from the POTWs and in the creeks were analyzed for PAH. The POTW samples ranged from 107 to 876 $ng \cdot L^{-1}$ TPAH while the creeks ranged from non-detect (~2 to 13 $ng \cdot L^{-1}$) to 22 $ng \cdot L^{-1}$ TPAH. All but one of the POTW samples showed a petrogenic source while all the creek samples showed no definitive PAH source type. For all three time periods, the POTWs acted as a source to the inlet while the creek concentrations always were below those of the receiving water. However, the source of PAH from the Bremerton POTW did not appear to produce consistently high levels of TPAH in the inner portion of the inlet.

**Table 15.** TPAH ($ng \cdot L^{-1}$) data for all discrete samples collected on this project. Sample ID suffix "R" refers to receiving water data and "E" to creek or POTW effluent.

| September Sample ID | TPAH ($ng \cdot L^{-1}$) | March Sample ID | TPAH ($ng \cdot L^{-1}$) | July Sample ID | TPAH ($ng \cdot L^{-1}$) |
|---|---|---|---|---|---|
| PS-01-02-R | 13.0 | PS10-01-R | 132.15 | PS16-01-R | 13.39 |
| PS-01-04-R | 3700.0 | PS10-02-R | 19.97 | PS16-03-R | 18.43 |
| PS-01-09-R | 36.0 | PS10-04-R | 16.41 | PS16-04-R | 24.46 |
| PS-01-10-R | 29.0 | PS10-06-R | 18.79 | PS16-05-R | 25.87 |
| PS-01-11-R | 27.0 | PS10-09-R | 31.47 | PS16-06-R | 18.68 |
| PS-05-10-R | 100.00 | PS10-10-R | 32.37 | PS16-07-R | 19.10 |
| PS-05-14-R | 48.00 | PS10-11-R | 44.73 | PS16-08-R | 24.74 |
| PS-05-20-R | 330 | PS11-02-R | 32.06 | PS16-09-R | 21.13 |
| PS-07-01-R | 380.00 | PS11-04-R | 32.69 | PS16-11-R | 54.22 |
| PS-07-03-R | 42 | PS11-06-R | 36.38 | PS16-12-R | 80.34 |
| PS-07-09-R | 35.00 | PS11-08-R | 40.84 | PS17-01-R | 23.34 |
| PS-07-14-R | 51.00 | PS11-10-R | 26.31 | PS17-06-R | 87.31 |
| PS04-01-E | 900.00 | PS11-12-R | 31.57 | PS17-08-R | 176.63 |
| | | PS11-14-R | 60.08 | PS17-10-R | 66.07 |
| | | PS15-01-R | 580.30 | PS17-11-R | 34.24 |
| | | PS15-02-R | 74.73 | PS17-12-R | 33.05 |
| | | PS15-04-R | 49.53 | PS18-12-E | 12.79 |
| | | PS15-05-R | 339.79 | PS18-13-E | 27.42 |
| | | PS15-06-R | 117.88 | PS18-14-E | 14.49 |
| | | PS15-08-R | 187.30 | PS18-15-E | 110.76 |
| | | PS15-01-E | 41.67 | PS18-16-E | 176.02 |
| | | PS15-02-E | 16.420 | | |
| | | PS15-03-E | 851.080 | | |
| | | PS15-04-E | 955.53 | | |

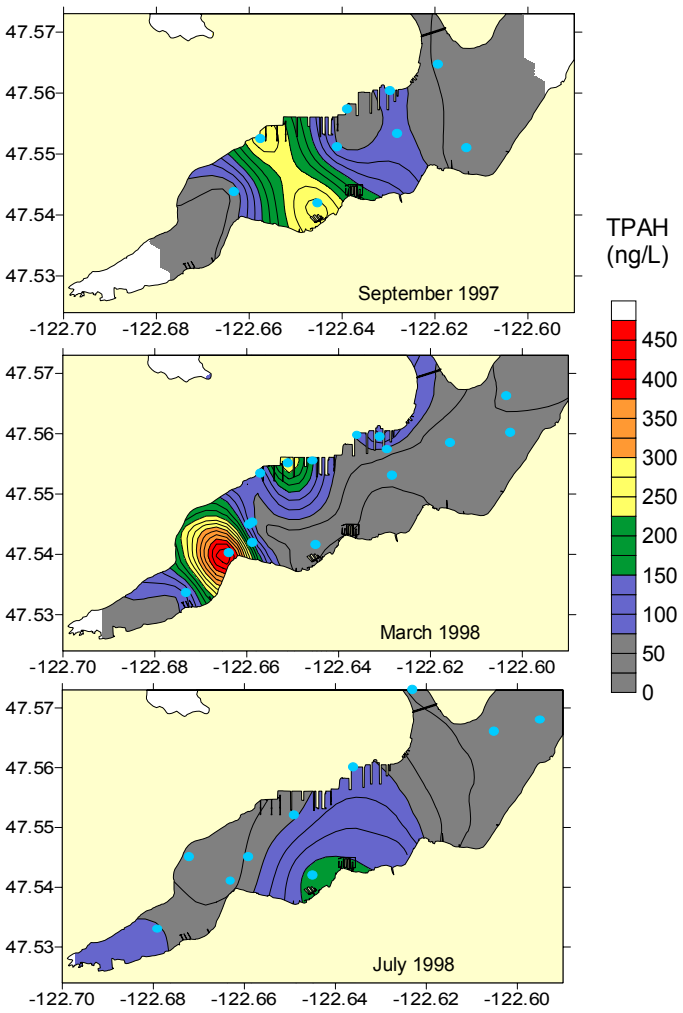


**Figure 45.** Distribution of total PAH ($ng \cdot L^{-1}$) $^{pooled}$ from all discrete sample data for the entire survey period.

**Table 16.** Recommended national water quality criteria for PAH by EPA as of April 1999.

| *PAH Analyte* | *EPA Criterion ($ng \cdot L^{-1}$)* |
|---|---|
| Acenaphthene | 1,200,000 |
| Acenaphthylene | na |
| Anthracene | 9,600,000 |
| Benzo(a)Anthracene | 4.4 |
| Benzo(a)Pyrene | 4.4 |
| Benzo(b)Fluoranthene | 4.4 |
| Benzo(ghi)Perylene | 4.4 |
| Benzo(k)Fluoranthene | 4.4 |
| Chrysene | 4.4 |
| Dibenzo(a,h)Anthracene | 4.4 |
| Fluoranthene | 300,000 |
| Fluorene | 1,300,000 |
| Indeno(1,2,3-cd)Pyrene | 4.4 |
| Naphthalene | na |
| Phenanthrene | na |
| Pyrene | 960,000 |

# 6.0 CONCLUSIONS

The data collected during this project provide the most comprehensive view to date of water quality in the Sinclair Inlet. The field effort was successful in establishing baseline water quality conditions throughout the inlet, identifying locations and extent of contaminants from storm water sources, and in collecting water current data for use in validating a hydrodynamic model for the inlet. This success was derived from the ability to make integrated, synoptic measurements at the necessary spatial and temporal scales to assess the processes affecting water quality distributions. The key findings from this effort are as follows:

**Circulation and Hydrography.** A complex gyral circulation pattern is generated at the mouth by interaction with the tidal flow through the Port Washington Narrows. This circulation dominates the flow and enhances flushing at mouth as a result of higher current speeds and a continuous outflow along the northern shore. Inside the inlet, circulation is influenced by both tides and estuarine conditions. The combination of freshwater sources that were higher in winter as reflected in the lower salinity, set up axial, lateral, and vertical gradients in the hydrography. These conditions combined with lower tidal flow lead to longer flushing times. Current and salinity data collected during these surveys allowed calculation of residence times. The residence time calculated for Sinclair Inlet was 57 days and for Dyes Inlet was 11 days.

**Conventional Water Quality Parameters.** Conventional measures of water quality of the inlet can be characterized as conditionally good. On average, the levels of these parameters were comparable to other estuarine environments. The term conditionally is used because there was visual evidence of large plankton blooms and exceptionally high chl-*a* levels seen inside the inlet on all occasions. These conditions also generated high oxygen, pH, and increased TSS levels as well. These are signs of eutrophication that appear to be driven by nutrient influx from the Bremerton POTW in the inner portion of the inlet. The nutrient source within this region of reduced circulation and mixing provides the necessary conditions to cause the high production.

While the nutrient flux to the inlet was greatest in winter, light limiting conditions keep the production levels in check. There was one small region along the south shore at the head of the inlet that had dangerously low oxygen levels presumably as a result of organic decomposition. This condition was observed on only one occasion and its extent in space and time is not fully known.

.

**Nutrients.** Nutrient distributions were influenced by inflow from the POTWs though silica was found at comparable levels in the creeks. Nutrient levels were highest in the inner portion of the inlet where the Bremerton POTW discharges into a region of lower flow and higher residence time. This condition enhanced primary production to exceptionally high levels as evidenced by large plankton blooms. The concentrations observed in the inlet in winter were considerably higher in winter than summer. The higher levels result primarily from increased mass loading by the Bremerton POTW with its higher winter concentrations and flow rates.

**Metals.** All metal concentrations measured in the inlet were well below water quality standards set by the State of Washington and EPA. The distribution of metals showed sources in the vicinity of the POTW and creek discharges, and within two pier areas of the shipyard, specifically the western pier area of the mothball fleet and along pier 3. Arsenic, copper, lead, selenium, and zinc were all significantly elevated in the POTW discharges relative to values measured in the inlet. Chromium, lead, and selenium were significantly elevated in the creeks relative to values measured in the inlet. The western shipyard pier area, the site of the mothball fleet was a source area for chromium, copper, silver, and zinc. The area east of pier 3 was elevated in all metals except for silver and dissolved lead. However, only copper and zinc were the only metals that were significantly higher within the shipyard area than outside. The likely source of these two metals are hull paint and cathodic protection anodes for the ships located in the western area and the dry dock discharges along pier 3. Though the seasonal signal was not consistent for all metals, average values were typically higher in the wet season than in the dry season. However, though the low levels overall indicate that the impact from stormwater is small.

**PAH.** All PAH concentrations measured in the inlet were well below water quality standards set by the EPA and adopted by the State of Washington. One sample measured outside the inlet contained a concentration of chrysene that was a factor of six above its limit of 4.4 $ng \cdot L^{-1}$. The general distribution of PAH was patchy and did not directly correspond to obvious sources. There was not obvious impact of stormwater on the distribution. The majority of samples (60%) contained PAH derived from background pyrogenic sources while 40% had a source derived at least partially from petrogenic sources.

There was no statistical difference between mean TPAH concentrations inside the shipyard region with those measured outside. The POTWs are a source of PAH to the inlet but its impact on the spatial distribution was not observed. The few creek measurements made suggest that they are not a source of PAH.

# 7.0 REFERENCES


Albertson, S.L., Newton, J.A., Eisner, L.B., Janzen, C.D., and Bell, A.B. (1995). *Sinclair and Dyes Inlet Seasonal Monitoring Report*, Report to the Washington State Department of Ecology, Environmental Investigations and Laboratory Services Program, Olympia, Washington.

Armstrong, F.A.J., Stearns, C.A., and Strickland, J.D.H. (1967). The measurement of upwelling and subsequent biological processes by means of the Technicon Autoanalyzer and associated equipment. In: Deep-Sea Research, 14, pp.381-389.

ASTM (1995) American Society for Testing and Materials (ASTM) manual, Biological Effects & Environmental Fate; Biotechnology; Pesticides Section, D 3731-87, Volume 11.05, Fluorometric method for chlorophyll a.

Bernhardt, H., and Wilhelms, A. (1967). The continuous determination of low level iron, soluble phosphate and total phosphate with the AutoAnalyzer. In: Technicon Symposia, I, pp. 385-389.

Bowden K.F. (1966). Mixing Processes in Estuaries. In: Estuarine Transport Processes (Kjerfve B. 1978), University of South Carolina Press, p. 11-36.

Chadwick, D.B, and M.H. Salazar (1991). Integrated measurement technologies for monitoring the marine environment. In: Proceedings of Oceans 91 Meeting, 1-3 October, 1991, Oceanic Engineering Society of IEEE, 91CH3063-5, p. 343-350.

Department of Ecology, Washington State, Chapter 173-201A WAC (1997). Water Quality Standards for Surface Waters of the State of Washington.

IEEE (1980). 1978 Practical Salinity Scale Equations, from IEEE. In: Journal of Oceanic Engineering, 5, pp 14.

Fisher, H.B. (1972). *Mass transport mechansinsm in partially stratified estuaries.* In: Journal of Fluid Mechanics, 53, 617-687.

Fisher, H.B., List, E.J., Koh, R.C.Y., Imberger, J., and Brooks, N.H. (1979*). Mixing in Inland and Coastal Waters.* Academic Press, Inc., Orlando, Florida, 32887, pp. 483.

Katz, C.N., and D.B. Chadwick (1993). Synoptic Mapping and Modeling of a Sewage Outfall Plume. In: Proceedings of the Marine Technology Society, 1993, p. 207-215.

Katz, C.N., Chadwick, D.B., and Douglas, G.S. (1991). Real-time Fluorescence Measurements Intercalibrated with GC-MS. In: Proceedings of Oceans 91 Meeting, 1-3 October, 1991, Oceanic Engineering Society of IEEE, 91CH3063-5, p. 351-358.

Katz, C.N., D.B. Chadwick, and L. Skinner (1995). Input of Polynuclear Aromatic Hydrocarbons to San Diego Bay from Creosote Pilings, In: Proceeding of Oceans 95 Meeting, October 1995, p. 17722-1729.

Lapota, D., D. Chadwick, C.N. Katz, B. Davidson, A. Patterson, and D. Duckworth (1993). 1993 Fall, Winter, Spring, and Summer Seawater Characteristics in San Diego Bay: Biological, Optical, Chemical, and Physical Measurements, Report to the Naval Research Laboratory Remote Sensing Division, December 1993, pp. 45.

Lavelle, J.W., H.O. Mofjeld, E. Lempriere-Doggett, G.A. Cannon, D.J. Pashinski, E.D. Cokelet, L.Lytle, and S.Gill (1988). A Multiply-Connected Channel model of Tides and Tidal Currents in Puget Sound, Washington and a Comparison with Updated Observations. In: NOAA technical memorandum ERL PMEL –84.

Lieberman, S.H., C. Clavell, and D.B. Chadwick (1989). Techniques for Real-Time Environmental Mapping and Monitoring. In: Proceedings, 16th meeting, US-Japan Marine Facilities Panel: United States-Japan Cooperative Program in Natural Resources on Marine Facilities, p. 495-499.

Lincoln, J.H. and E. Collias (1975). An Oceanographic Study of the Port Orchard System. In: URS

Micronautics Inc. (1984). Tide.1 Tide and Current Prediction Software. P.O. Box 1428, Camden, Maine, 04843.

Nakashima, S., R. E. Sturgeon, S. N. Willie, and S. S. Berman (1988). Determination of Trace Elements in Sea Water by Graphite-Furnace Atomic Absorption Spectrometry After Preconcentration by Tetrahydroborate Reductive Precipitation. Analytical Chimica Acta 207, p. 291-299.

Owens, W.B., and R.C. Millard (1985). A new algorithm for CTD oxygen calibration. In: Journal of Physical Oceanography, 15, p. 621-631.

Paulson, A.J., Feely, R.A., Curl, C., Crecelius, E.A., Geiselman, T. (1988). The impact of scavenging on trace metal budgets in Puget Sound. In: Geochimica et Cosmochimica Acta, 52, p. 1765-1779.

Ridley, E.L. and Ostericher, C.O. (1960). Flushing Study of Sinclair Inlet, Bremerton, Washington, U.S. Navy Hydrographic Office, Washington 25, D.C., Informal Oceanographic Manuscripts 21-60. UNPUBLISHED MANUSCRIPT.

Tetra Tech, Inc. (1988a). Puget Sound Estuary Program, Sinclair and Dyes Inlets Action Program: Initial Data Summaries and Problem Identification. In: Prepared for U.S. Environmental Protection Agency, Region X – Office of Puget Sound, Seattle, WA, TC-3338-13, Final Report.

Tetra Tech, Inc. (1988b). Puget Sound Estuary Program, Characterization of Spatial and Temporal Trends in Water Quality in Puget Sound. In: Submitted to U.S. Environmental Protection Agency, Region 10, Seattle, WA, U.S. EPA 503/3-88-003.

U.S. Department of the Navy (1983). Initial Assessment Study of Naval Shipyard Puget Sound, Bremerton, Washington. ESSA 13-022, Prepared for U.S. Navy Assessment and Control of Installation Pollutants (NACIP) Department, Port Hueneme, CA.